

APPLICATION OF ENERGY DISPERITIVE X-RAY
FLUORESCENCE TECHNIQUE FOR THE
DETERMINATION OF THE ELEMENTAL
COMPOSITION OF AIR PARTICULATE
MATTER IN KANPUR CITY

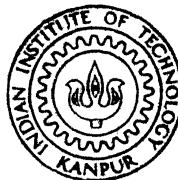
By

VEENA RAMRAO JOSHI

TH
PHY/1981/D

J

A70491



DEPARTMENT OF PHYSICS

INDIAN INSTITUTE OF TECHNOLOGY KANPUR

JULY, 1981

APPLICATION OF ENERGY DISPERITIVE X-RAY
FLUORESCENCE TECHNIQUE FOR THE
DETERMINATION OF THE ELEMENTAL
COMPOSITION OF AIR PARTICULATE
MATTER IN KANPUR CITY

A Thesis Submitted
in Partial Fulfilment of the Requirements
for the Degree of
DOCTOR OF PHILOSOPHY

By
VEENA RAMRAO JOSHI

to the

DEPARTMENT OF PHYSICS

INDIAN INSTITUTE OF TECHNOLOGY KANPUR
JULY, 1981

To

My Parents

70491

6 APR 1982

CERTIFICATE

This is to certify that the work presented in this thesis entitled 'Application of Energy Dispersive X-Ray Fluorescence Technique for the Determination of the Elemental Composition of Air Particulate Matter in Kanpur City' by Veena Ramrao Joshi has been done under my supervision and it has not been submitted elsewhere for a degree or diploma.

R. M. Singru

R. M. Singru
Department of Physics
Indian Institute of Technology,
Kanpur, India.

July 1981.

20.3.1982 126

ACKNOWLEDGEMENTS

I take this opportunity to express my deep sense of gratitude to Professor R.M. Singru for his encouragement and guidance throughout this work. I am also thankful to him for his considerate help in personal matters. I am grateful to Professor G.N. Rao for his guidance during the initial stages of my graduate research activities; he also introduced me to this interesting analytical technique, XRF.

This work was done under a project sponsored by the Department of Science and Technology, Government of India under grant no. DST/ES/127/75. Without the help and co-operation of persons working in this project, I could not have ventured to take up this problem. I express my sincere thanks to Dr. K.K. Dwivedi for his enthusiastic co-operation, useful discussions and ready help throughout the period of this work. I am equally grateful to Drs. Prem Sagar and V.V.V. Subrahmanyam for their help in the different stages of this work. My thanks are also due to all other person employed in the project for their help at various stages.

I wish to express my thanks to Shri Harish Chandra of I.T.R.C. Lucknow for lending the air sampling equipment. I convey my sincere thanks to the various organisations and persons for their ready help in providing power and place for air particulate sampling. The co-operation extended by Transport Section, I.I.T. Kanpur, in particular by Shri G.B. Vaidya needs a special acknowledgement.

I am thankful to Dr. Sudhir Sen and Professor G.K. Mehta for their co-operation during my work in the Nuclear Laboratory. I express my thanks to Professor P.S. Goel for providing the NIM standard samples. I convey my sincere thanks to Shri N.V. Blair for his help in electronic problems and Dr. Harish Verma for helping me in computer programming. I also express my thanks to the staff of Central Nuclear Laboratory, Glass blowing workshop, Physics workshop and Electronic workshop for their co-operation.

I am thankful to Shri B.K. Jain for preparing neat tracings, to Shri L.S. Bajpai for efficient typing and to Shri H.K. Panda for careful cyclostyling. I also thank Dr. T.R. Govindarajan, Shri Alhilesh Prasad, Shri A.K. Singh and Shri Ajit Mohan for their help in the final stages.

I am thankful to the Council of Scientific and Industrial Research, India and I.I.T. Kanpur for providing me with financial assistance.

Working in Central Nuclear Laboratory was a pleasure and I am thankful to all my colleagues for their friendly association.

I thank my brother, Raju for his patient help. I am also grateful to my parents-in-laws, Smt. and Shri M.V. Vallentyne for shouldering the responsibility of our son during the final stages of the thesis. Finally, I wish to express deep appreciation for my husband, Kishore, for

whatever he did to enable me to complete this work.

I cherish the memory of all those who have helped me in innumerable ways and have made my stay at I.I.T. Kanpur a memorable one.

VEDNA JOSHI

CONTENTS

LIST OF TABLES	viii
LIST OF FIGURES	xi
SYNOPSIS	xiv
CHAPTER 1 : AIR POLLUTION	1
1.1 Introduction	1
1.2 Pollutants and Sources	3
1.2.1 Introduction	3
1.2.2 Gaseous Pollutants	6
1.2.3 Air particulate matter	9
1.3 Air Quality Studies	16
1.3.1 Air quality criteria	16
1.3.2 Air quality monitoring	18
1.4 Air Pollution Studies in India	22
1.5 Motivation Behind the Present Work	23
References	26
✓CHAPTER 2 : TECHNIQUES FOR ELEMENTAL ANALYSIS OF AIR PARTICULATE MATTER	29
2.1 Introduction	29
2.2 Neutron Activation Analysis	31
2.2.1 Description of the method	31
2.2.2 Sensitivity, detection limit, precision and accuracy	34
2.3 Atomic Absorption Spectrometry	36
2.3.1 Description of the method	36
2.3.2 Interferences, accuracy and detection limit	39
2.4 Atomic Emission Spectroscopy	42
2.5 X-ray Spectrometry	43
2.5.1 Principle	43
2.5.2 Modes of X-ray detection	44
2.5.3 Modes of excitation	47
2.6 Solid Source Mass Spectrometry (SSMS) and Other Methods	53
2.7 Remarks	55
References	58
✓CHAPTER 3 : DESCRIPTION OF THE X-RAY FLUORESCENCE SPECTROMETER USED IN THE PRESENT WORK	61
3.1 Introduction	61
3.2 Experimental Set-up	61
3.2.1 Source and sample assembly	61
3.2.2 Electronic systems	67

	<u>Page</u>
3.3 Calibration of Our Spectrometer	77
3.3.1 Method	77
3.3.2 Preparation of the standards of pure elements	83
3.3.3 XRF analysis of the standards of pure elements	85
3.3.4 Accuracy	92
References	99
 CHAPTER 4 : SAMPLE COLLECTION AND XRF ANALYSIS OF THE SAMPLES	 101
4.1 Sampling Plan	101
4.1.1 Area description	101
4.1.2 Station locations	103
4.2 Sample Collection	110
4.2.1 Selection of the sampling sites	110
4.2.2 Sampling equipment	113
4.2.3 Collection of air particulate samples	116
4.3 XRF Analysis	121
4.3.1 Data acquisition	121
4.3.2 Method of analysis	121
References	127
 CHAPTER 5 : RESULTS AND DISCUSSION	 128
5.1 Analysis of Air Quality Data of Kanpur City	128
5.1.1 Introduction	128
5.1.2 Levels of TSF and amounts of trace elements in Kanpur city	130
5.1.3 Zone-wise analysis of Kanpur air quality results	135
5.1.4 Enrichment factor calculation	162
5.1.5 Correlation analysis	169
5.1.6 Factor analysis method	175
5.1.7 Factor analysis of the elemen- tal data in zones A, B and C of Kanpur city	181
5.2 Analysis of Air Particulate Matter Collected at the Breathing Level at Some Busy Traffic Crossings in Kanpur City	188
5.3 Analysis of Air Particulate Matter Collected Inside Some Factories	193
5.4 Summary of the Present Work and Conclusions Drawn	202
References	206

LIST OF TABLES

<u>Table No.</u>		<u>Page</u>
1.1	Summary of the gas composition of dry (water vapour-free) atmospheric air [5].	4
1.2	U.S. emission (in million metric tons/yr) of major air pollutants [7].	5
1.3	Mass emission of particles from main natural and anthropogenic sources [16].	10
1.4	Range of specific concentrations of elements in source materials [17].	12,13
1.5	Typical air quality in some cities of the world [18].	14
1.6	Sources and health effects of some trace elements in the atmosphere [21].	15
1.7	National ambient air quality standards promulgated by EPA on April 30, 1971 [27].	17
1.8	Threshold limit values (TLV) for work-room atmosphere.	19
2.1	Commonly used low energy X-ray (XR) and gamma-ray (GR) sources.	50
2.2	Elemental detection limits (ng/m^3) for different X-ray spectrometric methods.	52
2.3	Typical elemental detection limits (ng/m^3) in air particulate matter using different instrumental techniques.	56
2.4	Comparison of different instrumental techniques for elemental analysis.	57
3.1	Energies and intensities of some gamma-rays and X-rays from radioactive ^{241}Am source [2].	64
3.2	Sensitivities for different elements for the XRF spectrometer used in the present work.	91
3.3	Detection limits for different elements calculated from a XRF spectrum of a typical air particulate sample collected by us.	93

Table No.Page

3.4	K_{β}/K_{α} ratios for some elements	94
3.5	Analysis of NIM samples (concentration values are given in parts per million (ppm)).	96, 9
4.1	List of big industries in Kanpur shown in Fig. 4.1.	105, 1
4.2	Description of the sampling stations shown in Fig. 4.2.	109
4.3	List of sampling sites shown in Fig. 4.3.	112
5.1	Geometric mean and standard deviation for metals and TSP concentration ($\mu\text{g}/\text{m}^3$) in Kanpur and some other cities.	131
5.2	Arithmetic mean values and standard deviation of TSP and elemental concentration ($\mu\text{g}/\text{m}^3$) in Kanpur and some other cities.	132
5.3(a)	Information about the air particulate samples collected in thickly populated zone A.	136
5.3(b)	Information about the air particulate samples collected in thinly populated zone B.	137
5.3(c)	Information about the air particulate samples collected in industrial zone C.	138
5.4(a)	TSP and elemental concentrations ($\mu\text{g}/\text{m}^3$) at various locations in thickly populated zone A.	140, 1
5.4(b)	TSP and elemental concentration ($\mu\text{g}/\text{m}^3$) at various locations in thinly populated zone B.	142, 1
5.4(c)	TSP and elemental concentrations ($\mu\text{g}/\text{m}^3$) at different locations in industrial zone C.	144, 1
5.5	Range, geometric mean and standard deviation ($\mu\text{g}/\text{m}^3$) of the TSP and elemental concentrations in different zones of Kanpur.	159
5.6	Enrichment factors for different elements in Kanpur and other cities.	164
5.7	Enrichment factors for different elements in various zones of Kanpur city.	167

<u>Table No.</u>		<u>Page</u>
5.8	Identification of locations with high level of pollution due to sources other than soil.	168
5.9(a)	Linear correlation coefficients for samples in zone A.	171
5.9(b)	Linear correlation coefficients for samples in zone B.	172
5.9(c)	Linear correlation coefficients for samples in zone C.	173
5.10(a)	Factor analysis loadings (Rotated six-factor solution for zone A).	182
5.10(b)	Factor analysis loadings (Rotated six-factor solution for zone B).	183
5.10(c)	Factor analysis loadings (Rotated six-factor solution for zone C).	184
5.11	Elemental groups with large factor loadings on various factors in different zones.	186
5.12	Information about air particulate samples collected at breathing level at few busy crossings in Kanpur city.	189
5.13	Concentration of TSP and various elements ($\mu\text{g}/\text{m}^3$) in air particulate samples at some busy crossings in Kanpur city.	191,192
5.14	Linear correlation coefficients for samples collected at breathing level.	194
5.15	Factor analysis loadings (Rotated four-factor solution for samples at breathing level).	195
5.16	Information about air particulate samples collected inside some factories in Kanpur city.	197
5.17	TSP and elemental concentration ($\mu\text{g}/\text{m}^3$) at various places inside some factories in Kanpur city.	198,199
5.18	Maximum concentration in $\mu\text{g}/\text{m}^3$ recommended by the W.H.O. [29].	200

LIST OF FIGURES

<u>Fig. No.</u>		<u>Page</u>
2.1	Irradiation and counting scheme for the analysis of air particulates collected on filter paper.	33
2.2	Schematic diagram of atomic absorption spectrometer.	38
2.3	Flow chart for the atomic absorption analysis of atmospheric particulate samples collected on polystyrene filters.	40
2.4	Some of the basic atomic processes in X-ray fluorescence analysis.	45
2.5	Flow diagram of various X-ray spectrometric techniques.	46
3.1	Important gamma rays from radioactive ^{241}Am .	63
3.2	Photon spectrum from radioactive ^{241}Am .	65
3.3	Horizontal cross-section of the source holder.	66
3.4	Experimental arrangement for mounting the source and sample in front of the detector.	68
3.5	Energy resolution spectrum using radioactive ^{57}Co source.	72
3.6	Plot of FWHM vs. Energy.	73
3.7	Typical block diagram of the experimental set-up.	75
3.8	An energy calibration curve.	78
3.9	The filtration assembly used for thin element sample preparation.	84
3.10	Arrangement showing the preparation of thin samples from solutions using a nebulizer.	86

3.11	A plot of peak intensity vs. distance between sample and source holder.	88
3.12	A plot of deposition vs. intensity for Pb and Cr.	89
4.1	Map of Kanpur city showing important industries and main roads.	104
4.2	Map of Kanpur city showing sampling locations for air particulate samples.	108
4.3	Map of Kanpur city showing some busy crossings where air particulate samples were collected at breathing level.	111
4.4	A schematic diagram of the filter holder.	115
4.5	Experimental arrangement for air particulate sampling.	117
4.6	Photograph of some air particulate samples collected on the filter paper.	120
4.7	A typical XRF spectrum of an air particulate sample.	122
5.1	Map of Kanpur city showing the level of air particulate matter at various locations. The levels are indicated by a colour code.	139
5.2	Map of Kanpur city showing the level of Potassium detected in air particulate samples at various locations. The levels are indicated by colour code.	147
5.3	Map of Kanpur city showing the level of Calcium in air particulate samples at various locations. The levels are indicated by a colour code.	148
5.4	Map of Kanpur city showing the level of Titanium detected in air particulate samples at various locations. The levels are indicated by a colour code.	149
5.5	Map of Kanpur city showing the level of Vanadium detected in air particulate samples at various locations. The levels are indicated by a colour code.	150

<u>Fig. No.</u>		<u>Page</u>
5.6	Map of Kanpur city showing the level of Chromium detected in air particulate samples at various locations. The levels are indicated by a colour code.	151
5.7	Map of Kanpur city showing the level of Manganese detected in air particulate samples at various locations. The levels are indicated by a colour code.	152
5.8	Map of Kanpur city showing the level of Iron detected in air particulate samples at various locations. The levels are indicated by a colour code.	153
5.9	Map of Kanpur city showing the level of Nickel detected in air particulate samples at various locations. The levels are indicated by a colour code.	154
5.10	Map of Kanpur city showing the level of Copper detected in air particulate samples at various locations. The levels are indicated by a colour code.	155
5.11	Map of Kanpur city showing the level of Zinc detected in air particulate samples at various locations. The levels are indicated by a colour code.	156
5.12	Map of Kanpur city showing the level of Lead detected in air particulate samples at various locations. The levels are indicated by a colour code.	157
5.13	The range and typical values of urban trace element concentrations.	160

SYNOPSIS

APPLICATION OF ENERGY DISPERITIVE X-RAY FLUORESCENCE TECHNIQUE FOR THE DETERMINATION OF THE ELEMENTAL COMPOSITION OF AIR PARTICULATE MATTER IN KANPUR CITY.

By

VEENA RAMRAO JOSHI
Department of Physics
Indian Institute of Technology,
Kanpur 208016, India.

July 1981

In recent years, it has become possible to estimate the concentration of trace elements in environmental systems because of the advances in instrumental analytical techniques. In particular, instrumental techniques like energy dispersive X-ray fluorescence (XRF), instrumental neutron activation analysis (INAA), proton induced X-ray emission (PIXE) are being routinely used in the elemental analysis of air particulate matter. Due to the simplicity of analysis and its easy availability the XRF technique finds wide applications in the analysis of environmental systems. A number of investigators have obtained a large amount of information concerning the particulate concentration and distribution of trace elements in different kinds of atmosphere (heavily polluted, rural, marine, desert environment etc.) using these techniques. The measurement of chemical composition of air particulate matter provides us with important quantitative data about the extent of pollution and possible

health hazards. By analyzing the data it is possible to identify various natural and anthropogenic sources of pollution. Knowledge of sources of pollution is important in deciding the pollution control measures and it helps in understanding the distribution and transport of potentially toxic elements in the atmosphere.

To date, extensive air pollution studies and the use of instrumental techniques for elemental analysis of air particulate matter have been mainly confined to industrially developed countries where the problem of environmental pollution is more acute. There is little information available regarding the concentration and behaviour of trace elements in the cities of developing countries. Apart from other socioeconomic reasons the lack of instrumental techniques which are carefully standardized for this purpose is also an important reason for this drawback. A few studies carried out in India and Brazil already indicate that the concentrations of trace metals observed are comparable with those in industrially developed countries. Previous studies show that the amount of total suspended particulates (TSP) in the big cities of India (e.g. Bombay, Calcutta, Kanpur and Delhi) is very high (about 3-4 times) compared to the other cities in the world. A systematic study of the concentration of air particulate matter and its composition in an industrial city in India will enable us to understand the nature and sources of pollution giving rise to the high TSP concentration. This

information is also valuable while setting national air quality criteria for TSP.

We have selected Kanpur city to characterise the elemental composition of air particulate matter and to identify their sources. Kanpur is one of the most populous cities in India. It is an old industrial city where there is no urban planning and where the industrial pockets and residential colonies are situated in the same localities. It is also an important commercial centre of northern India. The modes of transport in the city are very diverse, varying from bullock carts to trucks and this gives rise to a large amount of suspended dust in the atmosphere. The extent of pollution in this city is expected to be very high and a systematic study of air particulate matter would be of great help in estimating the level of pollution and possible health hazards due to the toxic metals. Considering the large amount of dust raised in the atmosphere due to the old mode of heavy traffic, it is interesting to study the elemental concentration in air particulate matter at breathing level at the busy crossings. Keeping these aims in mind an energy dispersive X-ray fluorescence spectrometer was set up. The XRF spectrometer was standardized for accurate concentration measurements with the help of pure element specimens. The XRF spectra of various types of air particulate samples collected on filter papers were recorded. The identification of elements was done by determining the energies of

the peaks and the concentrations of various elements were measured by analyzing the area of the peaks. The air quality results obtained show that the levels of trace elements like Zn, Pb, Cu are comparable with those obtained at other cities of the world whereas elements like Ca, K, Fe show very high concentration in the atmosphere of Kanpur. Further analysis of the data is made by calculating enrichment factors and by applying statistical factor analysis method. The extent of pollution at the busy crossings is compared with the air quality data obtained at nearby localities. The results obtained for the atmosphere inside the factories are compared with the threshold limit values for the work-room atmosphere.

In Chapter 1 the problem of air pollution is introduced in general terms. A description of various important pollutants, their sources and sinks is given. Atmospheric levels of different pollutants and their possible health effects are discussed. The problem of trace metal pollution and possible health hazards are summarised. Various methods used in the analysis of the trace element data are outlined. The previous work done in India to measure TSP concentrations and their chemical composition is presented. The motivation behind the present work is described in the last section.

A review of various instrumental techniques used in the elemental analysis of the air particulate matter is given in Chapter 2. The detection limits obtained for various elements using different methods are compared and

the relative merits and demerits in using different techniques for elemental analysis are discussed.

In Chapter 3 we have described the characteristics of a Si(Li) solid state detector and other electronic systems used in the present experimental arrangement. Standardization of the X-ray fluorescence spectrometer was carried out by analyzing a number of thin samples of various pure elements or their compounds. These samples were prepared on Sartorius membrane filter papers by a nebulizer or by vacuum filtration technique. The accuracy of the standardization method used was determined by analyzing XRF spectra of standard NIM-rock samples. The standard NIM-rock samples are a set of geochemical standards and are obtained from South African Bureau of Standards. The agreement between the experimentally measured and certified concentrations of various elements is about 10%. The sensitivities (counts/sec/ $\mu\text{g}/\text{cm}^2$) of various elements and K_β/K_α ratios obtained from analysis of XRF spectra of pure element samples are tabulated. The detection limits are obtained by analyzing a typical air particulate sample.

In Chapter 4, the geographic, climatic and industrial conditions in Kanpur city are described. Criteria used in selecting sampling stations and sites to study the air quality of Kanpur city are described. Three types of air particulate samples were collected at different locations; viz. i) in different zones of Kanpur city to study the quality of Kanpur atmosphere ii) at busy crossing in the

city to study the extent of road side pollution iii) inside an iron and steel factory, a paints factory and a leather processing factory to study the work-room atmosphere. A portable GEC air sampler was used to collect air particulate samples on preweighed Sartorius membrane filters. Details of the sample collection are described. The method of recording the XRF spectra is described. The method followed for identification of element and for the calculation of peak area is described. Various corrections applied to obtain the net peak area corresponding to the actual concentration of the element are discussed. The method of converting peak area into $\mu\text{g}/\text{m}^3$ or parts per million (ppm) at NTP is outlined.

The results of elemental analysis are presented, analyzed and discussed in Chapter 5. The elemental data obtained for Kanpur city is compared with the air quality data for the other cities of the world. A zonewise examination of the data for the Kanpur city is made and it gives us an idea regarding the extent of pollution in various zones. The method of calculating enrichment factor, correlation coefficients and factor analysis is described. The results obtained from the elemental data by applying above methods are discussed and information regarding the sources of emission and their transport in the atmosphere is given.

It is hoped that the method of standardization, and the method of collection of air particulate samples outlined in this work will be useful in collection and analysis

of the air particulate samples involved in air monitoring studies. The elemental data analyzed by us have helped in understanding the high value of TSP and also in identifying the heavily polluted areas in Kanpur city. The data evaluation techniques used in the present analysis can be used in future studies to investigate the impact of current anthropogenic activities on the air quality of other industrial cities in India. It is hoped that the present work has illustrated how modern physical techniques can be applied to study problems of social relevance.

Chapter 1

AIR POLLUTION

1.1 Introduction

Problems of environmental pollution are byproducts of the development of civilization, the advancement in technology and the growing needs of mankind. The environment, defined as that outer physical and biological system in which man and other organisms live, is a complicated system with many interacting components. The environmental balance is a result of natural evolution of these interacting components, the history of which may be traced back to the evolution of life. Development of technology and industry has changed this environmental balance and has created a large number of problems affecting the air we breath, the water we drink and the soil in which our food is grown.

Among the various pollution problems the problem of atmospheric pollution demands greater attention as human health largely depends on the quality of air inhaled. Air has many other functions too. It is a storehouse and carrier of oxygen. It also carries sound and light. The atmosphere absorbs most of the damaging radiation that would otherwise reach earth from space. The chemical reactions that take place in our space are a mixture of desirable and undesirable ones. Air pollution is a global problem in the sense the transport of air pollutants is not affected by national boundaries.

The first documentation of the problem may have been the Roman complaints of the foulness of their city's air.

Coal burning was prohibited in London as early as 1273 A.D.

Air pollution episodes due to smog during which stagnant air trapped pollutants over a city or an industrial area became more prevalent with industrial development. A few of the places which suffered due to these episodes are London (1952) [1], Donora (1950) [2], the Meuse Valley in Belgium (1930) [3] etc. In all these situations excess deaths and a greater incidence of respiratory diseases were recorded. This led to the promulgation of clean air legislation in United States in 1955 and in England in 1956 and later to very extensive pollution studies in most of the developed countries.

In our country, the problem of environmental pollution is being recognised during the last few years. The public uproar against the Silent Valley project as well as against the installation of the Mathura Refinery; creation of a separate department of environment at the central government level and passing a legislation about air pollution provide evidence of public and government concern about the air pollution.

Air pollution has been defined in many ways. The Engineer's Joint Council defines [4] it as : "Air pollution means the presence in the outdoor atmosphere of one or more contaminants such as dust, fumes, gas, mist, odour, smoke

or vapour in quantities of characteristic and or duration such as to be injurious to human, plant or animal life or to property or which unreasonably interfere with the comfortable enjoyment of life and property".

1.2 Pollutants and Sources

1.2.1 Introduction

Composition of dry, natural air near the sea is given in Table 1.1. Depending on the level and kind of pollution this composition changes and also new pollutants are added into the atmosphere. World Health Organisation (WHO) has selected six most widespread pollutants for intensive international study, with the aim of setting criteria and guides for air quality [6]. The six pollutants selected are:

- i) sulphur dioxide ii) particles iii) carbon monoxide
- iv) oxidants v) nitrogen oxides and vi) lead.

The major anthropogenic sources of these pollutants are i) transportation ii) domestic heating iii) electric power generation iv) refuse burning v) industrial fuel burning and vi) process emissions. In Table 1.2 emissions of these various pollutants into the atmosphere due to different man-made sources are given. The emission data for other countries will be different depending on the type and intensity of its sources. A good part of these emissions are removed by natural processes and a part remains in the

Table 1.1

Summary of the Gas Composition of Dry (Water Vapor-Free) Atmospheric Air [5].

Type of Gas	Chemical Symbol	Concentration		Residence Time
		ppm	$\mu\text{g}/\text{m}^3$	
Principal gases				
Nitrogen	N_2	780000	$976 \cdot 10^6$	continuous
Oxygen	O_2	209400	$298 \cdot 10^6$	continuous
Argon	Ar	9300	$166 \cdot 10^6$	continuous
Trace gases				
Helium	He	5.2	920	about $2 \cdot 10^6$ years
Neon	Ne	18	$(1.6) \cdot 10^4$	continuous
Krypton	Kr	1.1	4100	continuous
Xenon	Xe	0.086	500	continuous
Carbon dioxide	CO_2	200-400	$(4-8) \cdot 10^5$	4 years
Carbon monoxide	CO	0.01-0.02	10-200	about 0.3 years
Methane	CH_4	1.2-1.5	850-1100	about 100 years
Formaldehyde	CH_2O	0-0.1	0-16	?
Nitrogen oxides	N_2O	0.25-0.6	500-1200	about 4 years
	NO_2	$(1-4.5) \cdot 10^{-3}$	2-8	a few days
Ammonia	NH_3	0.002-0.02	2-20	?
Hydrogen sulfide	H_2S	$(2-20) \cdot 10^{-3}$	3-30	about 40 day
Sulfur dioxide	SO_2	0-0.02	0-50	about 5 days
Chlorine	Cl_2	$(3-15) \cdot 10^{-4}$	1-5	a few days
Iodine	I_2	$(0.4-4) \cdot 10^{-5}$	0.05-0.5	?
Hydrogen fluoride	HF	$(0.8-18) \cdot 10^{-3}$	0.7-16	?
Hydrogen	H_2	0.4-1.0	36-90	?
Ozone	O_3	0-0.05	0-100	about 60 day

Table 1.2

U.S. Emission (in Million of Metric Tons/yr) of Major Air Pollutants [7].

Source	CO	Part Matter	SO _x	HC	NO _x
Motor vehicle (gasoline)	53.5	0.5	0.2	13.8	6.0
Motor vehicle (diesel)	0.2	0.3	0.1	0.4	0.5
Aircraft	2.4	0.0	0.0	0.3	0.0
Rail, Roads and others	2.0	0.2	0.5	0.6	0.8
Total transportation	58.1	1.1	0.7	15.1	7.3
Coal	0.7	7.4	18.3	0.2	3.6
Fuel oil	0.1	0.3	3.9	0.1	0.9
Natural gas	0.0	0.2	0.0	0.0	4.1
Wood	0.9	0.2	0.0	0.4	0.2
Total fuel combustion	1.7	8.1	22.2	0.6	9.1
Industrial processes	8.8	6.8	6.6	4.2	0.2
Solid waste disposal	7.1	1.0	0.1	1.5	0.5
Forest fires	6.5	6.1	0.0	2.0	1.1
Agriculture burning	7.5	2.2	0.0	1.5	0.3
Coal refuse burning	1.1	0.4	0.5	0.2	0.2
Structural fires	0.2	0.1	0.0	0.1	0.0
Total miscellaneous	15.3	8.7	0.5	7.7	1.5
Total	91.0	25.7	30.2	29.1	18.7

atmosphere for different periods depending on its residence time. The six pollutants can be broadly categorised as gaseous and particulate.

1.2.2 Gaseous pollutants

(a) Sulphur dioxide : Robinson and Robbins [8] have estimated that sulphur oxides from man's activities introduce 66 million metric tons of sulphur into the atmosphere annually, largely from coal and petroleum combustion. Natural sulfur sources are biologically produced H_2S (arising from decay of organic matter) that is eventually oxidised to sulfur oxides and sulfates from sea spray. The total natural emission of sulfur is 129 million metric tons per year.

The major portion of sulfur oxides emitted is SO_2 and emission of SO_3 is only a few percent of SO_2 . SO_2 is readily oxidised to SO_3 in the atmosphere by photochemical or catalytic processes and in the presence of moisture SO_2 becomes H_2SO_4 or a sulphate salt and soon precipitates out to the atmosphere. The SO_2 in the atmosphere lasts only a few days and SO_2 concentration in atmosphere is small compared to annual emissions by man.

The actual amount of sulfur dioxide found in the air varies from almost nil in some rural areas to 3 parts per million (ppm) in heavily industrialized areas. During the mid - 1960's data obtained by the Air Monitoring Project in U.S. showed mean annual concentrations of SO_2 ranging from 0.01 ppm in San Francisco to 0.18 ppm in Chicago [9].

Individual SO_2 concentration exhibited a log-normal frequency distribution. Data showed that the 1-hour maximum values for the year were about 10 to 20 times the annual average and 1 day maximum values for the year were about 4 to 7 times the annual average.

Sulphur dioxide (SO_2) has been the suspect in several air pollution disasters - notably Donora, the Meuse Valley and several episodes in London. Sulphur oxides can damage materials and property through their conversion into the highly reactive H_2SO_4 . The corrosion of metals like Fe, steel, Zn is accelerated by atmospheres polluted by SO_2 and particulate matter. Humidity and temperature play an important synergistic roles. SO_2 has been found to affect the vegetation even at 0.03 ppm level. SO_2 and H_2SO_4 are capable of irritating the respiratory system of animals and human beings.

In India, Rao et al. [9] have shown that operation of Mathura refinery will endanger Taj Mahal and the life of people in the neighbouring areas due to the high level of SO_2 emission.

(b) Carbon monoxide : CO originates from the incomplete combustion of carbonaceous materials and is the air pollutant emitted in the largest quantities. It is estimated that man's activities are producing 250 million metric tons annually and there exist some biological sources of CO. Oceans are a natural source of CO (10 million metric tons/yr) [11]. Residence time of CO is found to be 0.1 yr [11].

Oxidation of CO to CO_2 is very slow. Removal processes of CO are not well understood. The various possibilities are: i) CO is adsorbed and oxidized on surfaces; perhaps it is removed and utilized by plants and animals ii) or perhaps photochemical or catalytic processes are involved in its removal [12]. Recent research indicates that soils are capable of removing large amounts of CO from the atmosphere probably due to the activity of soil microorganisms [13].

In the urban areas of U.S.A. CO concentration of several ppm are common [11].

A variety of toxic effects of CO on human beings and animals arise from its combination with hemoglobin in the blood [12].

(c) Nitrogen oxides : Nitrous oxide is a normal constituent of the atmosphere and is found in concentration of about 0.5 ppm. Out of the many oxides of nitrogen only nitrogen oxide (NO) and nitrogen dioxide (NO_2) are emitted into the atmosphere by man in significant quantities. Estimated biological production of NO and N_2O amounts to about 1 billion metric tons annually, while man's combustion processes produce about 48 million metric tons of NO_x annually [14].

The concentration of NO and NO_2 in nonurban areas are only a few parts per billion and these gases have a residence time in the atmosphere of only 3 or 4 days [15].

Concentration of 100 ppm or more for a few minutes can be lethal to humans and animals, and exposures to 5 ppm

for a few minutes leads to effects on the respiratory system. Long-term exposures to 0.06 ppm have been related to an increase in acute respiratory disease in humans [15].

(d) Oxidants : These are a result of reactions induced by sunlight on automobile exhaust. They are typical of Los Angeles Smog and cause eye irritation and asthmatic attacks and are found in many cities with abundant sunlight and much pollution from automobiles.

1.2.3 Air particulate matter

Historically, the oldest air pollution problem is that of smoke and soot i.e. particulate matter. Natural sources of atmospheric particles are ocean spray resulting in salt particles, volcanoes, biological sources emitting spores, pollen, viruses or bacteria. Forest, grass and brush fires produce 5×10^{18} particles/m². Dust and sand-storms also contribute to the particulate burden of atmosphere. During the last century man's activities have caused a significant change in the amount and composition of the particulate matter. The increasing need for energy and raw materials to feed a metal-based technology has contributed large quantities of normally unavailable trace elements in the environment. This sudden availability of trace elements, coupled with their toxicity to living organisms, constitutes the problem of trace element pollution. In Table 1.3 mass emissions of particles from main natural

Table 1.3

Mass Emission of Particles from Main Natural and Anthropogenic Sources [16].

Source	Natural		Anthropogenic	
	$\times 10^6$ tons	%	$\times 10^6$ tons	%
	year $^{-1}$	year $^{-1}$		year $^{-1}$
Primary particle production				
Coal fly ash			39.7	1.4
Iron and steel industry emission			9.9	0.34
Nonfossil fuels (wood, mill wastes)			8.8	0.31
Petroleum combustion			2.2	0.08
Incineration			4.4	0.15
Cement manufacture			7.7	0.27
Agricultural emission			11.0	0.38
Miscellaneous			17.6	0.61
Sea salt	1102	38		
Soil dust	220	7.7		
Volcanic particles	4.4	0.15		
Forest fires	3.3	0.12		
Subtotal	1329.7	46.3	101	3.5
Gas-to-particle conversion				
Sulfate from H_2S	225	7.8		
Sulfate from SO_2			162	5.6
Nitrate from NO_x	476	16.6	33	1.1
Ammonium from NH_3	297	10.3		
Organic aerosol from terpenes, hydrocarbons, etc.	220	7.7	30	1.1
Subtotal	1218	42.4	225	7.8
Total	2548	88.7	326	11.3

and anthropogenic sources are given. Table 1.4 gives the range of specific concentrations (ppm) of elements in various source materials. From Table 1.3 and 1.4 we can see that man's contribution to total air particulate matter is about 10 per cent of that due to natural source, but man-made sources are major contributors of trace elements like Zn, V, Pb, Ni, Mn, Cu, and Cr etc.

The main sink of atmospheric particulates is precipitation and its rate depends on the density and diameter of the particles according to the Stokes' law. Deviation from Stokes' law occurs as a result of irregular particle shapes, turbulent flow around large particles, random Brownian motions of very small particles and weather effects.

Air quality data for different pollutants at various places are given in Table 1.5. The high values of total suspended particulates (TSP) in India is a striking feature of these data.

The effects of air pollution due to particulate matter depend on the composition as well as on the particle size of the suspended dust. The general effect of particulates is to reduce visibility as well as the amount of solar radiation reaching the earth. Lipfert [19] observed that particulates are associated with excess deaths especially during the air pollution episodes.

Effects of particulate dust on human beings depend on the particle size and composition. In Table 1.6 health

Table 1.4

Range of Specific Concentrations of Elements in Source Materials [17].

Element	Crustal Dust*	Sea Salt*	Coal-Fired Power Plant Ash*	Oil-Fired Power Plant Ash*
Al	8.6 %	4.6-5.5	1-10 %	100-5000
As			10-500	30
Ba	588	1.4	100-1000	0.05-1 %
Be	2.4		1-10	
Br		0.19 %		
Ca	1.25 %	1.16 %	1-5 %	10-1000
Cd			10-100	
Cl		55 %		
Co	17		10-100	90
Cr	98		10-1000	66
Cu	48		10-1000	50-2000
Fe	4.8 %	0.5-5	1-50 %	1-10 %
Hg	0.37		0.1-1	
K	1.68 %	1.1 %	0.5-5 %	1000
Mg	1.62 %	3.7 %	0.1-1 %	500-5000
Mn	550	0.025-0.25	100-1000	1-100
Mo			10-100	
Na	0.9 %	30.6 %	0.5-5 %	0.2-5 %
Ni	57		10-1000	
Pb	168	0.12-0.14	100-5000	200-2000
Sb			1-100	5
Se	15		10-100	5
Si	24 %	1.4-94	10-50 %	0.1-1 %
Sn	11		1-10	
Sr				
Ti	0.51 %		0.1-2 %	
V	100	0.009	50-5000	0.01-20 %
Zn	281	0.14-0.40	100-10,000	200-3500

Continued

Table 1.4

Range of Specific Concentrations of Elements in Source Materials [17].

Element	Municipal Incinerator Ash*	Cement Manufacturing Ash*	Automotive Exhaust Particulates*	Iron and Steel Foundry Emission*
Al	1-10 %			10-1000
As	10-500			
Ba	100-5000			
Be	1-10	1-10		
Br	50-2000		7.9 %	
Ca	1-10 %			
Cd	10-5000	10-1000		
Cl	0.5-20 %		6.8 %	
Co	10-1000			
Cr	100-5000	100-1000		10-100
Cu	100-5000	0.01-1 %		10-100
Fe	0.1-10 %		0.4 %	0.1-10 %
Hg				
K				
Mg	10-1000			100-1000
Mn	50-5000	100-1000		10-1000
Mo				
Na	1-10 %			
Ni	10-1000	100-1000		10-1000
Pb	1-10 %	100-1000	40 %	10-1000
Sb	10-1000	100-1000		
Se	1-10			
Si				
Sn				
Sr		0.01-1 %		
Ti	0.2-2 %			
V	10-100	10-100		
Zn	1-10 %		0.14 %	0.1-1 %

*Concentrations are micrograms per gram unless noted as percentage.

Table 1.5

Typical Air Quality in Some Cities of the World [18].

Place	SO ₂ (ppm)		Air Pollutant		
	Summer	Winter	NO ₂ (ppm)	Oxidant (ppm)	Suspended Particulate (μg/m ³)
London	0.087	0.177	0.029	-	221
Chicago	0.135	-	0.042	0.004	280
Cincinnati	0.029		0.030	0.014	176
SanFransisco	0.008		0.042	0.018	104
Tokyo	0.059		0.062	-	261
Bombay	0.039		0.011	0.006	238
Calcutta	0.022		0.012	0.015	527
Kanpur	0.041		0.040	0.048	488
Delhi	0.015		0.011	0.009	700

Table 1.6

Sources and Health Effects of Some Trace Elements in the Atmosphere [21].

Substance	Sources	Health effects
Lead	Auto exhaust, industry, solid waste disposal, coal combustion, paint	Brain damage, behavioral disorders, convulsions, death
Vanadium	Coal and petroleum combustion, industry	Inhibits formation of phospholipids and S-containing aminoacids
Manganese	Industry, coal combustion	Fever, pneumonia
Nickel	Coal combustion, industry	Dermatitis, dizziness, headaches, nausea, and carcinogenesis [also $\text{Ni}(\text{CO})_4$]
Cadmium	Industry	Gastrointestinal disorder, respiratory tract disturbance, carcinogenic and mutagenic
Mercury	Coal combustion, commercial, industry	Tremor, skin eruption, hallucinations
Beryllium	Coal combustion, industry	Lung damage, enlargement of lymph glands, emaciation
Selenium	Ore refining, sulfuric manufacture, coal combustion	Depression, jaundice, nose-bleed, dizziness, headaches.

effects and sources of few particulate pollutants are given. The role of trace elements in bioenvironmental systems is discussed by Morgan et al. [22] and Dulka et al. [23]. Trace elements like Cu, Zn, V, Cr, Fe, Ni, Co are essential for body functioning but excess of these seem to cause various disorders. The elements Be, Ba, Hg, Cd, Pb are known to be toxic. One way through which the trace elements enter our body is through the inhalation of air. Particles of size 0.1 μm are retained in the lungs. Recent studies have shown that many trace elements like Cr, Pb, Ni, V, and Zn exhibit increasing specific concentrations with decreasing size in particles [24]. The studies of chemical composition of aerosols and their possible health effects are assuming great importance. It has been observed that the levels of Cd and Pb in the blood for most children in the U.S.A. are very high [25,26].

1.3 Air Quality Studies

1.3.1 Air quality criteria

A few countries like Czechoslovakia, the Federal Republic of Germany, Poland, Romania, the Soviet Union and the United States of America have adopted criteria for the air quality by setting standards for a few contaminants. The standards are meant to protect the public from adverse health effects. These represent the lowest level at which available evidence suggests that an effect will be produced within a reasonable margin. In Table 1.7 National Ambient

Table 1.7

National Ambient Air Quality Standards Promulgated by EPA on April 30, 1971 [27].

Sulfur oxides :	80 $\mu\text{g}/\text{m}^3$ (0.03 ppm) as annual arithmetic mean and 365 $\mu\text{g}/\text{m}^3$ (0.14 ppm) as maximum 24-hr concentration not to be exceeded more than once a year.
Suspended particulate matter :	75 $\mu\text{g}/\text{m}^3$ as annual geometric mean and 260 $\mu\text{g}/\text{m}^3$ as maximum 24-hr concentration not to be exceeded more than once a year.
Carbon Monoxide :	10 mg/m^3 (9 ppm) and 40 mg/m^3 (35 ppm) as maximum 8-hr and 1-hr concentration respectively, not to be exceeded more than once a year.
Hydrocarbons :	160 $\mu\text{g}/\text{m}^3$ (0.24 ppm) as maximum 3-hr concentration (6 to 9 AM) not to be exceeded more than once a year.
Nitrogen oxides :	100 $\mu\text{g}/\text{m}^3$ (0.05 ppm) as annual arithmetic mean.
Photochemical oxidants :	160 $\mu\text{g}/\text{m}^3$ (0.08 ppm) as maximum 1-hr concentration not to be exceeded more than once a year.

Quality Standards in USA are given. In addition to this Environmental Protection Agency (EPA), USA, has recently announced [28] ambient air quality standard for airborne lead. The lead standard is $1.5 \mu\text{g}/\text{m}^3$ on a monthly average. The level is based on the need to protect young children (1-5 years). Threshold level values (TLV) for work-room atmosphere are different and are for 8 hr/day whereas air quality data are for 24 hr average. TLV adopted by the American Conference of Governmental Industrial Hygienists (1971) are given in Table 1.8. Standards for emission rates have also been prescribed to control the emission of pollutants.

1.3.2 Air quality monitoring

In the study of air pollution, air quality monitoring is very important and can serve many objectives, some of which are outlined below.

- i) effects of specific human activities on the environment.
- ii) survey and study of the effects of environmental changes on man's health, human activities etc.
- iii) the detection and provision of an early warning of significant changes in the environment.
- iv) the checking of the compliance with established environmental quality criteria and standards.
- v) the checking of the efficiency of control systems and corrective measures.

Table 1.8

Threshold Limit Values (TLV) for Work-Room Atmosphere.

Element	TLV μg/m ³
V	100
Cr	500
Mn	5000
Fe	10000
Ni	1000
Cu	100
Zn	5000
Pb	150

Suess [29] has summarized the efforts made at the international level to perform world-wide air quality monitoring. The United Nations Environment Programme (UNEP), with the support and co-operation from several other intergovernmental agencies has launched a programme for the development of a Global Environmental Monitoring System (GEMS). This is supplemented by the background level pollution study by World Meteorological Organisation (WMO). To start with the study is limited to two of the more ubiquitous pollutants namely suspended particulate matter and SO_2 . Apart from this most of the developed countries have national air quality monitoring network to study the problem on a national scale.

During the past few years a large amount of work has been carried out to assess the atmospheric pollution due to trace elements in different kinds of atmosphere viz. i) heavily polluted [30], ii) desert [31], iii) non-urban [32] and iv) marine [33] etc. In addition to this, specific air pollution studies have been carried out by studying air-particulate matter near an urban road [34], near a lead smelting complex [35] etc. The levels of heavy metals measured in these studies serve as an index of the extent of pollution. The behaviour of trace metals in the atmosphere depends on their chemical nature and also on their size distribution. These two characteristics are mostly dependent on the sources and the ambient atmospheric conditions. The study of elemental constituents as a function

of particle size is made to understand their effects on health and on atmospheric properties and also to identify their sources and sinks [36,37]. Another widely used method of examining the relative importance of sources on the measured trace element concentrations, is to compare the relative abundance of elements in source material to that found in the atmosphere. The enrichment factor is calculated by obtaining the ratio of the concentration of an element in air particulate matter normalized to a reference element, to the soil concentration of the element normalized to the same reference element. Ragaini et al. [35] have applied this method to study the trace element contamination near a lead smelting complex in Kellog, Idaho, U.S.A. Moyers et al. [31] calculated linear correlation coefficients for all possible element pairs to see the interrelations that exist among various elements in the atmosphere of the Southwest desert near Tucson, Arizona, U.S.A. Highly correlated species may come from the same primary source or secondary transformation process or the correlation may indicate that the species are carried together in the same air mass. Identification of air pollution sources is usually done either by the method of chemical element mass balances [38] or by statistical methods like factor analysis [39]. Application of the method of chemical element mass balance needs the knowledge of elemental emissions from various sources. Factor analysis is a statistical method to obtain information about the

sources of pollution. It differentiates the separate patterns of relationships in the matrix of correlation coefficients by factoring the matrix into its basic dimensions. Factor analysis condenses large sets of data into uncorrelated sets of factors which correspond to various sources of pollution.

1.4 Air Pollution Studies in India

India is a leading developing country. It has many big industrial cities and the growth of industry is generally unplanned from environmental point of view. Because of the socioeconomic problems of a developing country, controlling air pollution in India is a very difficult task. Data on air quality monitoring is scanty. However, a few groups have been working to assess the present air pollution situation in the main cities of the country. The results obtained by Yennawar et al. [40] in the air quality survey of four major cities of India are given in Table 1.5. High values of TSP in all the four cities is a striking feature. A short term air quality study at Kanpur was done by Sharma et al. [41] in 1973. Their results of TSP are in agreement with those reported in Table 1.5. Despite its effect on visibility, human health and soil material very little has been done to determine the chemical composition of the particulate matter. Recently trace element analysis for Pb, Cd, Zn, Cu and Fe in the particulate matter of Greater Bombay is done by Khandekar et al. [36].

The elemental levels obtained for toxic elements like Cu, Zn, Pb, Cd are comparable to those obtained in highly polluted cities. Some trace element studies have been made near the west coast of India and over the sea [42,43]. Industry related environmental pollution studies have been carried out for Kanpur City [44]. SO₂ pollution in Bombay and its effects on people is studied by Zutshi et al. [45] and Deoras [46].

1.5 Motivation Behind the Present Work

In view of the very high level of TSP values in India it was felt that a trace elemental analysis of air particulate matter may throw some light on the origin of this large amount of suspended dust in the atmosphere. According to the air quality criteria set by different countries the values obtained in our country are very high. The reasons could be many, as for example 'i) natural dust emissions may be high due to the climatic conditions characteristic of tropical countries, ii) the old and outdated mode of industrial production followed by most of the factories, iii) the diverse means of transportation (i.e. diesel trucks to bullock cart) on dusty roads may be releasing large amount of dust into the atmosphere.

Kanpur has all the above-mentioned characteristics compounded in a worst fashion. Among the industrial cities in India it is an old industrial city. Though it is the eighth populous city, its air quality is as poor as

that of the other three cities (Bombay, Calcutta, Delhi, Table 1.5). One of the reasons that can be attributed to this observation is the concentration of a large number of industries in a relatively small area with high population density. The climatic conditions like dry hot summers with frequent duststorms and cold winters where temperature inversions are common, aid in increasing the level of pollution. All these factors make the study of air pollution in Kanpur city very significant.

A study of air particulate matter for trace elements in Kanpur city was planned to investigate the possible reasons for the high value of TSP and also to study the extent of pollution in an industrial city of India. A suitable analytical technique described in Chapter 2 was standardized for elemental analysis. The standardization procedure is described in Chapter 3. Details of the air quality monitoring for TSP in Kanpur city will be discussed in Chapter 4.

A zone-wise analysis of the data for TSP and various heavy/toxic elements (K, Ca, Ti, V, Cr, Mn, Fe, Cu, Ni, Zn Ba and Pb) is carried out to point out the polluted zones and the level of pollution and to suggest some correlations. Enrichment factors are calculated for various elements to investigate the nature of sources. Further analysis of the trace element data to obtain information regarding their sources is done by statistical methods.

It is felt that the present study will help in understanding the nature of TSP in India and may be of use in setting air quality criteria for TSP. On the local level it points out the polluted regions in the city which need greater attention. The present work can lead to the studies of health effects of these pollutants.

REFERENCES

1. E.T. Wilkins, Quart. Jour. Roy. Met. Soc., 80, 267 (1954).
2. H.H. Schrenk et al. Air Pollution in Donora, Public Health Service Bulletin No. 306 (1949).
3. J. Mage and G. Batta, Chim. and Ind. (Paris), 27, 961 (1932).
4. C.A. Bishop, Chem. Eng. Progr., 53, 146 (1957).
5. C.E. Junge, Air Chemistry and Radioactivity, Academic Press, New York (1963).
6. Indian J. Environ. Health, 13, 245 (1971).
7. National Inventory of Air Pollutant Emission, NAPCA Publication No. AP-73, (1968).
8. E. Robinson and R.C. Robbins, J. Air Pollut. Control Assoc., 20, 233 (1970).
9. K.S. Rao, R.S. Soin and T. Shivaji Rao, Chem. Age of India, 30, 903 (1979).
10. J.W. Swinnerton, V.J. Linnenbom and R.A. Lamontagne, Science, 167, 984 (1970).
11. B. Weinstock, Science, 166, 224 (1969).
12. Air Quality Criteria for Carbon Monoxide, NAPCA Publication No. AP-62, (1970).
13. R.E. Inman, Science, 172, 1229 (1971).
14. E. Robinson and R.C. Robbins, J. Air Pollut. Control Assoc., 20, 303 (1970).
15. Air Quality Criteria for Nitrogen Oxides, U.S. Environ. Prot. Agency Publication No. AP-84 (1971).
16. S.S. Butcher and R.J. Charlson, An Introduction to Air Chemistry, Academic Press, New York (1972).
17. W. Strauss, ed. Air Pollution Control Part III, John Wiley and Sons (1978), p. 221 and references therein.
18. K.V. Ramchandran, Proc. Symp. on Environ. Pollut., held at Nagpur, 17-19 January (1973), p. 267.

19. F.W. Lipfert, *J. Air Pollut. Control Assoc.*, 30, 366 (1980).
20. Air Pollution Emission Factors, U.S. Environ. Prot. Agency Publication No. AP-42, (1973).
21. G.L. Waldbott, Health Effects of Environmental Pollutants, Mosby, St. Louis, Missouri (1973).
22. G.B. Morgan and E.W. Bretthauer, *Anal. Chem.*, 49, 1210A (1977).
23. J.J. Dulka and T.H. Risby, *Anal. Chem.*, 48, 640A (1976).
24. D.F.S. Natshu, J.R. Wallace and C.A. Evans, Jr., *Science*, 183, 202 (1974).
25. C.J. Cohen, G.N. Bowers and M.L. Lepon, Jr., *Ame. Med. Assn.*, 226, 1430 (1973).
26. H.A. Waldran, *Nature*, 253, 345 (1975).
27. S.S. Miller, *Environ. Sci. Technol.*, 5, 503 (1971).
28. News Focus, *J. Air Pollut. Control Assoc.*, 28, 162 (1978).
29. M.J. Suess, *Atmos. Environ.*, 13, 211 (1979).
30. C. McDonald and H.J. Duncan, *Atmos. Environ.*, 13, 413 (1979).
31. J.L. Moyers, L.E. Ranweiler, S.B. Hopf and N.E. Korte, *Environ. Sci. Technol.*, 11, 789 (1977).
32. T.B. Johansson, R.E. Van Grieken and J.W. Winchester, *J. Geophys. Res.*, 80, 1039 (1976).
33. J.W. Winchester, *Nucl. Instrum. Methods*, 142, 85 (1977).
34. G. Desaedeleer, J.W. Winchester, J.O. Pilotte, J.W. Nelson and H.A. Moffitt, PIXE Analysis of Roadway Aerosol, IAEA-SM 206/18, (1976).
35. R.C. Ragaini, H.R. Ralston and N. Roberts, *Environ. Sci. Technol.*, 11, 773 (1977).
36. R.N. Khandekar, D.N. Kelkar and K.G. Vohra, *Atmos. Environ.*, 14, 457 (1980).
37. K.A. Hardy, R. Akselsson, J.W. Nelson and J.W. Winchester, *Environ. Sci. Technol.*, 10, 176 (1976).
38. S.K. Friedlander, *Environ. Sci. Technol.*, 7, 235 (1973).

39. P.K. Hopke, E.S. Gladney, G.E. Gordon, W.H. Zoller and A.J. Jones, *Atmos. Environ.*, 10, 1015 (1976).
40. P.K. Yennawar, S.N. Dixit, V.L. Pampattiwar, J.M. Dave and S.J. Arceivala, *Environ. Health*, 12, 355 (1970).
41. V.P. Sharma, H.C. Arora, S.N. Chattopadhyaya and Tapan Routh, *Indian J. Environ. Health*, 15, 133 (1973).
42. S. Sadasivan, *Atmos. Environ.*, 12, 1677 (1978).
43. S. Sadasivan, *Atmos. Environ.*, 14, 33 (1980).
44. V.K. Kumar and Rahul Singh, *Chem. Age India*, 31, 1143 (1980).
45. P.K. Zutshi, T.N. Mahadevan, M. Vidynathan and A.P. Sathe, *Chem. Age India*, 28, 637 (1977).
46. P.J. Deoras, *Chem. Age India*, 28, 648 (1977).

Chapter 2

TECHNIQUES FOR ELEMENTAL ANALYSIS OF AIR PARTICULATE MATTER

2.1 Introduction

Experimental studies of the chemical composition of air particulate matter have shown that the concentrations of many elements are found to be above the background level in the local [1,2] as well as the global [3,4] atmosphere. An estimation of levels of various elements is necessary to determine their toxic nature [5] and it also helps in studying the effect of trace elements in chemical reactions that take place in the atmosphere [6,7]. Dulka et al. [8] have discussed in detail the role of trace elements in some environmental and biological systems.

In general, the concentrations of different elements are measured in $\mu\text{g}/\text{m}^3$ or $\mu\text{g}/\text{gm}$ and sometimes they are determined as a function of the particle size of air particulate matter. These measurements help in establishing air quality, source emission rates, amounts of trace elements that can be inhaled or are available for interaction with other atmospheric constituents.

A number of chemical and instrumental analytical techniques are used to determine elemental concentrations of air particulate matter [9]. The choice of an analytical method depends on various factors like : (i) elements of interest, (ii) the nature and chemical composition of the

sample, (iii) amount of sample available, (iv) complex nature of matrix effects and (v) precision and accuracy required in the final analysis. Sometimes considerations like availability of the instruments, speed of analysis and cost of analysis play an important role in choosing a particular method. These aspects of different spectroscopic methods are compared by Winefordner [10].

Generally, air particulate matter collected on a filter paper is used to estimate the levels of various elements in air. Concentrations of the interesting elements found in the atmosphere are very small (i.e. in the nanogram to microgram range). Hence the analytical method should have a good detection limit and high accuracy for different elements of interest. It is also necessary to analyze a large number of air particulate samples for different elements. Therefore a fast analytical technique, capable of simultaneous quantitative determination of many elements is desirable. A non-destructive method, which uses air particulate sample without any pretreatment is generally preferred. In this case, inaccuracy due to sample preparation is avoided and also the samples can be kept for further analysis.

Dulka et al. [8] give a list of analytical techniques suitable for trace analysis. Current developments in elemental analysis of air particulate matter using different methods are summarized by Fox et al. [11]. Some of the more frequently used techniques in the elemental analysis of

air particulate matter, are : (i) Neutron Activation Analysis, (ii) Atomic Absorption Spectrometry, (iii) Atomic Emission Spectroscopy, (iv) X-ray Spectrometry and (v) Solid Source Mass Spectrometry. In the following we shall describe the basic principles of each of these methods.

2.2 Neutron Activation Analysis

2.2.1 Description of the method

Neutron activation analysis can be carried out either by chemical separation method or by energy dispersive gamma-ray spectrometer. The latter method is known as instrumental neutron activation analysis (INAA) and it is preferred to the chemical separation method for multielemental analysis of environmental samples [12,13].

In the INAA method the sample is bombarded with thermal neutrons from a nuclear reactor. These neutrons interact with the nuclei of various elements mainly through (n,γ) reaction and as a result of this reaction radioactive isotopes with one higher mass number are formed. Most of these radioactive isotopes decay by emitting gamma rays whose energy is characteristic of the decaying nucleus.

The energy spectrum of an irradiated sample is recorded with the help of a high-resolution Ge(Li) detector and a multichannel analyzer. Various radionuclides are identified by the energies of their gamma rays. Matrix effects are negligible in the case of INAA due to high penetrating power

of neutrons and gamma rays. Hence the relation between the gamma-ray intensity and the concentration of an element is linear. Normally a calibration curve, which relates intensity of the gamma ray to the concentration of an element is established by recording a gamma ray spectrum of a standard solution. The standard solution contains known amounts of all analyzable elements and is irradiated along with the given sample [14]. Concentration of an element in the sample is estimated by comparing the intensities of the gamma rays from the element in the sample and in the standard solution.

Analysis of air-particulate samples by the INAA method is usually carried out as follows. Air-particulate samples collected on different kinds of filters are cut and sealed in clean polyethylene vials. Several vials containing different air-particulate samples and a standard sample are simultaneously irradiated by thermal neutron flux in the range of 10^{12} to 10^{13} neutrons/sec/cm² [15]. Usually two separate irradiations, each lasting for different time periods are carried out so that the spectral interference between long- and short-lived isotopes are minimised. The entire irradiation and counting scheme normally followed in the analysis of air-particulate matter is shown in Fig. 2.1. The radioactive isotopes used for gamma ray detection at each counting stage are also shown in Fig. 2.1. The major interference in the gamma-ray spectrum of air-particulate samples arises from the following : (i) large concentration

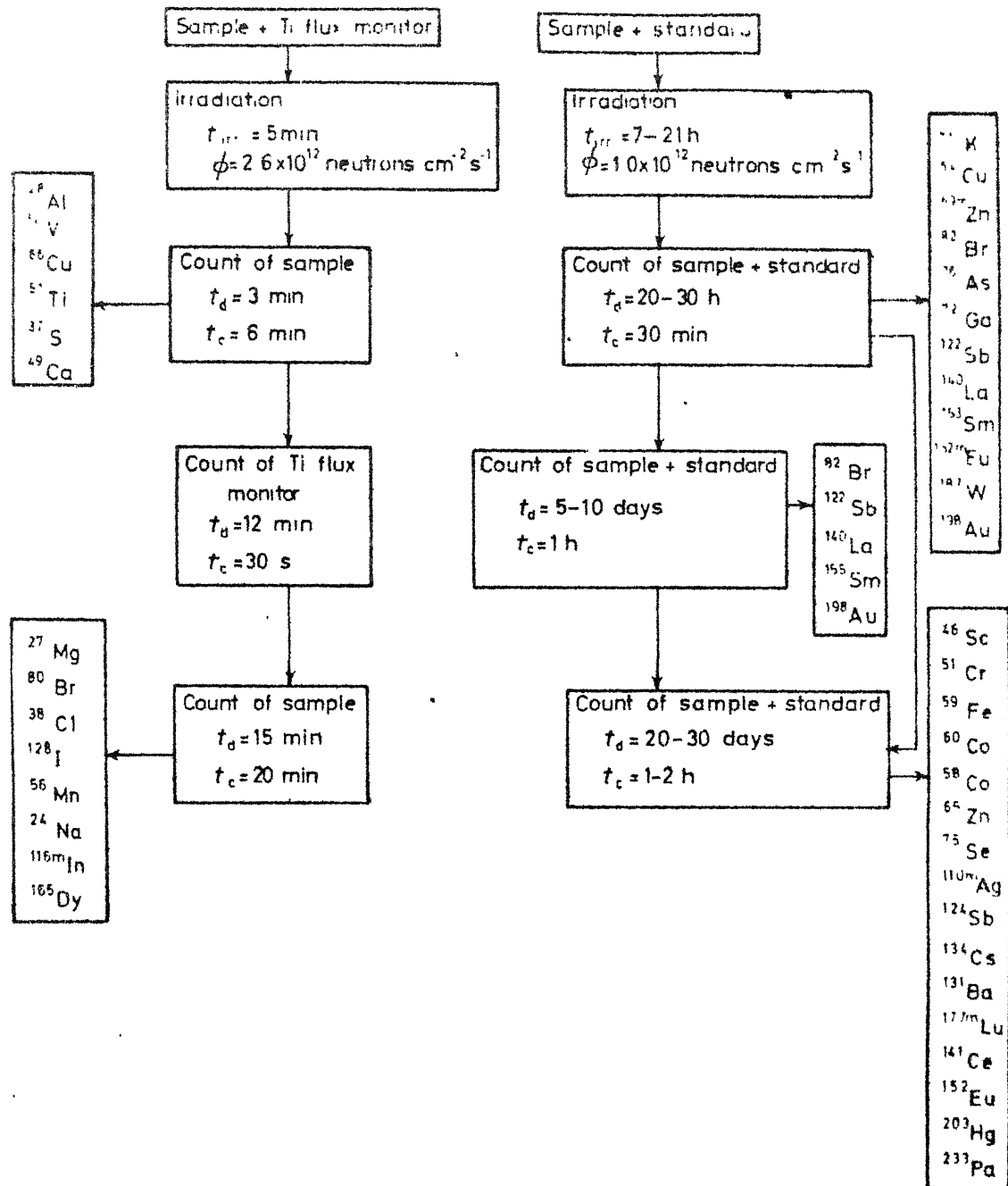


Fig. 2.1 Irradiation and counting scheme for the analysis of air particulates collected on filter paper. ϕ = thermal neutron flux; t_{irr} = irradiation time; t_d = time between end of irradiation and start of counting; t_c = counting time [12].

of Na in marine aerosol gives rise to the troublesome ^{24}Na ($T_{1/2} = 15$ hrs.) activities (ii) in urban aerosols, the ^{82}Br ($T_{1/2} = 36$ hrs.) activity is predominant from 1 to 7 days after the end of irradiation.

2.2.2 Sensitivity, detection limit, precision and accuracy

Radioactive counting techniques are highly sensitive. Hence in the INAA method it is possible to attain very low detection limits for a large number of elements. Detection limits for various elements depend on the following : (i) the size and composition of the sample (ii) the experimental conditions like neutron flux, irradiation and counting scheme used. When these conditions are defined in an experiment, the inherent limitation on detection limit comes from the neutron capture cross-section of the isotope being activated, its radioactive half-life ($T_{1/2}$) and its fractional abundance. These quantities vary within large limits from element to element and the detection limit is not uniform for all the elements. Some elements, for example sulfur, can be determined by the INAA method only when they are present in high concentrations. Several elements like Be, Cd, Pb, do not emit gamma rays under normal conditions of thermal neutron activation and such elements cannot be determined by INAA. Detection limits for various elements by the INAA technique are shown in Table 2.3, which also provides a comparison of the detection limits reached by different techniques and

will be described later. The INAA detection limits are obtained with samples collected on polystyrene filters. Approximately 5-80 m^3 of air was passed through the filters. Neutron flux of 10^{12} to 10^{13} n/sec/cm^2 was used for irradiation and a 30 cm^3 Ge(Li) detector was used for counting [12].

Accuracy of an analytical technique ultimately depends on the systematic errors involved at each step in the method of analysis. The main errors in INAA are due to flux inhomogeneity, error in irradiation time, uncertainty in the value of flux etc. In general an accuracy and precision of about 10 % can be achieved [16].

The INAA method, is probably the best available technique for the precise determination of a large number of elements in airborne particulate samples. The high sensitivity of the technique makes it especially useful for analyzing small amounts of material, such as obtained from the individual stages of low volume cascade impactors. Since the method is nondestructive the samples can also be kept for further analysis.

Some of the major drawbacks of the method are : (i) the results for the most important elements become available only after long irradiation, cooling and counting times, (ii) cost per sample is high and some key elements such as Pb and Be cannot be easily determined. The scarcity of neutron irradiation facilities is another obstacle in using the INAA method for routine analysis.

The INAA method is extremely valuable for checking results obtained by other techniques. Because of the large number of elements it can analyze, activation analysis is ideally suited for area-wide studies, individual source studies and chemical fingerprinting. Its ability to determine isotopes precisely makes it potentially useful for isotope tracing studies.

2.3 Atomic Absorption Spectrometry

2.3.1 Description of the method

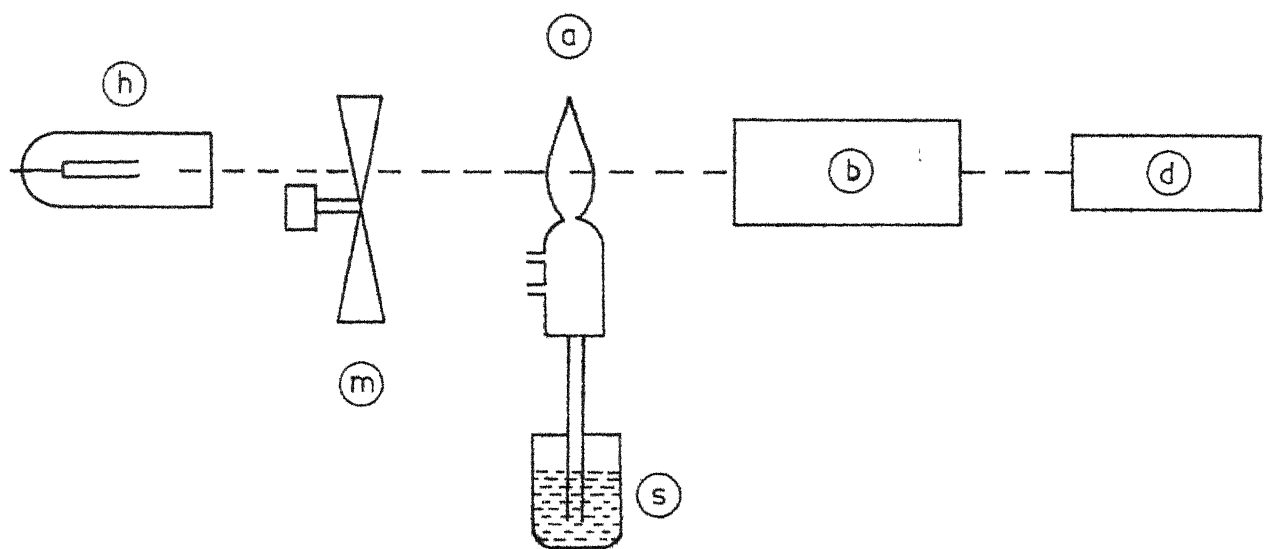
Atomic absorption spectrometry (AAS) is a simple, cheap, widely available and rapid technique. Hence it is extensively used in elemental analysis of airborne particulates [17,18]. A radiation of frequency ν and intensity I_0 is passed through an absorption cell containing atomic vapor of the sample atom capable of emitting radiation of frequency ν . Upon absorption the incident beam intensity is attenuated according to Beer's law. Absorption occurs only in the direction of incident radiation. The resulting emission does not compensate this absorption because it is omnidirectional. The absorption, is measured as absorbance A and is given by

$$A = \log (I_0/I) \quad (2.1)$$

where I_0 and I are the intensities of incident and outgoing radiation respectively. Measurement of absorbance helps in estimating the concentration of elements in the

atomic vapor.

Basically atomic absorption spectrometers consist of a source, some means of atomization, a monochromator, a detector and a mechanical chopper for modulating the source. A schematic diagram of an atomic absorption spectrometer is shown in Fig. 2.2. The light source is a hollow cathode lamp, the cathode of which is made of the element to be determined. The sample to be measured is generally atomized in a flame supported by a fuel-oxidant mixture such as hydrogen and air, or hydrogen and oxygen or acetylene and nitrous oxide or some other suitable mixture. Normally the flame is extended along the axis of the light beam to provide a long absorption path. Samples in solution form are aspirated into the flame, where evaporation of the solvent and the analyte occur. Since a high steady state concentration of ground state atoms is desirable, flame temperatures must be sufficient to achieve atom production. However it should not be so hot that extensive thermal excitation is caused to electronic energy levels above the ground state. To improve the detection limits for various elements other flameless methods of atomization like electrically heating the sample in a graphite tube or heating the sample in tantalum boat are used. Radiation from the source traverses the atomic population representing the sample and enters the entrance slit of a monochromator which separates the desired resonance line from the other lines that may be



(h) Hollow cathode lamp

(m) Modulator

(a) Atomiser

(b) Monochromator

(s) Sample

(d) Detector

Fig. 2.2. Schematic diagram of atomic absorption spectrometer.

present. The net radiation intensity is measured by a conventional photomultiplier tube and amplifier. Quantitative determination of the concentration of elements is done using appropriate calibration curves.

The AAS method can analyze only one element at a time hence a large amount of air particulate matter is needed to analyze many elements. Normally, about 2000 m^3 of air is sucked to collect enough sample for analysis. As the sample is needed in solution form, filters along with the sample are subjected to acid digestion. A typical sample preparation scheme is given in Fig. 2.3. This scheme allows a determination of 22 elements in airborne particulate matter. Begnoche et al. [18] have described a method to determine metals in atmospheric particulates using flameless atomic absorption spectrometry.

2.3.2 Interferences, accuracy and detection limit

Chemical interferences like formation of alkaline earth phosphates and lead silicate can occur for many elements and can result in reduction of the free atom population available for absorption of radiation. Spectral interferences can be due to reduction of transmitted radiation both by scattering from particles present in the atom reservoir and by molecular absorption at the analytical wavelength. Occasionally more than one element has an absorption line at the same wavelength.

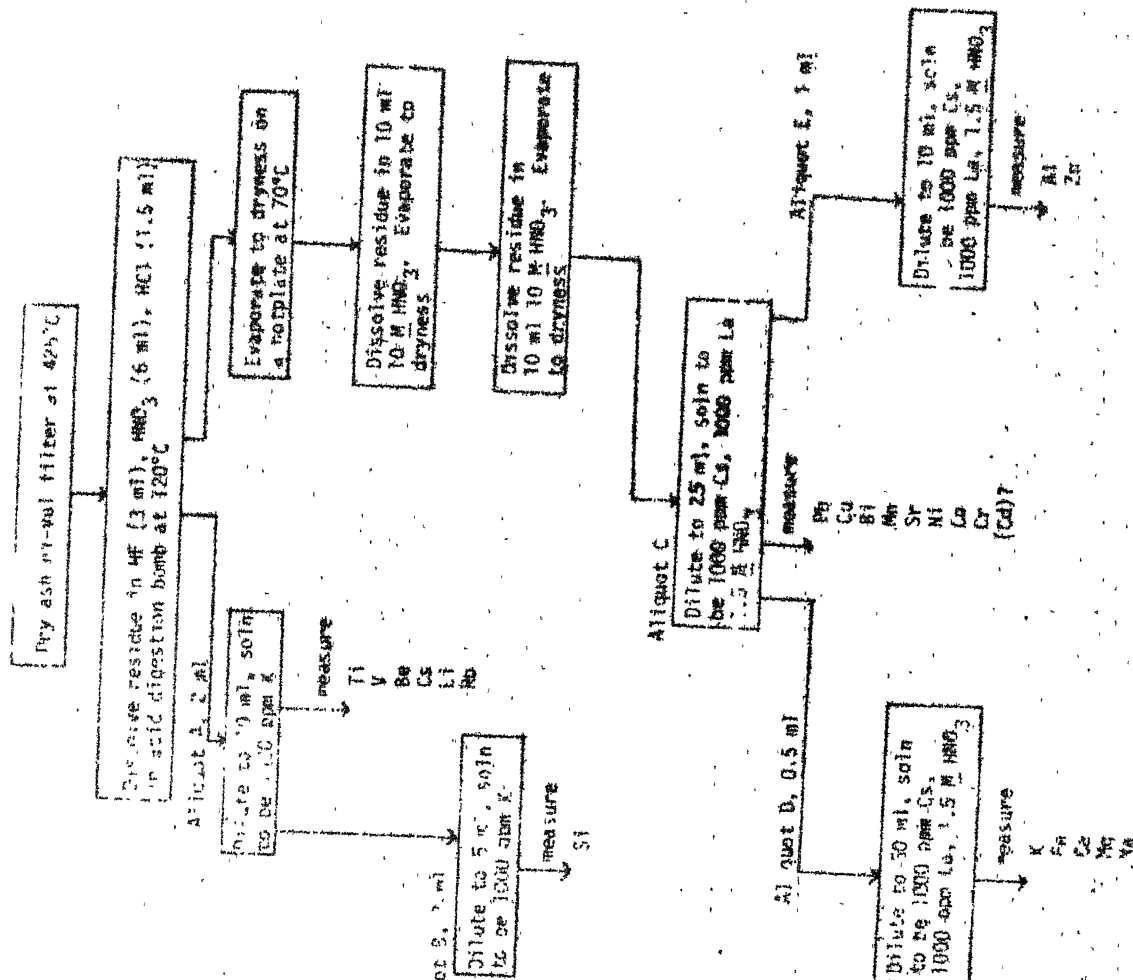


Figure 2.3 Flow chart for the atomic absorption analysis of atmospheric particulate samples collected on polystyrene filters

The precision attainable with conventional flame atomic absorption spectrometry is 1 to 5 % but is only 5 to 15 % when a graphite furnace is used. Accuracies of the order of 5 % can be obtained using flame instruments [19]. Typical detection limits for various elements in air particulate samples using flame and flameless atomic absorption spectrometer are given in Table 2.3. Detection limits for flame AAS were obtained by passing 2000 m³ of air through polystyrene filters. Samples were solubalized by a combination of dry and wet ashing [17]. Flameless AAS detection limits were obtained from absolute detection limits by assuming 2000 m³ of sample volume [39].

Simplicity, easy availability, accuracy and speed are the main advantages of AAS. But it suffers from serious disadvantages like : (i) it is a destructive method, i.e. sample has to be destroyed; (ii) simultaneous multielement analysis is very difficult; (iii) large amount of sample is needed if many elements are to be determined; (iv) impurities in the blank may cause serious problems; (v) during acid digestion volatile elements like Hg, As, Cd are lost and hence it is difficult to estimate the concentration of these elements by AAS. Hence this method is not suitable for low volume samples and particle size distribution of trace elements.

2.4 Atomic Emission Spectroscopy

In Atomic emission spectroscopy (AES), the sample to be analyzed can be in the form of a solid or a solution. The sample is first subjected to a high temperature generated by an electrical discharge, a flame or a sustained plasma and various elements in the sample are vaporized and dissociated into atoms, which are then thermally excited to higher energy levels. These excited atoms emit radiations while returning to the ground state. The wavelength of emission lines is characteristic of the emitting atom and the intensity is proportional to the number of emitting atoms of each type. Emitted radiation can be isolated with a conventional monochromator and detected by a photomultiplier or dispersed across a photographic plate.

Air particulate matter collected on filter paper cannot be analyzed directly by AES utilizing an electrical discharge. Direct analysis is possible if the particles or vapors are collected in the graphite cup electrode. Seeley et al. [20] have developed this method fully. Quantification using this method is difficult and time-consuming and the detection limits are often not sufficient for several elements of interest in airborne particles. Detection limits are improved by using various types of plasma sources. The source most fully developed for analytical purposes is the inductively coupled radiofrequency plasma (ICP). In

this case sample to be analyzed should be in the form of a solution. At present ICP-AES is potentially a very attractive technique for the multielement analysis of airborne particles. Detailed description of this method is given by Barnes[21]. Spectral line and background interferences are generally very large in this method. Precision and accuracy of about 10 % is possible after careful quantitative analysis.

Typical detection limits for various elements in airborne particulate matter is given in Table 2.3. These detection limits are adopted from solution values ($\mu\text{g/ml}$) by assuming a 10 m^3 sample volume [38].

2.5 X-Ray Spectrometry

2.5.1 Principle

The three main components of a X-ray spectrometer are (i) an excitation source (ii) a sample to be analyzed and (iii) a X-ray detection system. In X-Ray spectrometry (XRS) sample can be excited by any form of radiation capable of producing vacancies in the inner electron shells of the atoms in the sample. These vacancies are filled by transitions of electrons from outer atomic orbitals with simultaneous emission of X-rays whose energies are characteristic of the elements in the sample. Measurements of energies of these X-rays for the identification of the elements and the determination of their intensities to estimate the concentration of various elements is the basic problem of X-ray

spectrometry. A simplified version of some of the basic atomic processes occurring in X-ray fluorescence method is shown in Fig. 2.4. A number of X-ray spectrometric techniques, based on the different modes of excitation and detection exist. A flow diagram of various X-ray spectrometric techniques is shown in Fig. 2.5.

2.5.2 Modes of X-ray detection

Two types of X-ray detection systems are employed in X-ray spectrometry viz. wavelength dispersive detection and energy dispersive detection [22].

In wavelength dispersive detection the emitted X-rays are collimated and diffracted by an analyzing crystal. Here the angle of diffraction is related to the wavelength according to Bragg's law and X-rays having different wavelengths are diffracted at different angles. A Geiger counter or NaI(Tl) scintillator or proportional counter is used to register the X-rays after diffraction.

Wavelength dispersive detection systems exhibit excellent energy resolution (~ 0.5 eV) so that spectral interferences due to overlap (from other wavelengths) are not there. Occasionally interference due to second and higher order lines occurs with the line of interest. The transmission efficiency of wavelength dispersive spectrometers is low, and the wavelength analysis requires a point-by-point scan over lengthy counting periods at each wavelength of interest. Because of these limitations this method

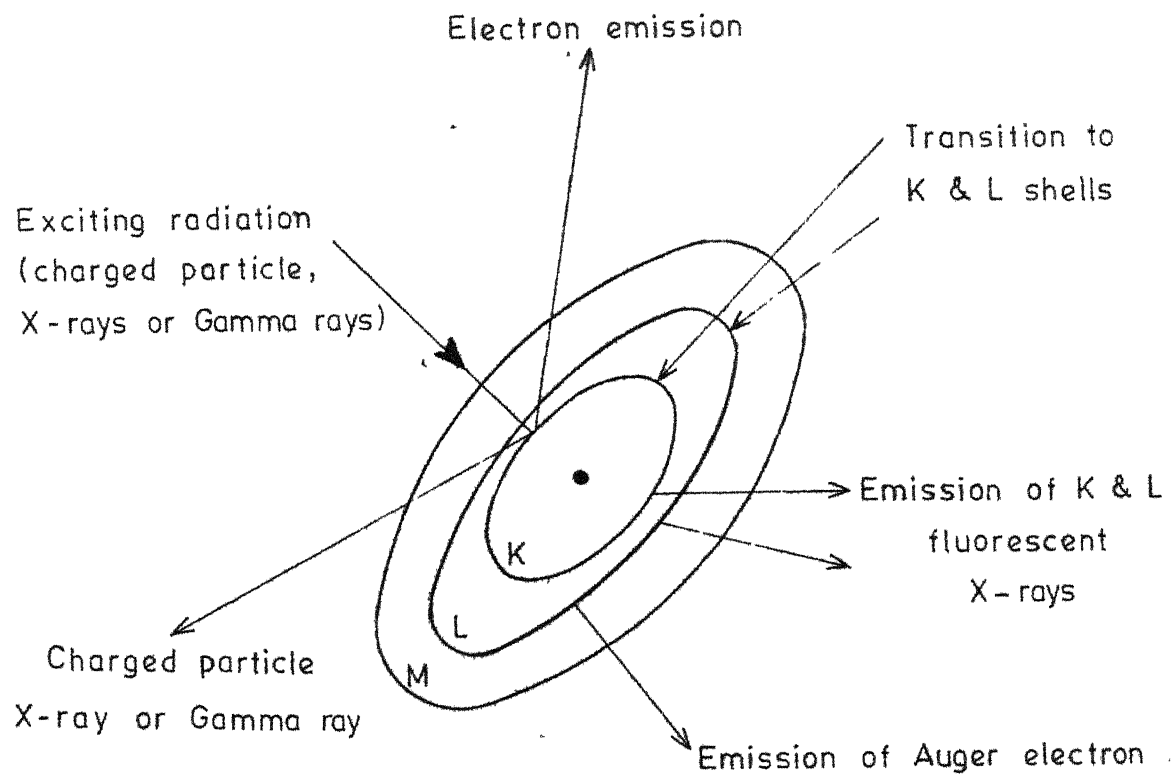


Fig. 2.4. Some of the basic atomic processes in X-ray fluorescence analysis.

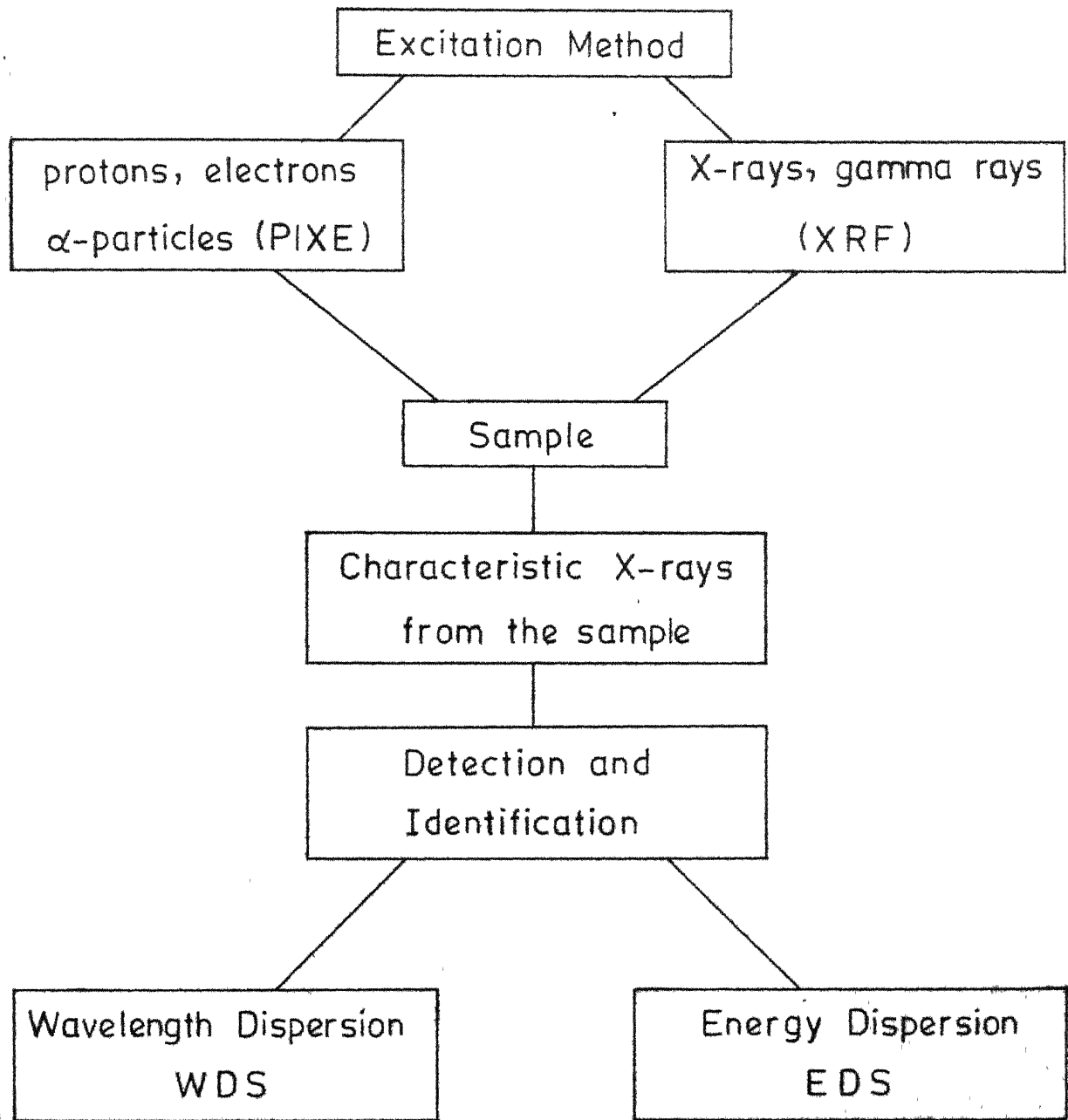


Fig. 2.5. Flow diagram of various X-ray spectrometric techniques

is not suitable for multielemental analysis and is generally not used in air pollution work.

The energy dispersive detection system employs a lithium-drifted silicon detector (Si(Li)) in conjunction with an amplifier and a multichannel analyzer. All X-rays entering this detector are sorted according to their energies and stored as digital signals in different channels of the multichannel analyzer. Consequently a complete X-ray spectrum of the elements in the sample is recorded simultaneously.

The energy resolution normally achieved is about 180-200 eV and it is inferior to wavelength dispersive systems, so spectral interferences due to overlap are common. This mode of detection is widely used in air pollution work [23,24] because of its capacity to quantitatively determine many elements simultaneously.

2.5.3 Modes of excitation

The different types of exciting radiation used in energy dispersive X-ray spectrometry are (i) charged particles such as electrons, protons or α -particles, (ii) photons from monochromatic or polychromatic X-rays and (iii) gamma rays from radioactive isotopes.

Excitation of X-ray emission by charged particle bombardment primarily involves the use of electrons and protons. Major advantage of electron excitation is in its ability to analyze light elements like Na, Mg, Al etc. where all other techniques fail. It suffers from poor detection

limits for other elements because of large bremsstrahlung background caused by deceleration of exciting electrons in the sample. Hence it is rarely used in the analysis of airborne particles [22].

Proton induced X-ray emission (PIXE) has been used extensively in trace element analysis of a variety of samples [24,25]. Folkman et al. [26] have shown that proton beams with energies near 3 MeV and α -particles of 16 MeV are about the best choice for optimum sensitivity in most analytical applications. The bremsstrahlung background due to protons is much less than that of electrons and below 12 keV the bremsstrahlung due to secondary electrons in the sample is the dominant source of background for 3 MeV protons. Good detection limits [24] have been demonstrated for the analysis of airborne particles. A significant disadvantage is that such experiments are limited to laboratories where a Van de Graaff accelerator is available.

Photon induced X-ray emission is known as XRF or X-ray fluorescence and we shall adopt the same abbreviation. Excitation of X-ray emission by photons requires that the exciting radiation should possess energy greater than that of the K or L absorption edge, which increases approximately linearly with atomic number Z. The efficiency of excitation and hence the sensitivity of detection falls off steeply as the energy of the exciting radiation increases above this absorption edge [27]. Consequently maximum sensitivity is

achieved for a given element when the exciting radiation has an energy just above that of the absorption edge.

The methods of photon excitation include X-rays from X-ray tubes and X-rays and gamma rays from radioactive sources in direct or secondary fluorescence configuration. In direct configuration monochromatic X-rays from the X-ray tubes or X-rays and gamma rays from the radioisotopes are used directly to excite the sample. In secondary fluorescence system, X-rays are first excited from a suitable target and these X-rays are used to excite the sample. X-ray tubes with 3 to 4 kW power are commonly used with W or Mo or Cu as anode material. Gamma rays used for irradiation of samples are derived from a radioactive isotope whose choice and strength is limited by safety and half-life considerations. The most useful radioactive isotopes used in XRF analysis are given in Table 2.1. Radioactive sources are used mainly because of their low cost and simplicity of operation. Annular sources are generally used because of the large solid angle subtended by the source in such geometries. In our work we have used a radioactive ^{241}Am source as a source of excitation and these details will be described in Section 3.2. Recently a polarized X-ray beam derived from synchrotron radiation has been used [28] and this offers the advantage of reduction in the background. Calibration of X-ray spectrometers is done by various methods depending on the nature of the sample and the method of excitation and detection of X-rays [29].

The method of calibration used in the present work for the analysis of air particulate matter is discussed in Chapter 3.

X-ray spectrometry has the major advantage that air-borne particles can be analyzed nondestructively from a surface (e.g. filter paper) on which sample is collected. It can determine all elements with $Z \geq 11$ with fairly uniform sensitivity and detection limit. It is capable of high precision (~ 2 to 5 %) and reproducibility in the analysis of air-borne particles. Accuracy of the method depends on the calibration method used and is generally about 10 %. In Table 2.2 we give typical elemental detection limits for different elements for several X-ray spectrometric techniques. Typical elemental detection limits for different elements in air-particulate samples are given in Table 2.3. These are obtained by passing 2.25 m^3 of air through 3 cm^2 of Gelman filter. Counting time is approximately 1000 sec. [23].

Comparison of various modes of excitation and detection has been studied [30-32] and there is a general agreement that as far as detection limit and sensitivity are concerned both XRF and PIXE are equally good. XRF is preferred over PIXE for routine analysis of air particulate matter collected on filter paper because of ease of operation and maintenance of XRF system. Again the errors arising from the microinhomogeneities are smaller [33,34] in the XRF method.

70491

Elemental Detection Limits (ng/m³) for Different X-ray Spectrometric Methods

Detection	Excitation	Elements						Zn	Eb
		Al	S	Si	Ca	V	Fe		
Wavelength dispersion	X-Ray Tube Cr	110	15	0.9	3.1	17	47	51	55
	Rh	26	4		9.1	1	9.5	15	16
	W		16		9	11		13	83
Energy dispersion	X-Ray Tube Mo				110	50	38	38	35
					10	11	12	52	60
Secondary fluorescer									
Isotope	In				18	16			
	Cu				220	22	14		
	Ag				97	120		57	60
Particle	55 Fe (7 mCi)				35	57			
	109 Cd (70 mCi)				1900	680	680	440	224
Proton		0.01	0.1	0.01	0.01	0.01	0.01	0.02	0.1

2.6 Solid Source Mass Spectrometry (SSMS) and other methods

In conventional SSMS the sample is presented in the form of two identical electrodes between which a high voltage radiofrequency spark discharge is established. Ions characteristic of the electrode material are sputtered from the electrode surface and are accelerated into a double-focussing mass spectrometer for mass analysis. Photographic detection is usually preferred for multielemental analysis because it averages out fluctuations in the electrical discharge and records all ions passing through the spectrometer.

Airborne particles can be analyzed directly as solids after ashing or in solution. Solids are homogeneously mixed with spectroscopic graphite or silver powder and pressed into an electrode. Samples in the form of solutions are evaporated to dryness. SSMS is free of chemical interference but there can be severe spectral interferences resulting from the formation of multiply charged ions whose mass to charge ratio is close to that of a single charged species of interest. The precision and accuracy attainable depend very much on the way an analysis is performed. The most common procedure is to obtain a quantitative estimate of one element by another technique and to assume that spectral intensities are proportional to the amount of each element present. Such a method, involving an internal standard, provides analysis that is usually accurate to within a factor of 3 when account is taken of the abundances

of each isotope of an element. More precise calibration with precision in the range of 10 to 20 % is possible by establishing sensitivity factors for each element of interest by standard addition [32]. It is a time-consuming method and requires that at least one element be determined precisely in each sample. Excellent precision can be obtained by using the method of isotope dilution which involves standard addition of one or more isotopes of each element being calibrated [36]. This procedure is also very time-consuming.

SSMS is best suited for semiquantitative analysis. It also offers similar sensitivity for all the elements determined. The main disadvantages of the technique are the high cost of the instrumentation and the long time required to extract numerical data from photographic plates. In Table 2.3 we have given detection limits for various elements using SSMS. These are detection limits adopted by assuming 10 m^3 of sampling volume [38].

Apart from the spectroscopic methods a variety of electrochemical methods have been used for determining several elements present in airborne particles. These are potentiometry using ion selective electrodes, polarography and stripping voltammetry in their dc pulse and differential pulse modes [37]. All these methods require sample in solution form, and are easy to calibrate. These methods are rarely used in routine air pollution studies because of the elaborate sample preparation methods.

2.7 Remarks

In Table 2.3 we have summarized the typical detection limits for various elements using different techniques. Some of the other characteristics of various techniques are given in Table 2.4. Of the four multielemental techniques only two are capable of non-destructive analysis viz. INAA and XRS. XRS is more widely used in routine air pollution studies because of its easy availability, simplicity of operation. It can quantitatively analyze all elements of interest in air particulate samples with good accuracy and precision. It seems to be ideally suited for air pollution studies.

Table 2.3

Typical Elemental Detection Limits (ng/m³) in Air- Particulate Matter Using Different Instrumental Techniques.

Element	TNAA	AAS (flame)	AAS (flameless)	Technique	XRF	SSMS
Na	40	30	0.00005	-	-	0.0002
Al	8	400	0.15	2	-	0.0002
S	5000	-	-	-	-	0.0003
K	7.5	40	0.00005	-	-	0.0003
Ca	200	30	0.00005	-	-	0.0003
Ti	40	70	0.5	3	20	0.0005
V	2	6	0.2	6	16	0.0004
Cr	0.25	0.3	0.01	1	13	0.0005
Mn	0.6	0.3	0.0035	0.7	9	0.0005
Fe	0.02	70	0.05	5	10	0.0005
Ni	20	2	0.1	6	4	0.0007
Cu	5	3	0.005	1	6	0.0008
Zn	1	30	0.0005	2	4	0.01
Ba	0.1	-	0.005	-	-	0.02
Pb	-	7	0.005	8	7	0.03

Table 2.4

Comparison of Different Instrumental Techniques for Elemental Analysis.

Method	INAA	SSIMS	AES	AAS	XRS
Quantitation	difficult	time-consuming	difficult	easy	easy
Speed	moderate	slow	fast	fast	fast
Range	most elements	most elements	most elements	most elements	2 \times 11
Analysis time	a few min. to a few days	a few hrs.	1-2 hrs.	1-2 hrs.	1 hr.
Precision(%)	2-10	20-30	5-20	2-5	1-2
Detection limit (g)	$>10^{-12}$	10^{-3} - 10^{-9}	10^{-5} - 10^{-6}	10^{-6} - 10^{-7}	10^{-3} - 10^{-5}
Sample size	a few mg to few g	a few mg	10 mg-1 g	10-100 mg	0.1-2 mg
non-destructive	Yes	No	No	No	Yes
Multielemental	Yes	Yes	Yes	No	Yes

REFERENCES

1. D.H. Pierson, P.A. Cawse, L. Salmon and R.S. Cambray, *Nature*, 241, 252 (1973).
2. A.W. Struempler, *Atmos. Environ.*, 10, 33 (1976).
3. W.H. Zoller, E.S. Gladney and R.A. Duce, *Science*, 183, 198 (1974).
4. H.I. Blifford and D.A. Gillette, *Atmos. Environ.*, 6, 463 (1972).
5. D.F.S. Natusch and J.R. Wallace, *Science*, 186, 695 (1974).
6. P. Urone and W.H. Schroeder, *Environ. Sci. Technol.*, 3, 436 (1969).
7. R.F. Pueschel, C.C. Van Valin and F.P. Parungo, *Geophys. Res. Lett.*, 1, 51 (1974).
8. J.J. Dulka and T.H. Risby, *Anal. Chem.*, 48, 640A (1976).
9. M. Pinta, Modern Methods for Trace Element Analysis, Ann Arbor Science Publishers Inc., Michigan (1978).
10. J.D. Winefordner, ed. Trace Analysis, John Wiley and Sons Inc., (New York), (1976), p. 419.
11. D.L. Fox and H.E. Jeffries, *Anal. Chem. Reviews*, 57, 22R (1979)
12. R. Dams, J.A. Robbins, K.A. Rahn and J.W. Winchester, *Anal. Chem.*, 42, 861 (1970).
13. M. Grosch, W. Grosch, G. Wolf and H. Kreyling, *Atmos. Environ.*, 12, 1235 (1978).
14. W.H. Zoller and G.E. Gordon, *Anal. Chem.*, 42, 257 (1970).
15. I. Olmez, N.K. Aras, G.E. Gordon and W.H. Zoller, *Anal. Chem.*, 46, 935 (1974).
16. R. Dams, K.A. Rahn and J.W. Winchester, *Environ. Sci. Technol.*, 6, 441 (1972).
17. L.E. Ranweiler and J.L. Moyers, *Environ. Sci. Technol.*, 8, 152 (1974).

18. B.C. Begnoch and T.H. Risby, *Anal. Chem.*, 47, 1041 (1975).
19. G.E. Marks and C.E. Moore, *Appl. Spectro.*, 26, 523 (1971).
20. J.L. Seeley and R.K. Skogerboe, *Anal. Chem.*, 46, 415 (1974).
21. R.M. Barnes; ICP-AES in Air and Water Pollution Analysis, Presented at the 8th Annual Symposium on the Anal. Chem. of Pollutants, April, 1978, Geneva, Switzerland.
22. G.L. Macdonald, *CRC Crit. Rev. Anal. Chem.*, 4, 281 (1974).
23. R.D. Giaque, L.Y. Goda and N.E. Brown, *Environ. Sci. Technol.*, 8, 436 (1974).
24. T.B. Johansson, R. Akselsson and S.A.E. Johansson, *Nucl. Instrum. Methods*, 84, 141 (1970).
25. C.Q. Orsini, H.C. Kaufmann, K.R. Akselsson, J.W. Winchester and J.W. Nelson, *Nucl. Instrum. Methods*, 142, 91 (1977).
26. F. Folkmann, J. Borggren and A.K. Jeldgaard, *Nucl. Instrum. Methods*, 119, 117 (1974).
27. H.A. Liebhafsky, P.A. Pfeiffer, E.H. Winslow and P.D. Zemany, X-rays, Electrons and Analytical Chemistry, Wiley-Interscience, New York (1972).
28. T.G. Dzubay, B.V. Jarrett and J.M. Jaklevic, *Nucl. Instrum. Methods*, 115, 297 (1974).
29. H.K. Herglotz and L.S. Birks, eds. X-ray Spectrometry, Marcel Dekker, Inc. (1978).
30. J. Gilfrich, P.G. Burkhalter and L.S. Birks, *Anal. Chem.*, 45, 2002 (1973).
31. J.A. Cooper, *Nucl. Instrum. Methods*, 106, 525 (1973).
32. F.S. Goulding and J.M. Jaklevic, *Nucl. Instrum. Methods*, 142, 333 (1977).
33. R.L. Walter and R.D. Willis, X-ray Spectrometry, Marcel Dekker, Inc. New York (1978).
34. M.S. Ahlberg and F.C. Adams, X-ray Spectrometry, 7, 73 (1978).

35. R.L. Davison, D.F.S. Natusch, J.R. Wallace and C.A. Evans, *Environ. Sci. Technol.*, 8, 1107 (1974).
36. A.J. Ahearn, ed. Trace Analysis by Mass Spectrometry, Academic Press, New York (1972).
37. B.B. Damaskin, Principles of Current Methods for the Study of Electrochemical Reactions, McGraw-Hill, New York (1967).
38. G.H. Morrison, ed. Trace Analysis, Wiley-Interscience, New York (1965).
39. J.Y. Hwang, P.A. Ullucci and C.J. Mokeler, *Anal. Chem.*, 44, 2018 (1972).
40. T.B. Johansson, R.E. Van Grieken, D.M. Nelson and J.W. Winchester, *Anal. Chem.*, 47, 855 (1976).

Chapter 3

DESCRIPTION OF THE X-RAY FLUORESCENCE SPECTROMETER USED IN THE PRESENT WORK

3.1 Introduction

In this chapter (Section 3.2) we have described the experimental set-up used in the present work. It consisted of a source-sample assembly, a Si(Li) detector and other associated electronics necessary for energy dispersive analysis of a X-ray fluorescence (XRF) spectrum. Performance characteristics, viz. energy resolution, stability and linearity of our XRF spectrometer are also reported in Section 3.2. Calibration method used for the analysis of air particulate samples is explained in Section 3.3.

3.2 Experimental Set-up

3.2.1 Source and sample assembly

In our spectrometer we used the radiations from a radioactive source of ^{241}Am . This source had a strength of 100 mCi and was in an annular geometrical shape. It was obtained from the Radiochemical Centre, Amersham, U.K. Various dimensions of the source were as follows: outer diameter = 38 mm, inner diameter = 22.5 mm and height = 6.5 mm. It had a 50 μm . Be window in the front for protection, and tungsten alloy at the back to cut-off radiations from the source in backward direction. The photon output in the units of photons/sec/steradian was 3×10^7 for

17.7 keV and 6.5×10^7 for 59.54 keV. The source is made by incorporating Americium-241 in a ceramic enamel and is kept in a stainless steel holder with tungsten alloy backing.

Half-life of ^{241}Am is 458 years. It is an alpha emitter and it decays to ^{237}Np . The complex decay scheme of ^{241}Am is given by Lederer [1]. In Fig. 3.1 we have shown important gamma rays emitted by radioactive ^{241}Am . We have given a list of prominent gamma rays, Np X-rays and their relative intensities in Table 3.1. A typical spectrum of the ^{241}Am source is shown in Fig. 3.2.

A schematic diagram of the source holder designed and used by us is shown in Fig. 3.3. It is made out of an aluminium block to avoid characteristic X-rays interfering in the energy range of interest. The essential features of the source holder are a groove to hold ^{241}Am source, and a through hole for beam collimation. To minimize interference in the sample spectrum it is necessary that X-rays and gamma rays from the source should not reach the detector directly. Calculations using linear absorption coefficient show that a 1.25 mm thick Pb shielding can effectively absorb 99.9 % of the highest energy ($E_\gamma = 59.54$ keV which is the most intense) gamma rays from the source. Lead shielding gives rise to Pb L X-rays (energy 10.55 to 14.76 keV). These X-rays can be absorbed with 99.9 % efficiency by using a 3.9 mm aluminium. Shielding arrangement incorporated in the source holder is shown in Fig. 3.3.

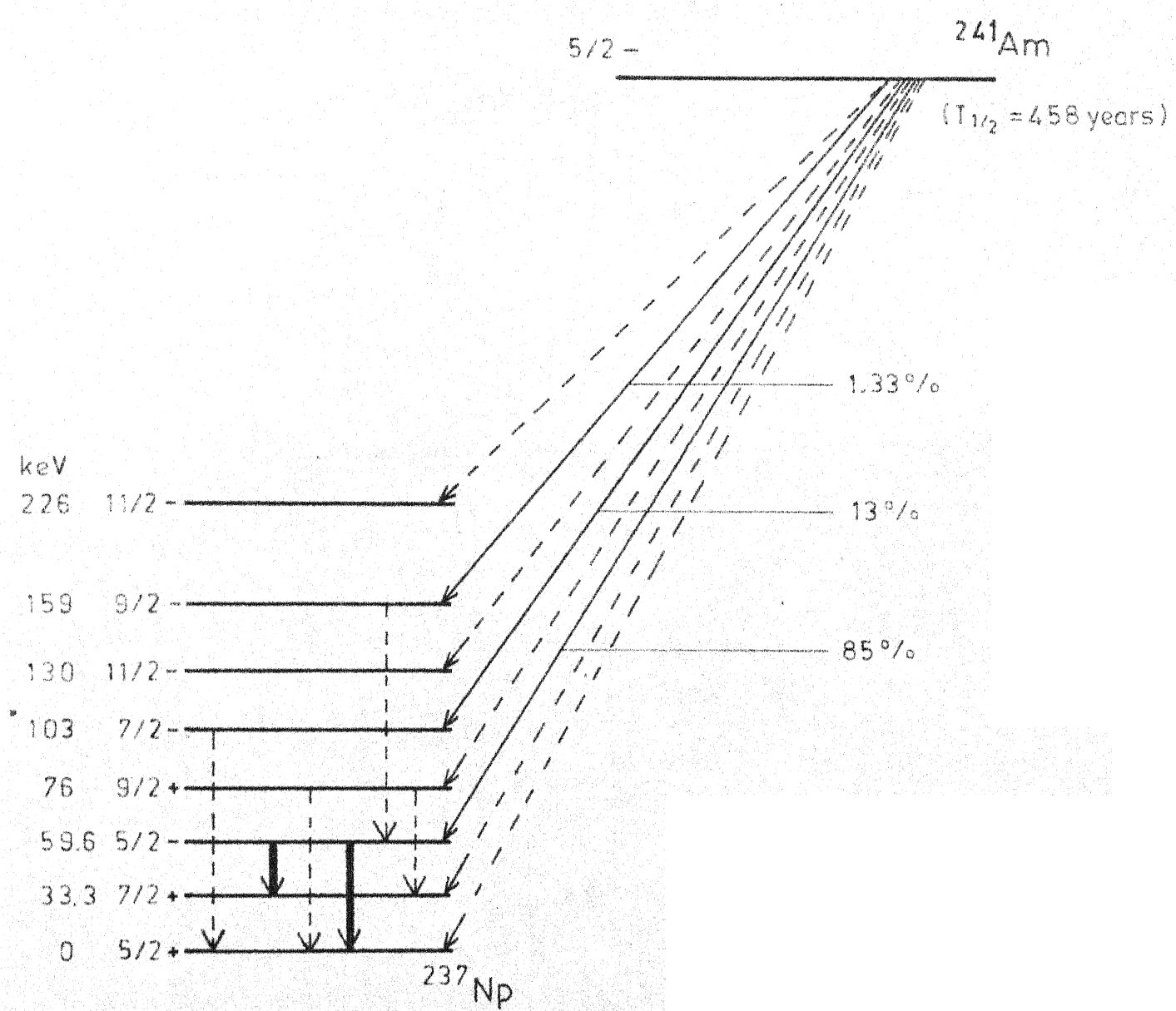


Fig. 3.1. Important gamma rays from radioactive ^{241}Am .

Table 3.1

Energies and Intensities of Some Gamma Rays and X-rays
from Radioactive ^{241}Am Source [2].

Line	Energy keV	Intensity	
		Relative	Absolute (photons/100 ^{241}Am α -decay)
<u>Np X-rays</u>			
L_{α}	11.89	2.2	0.8
L_{α_2}	13.76	37.5	13.5
L_{α_1}	13.95		
L_{β_2}	16.84	51.2	18.0
L_{β_1}	17.74		
L_{γ}	20.77	13.8	5.0
<u>Gamma rays</u>			
^{241}Am	26.35	7.0	2.5
Gamma ray	59.54	100	35.9

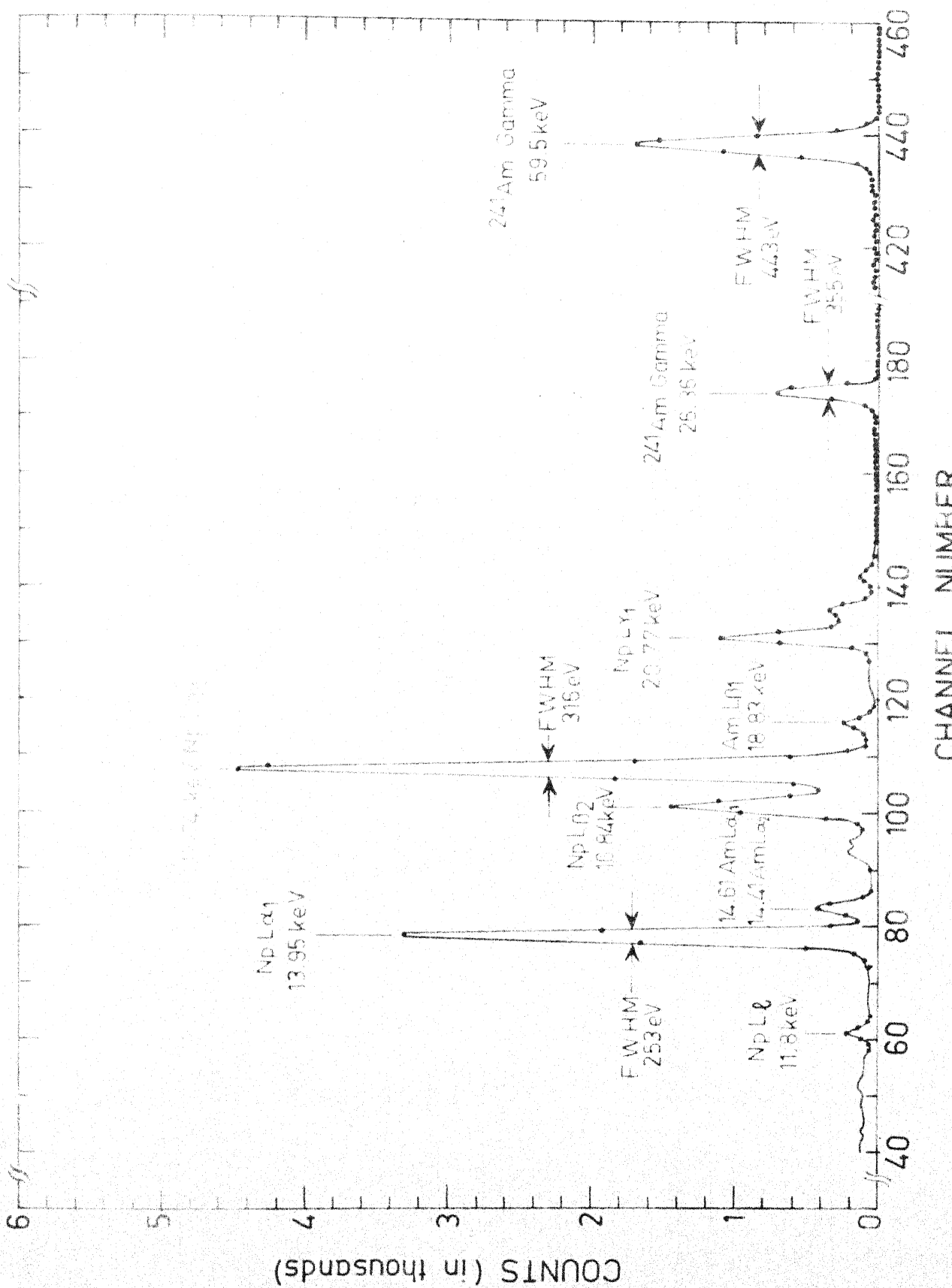
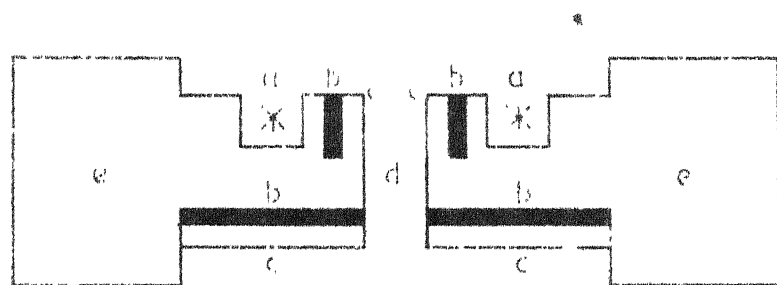


Fig. 3.2. Photon spectrum from radioactive 241Am.



6. Gluove for ^{241}Am source

267. 1900-1901

3. Local shielding

c - Aluminum shielding

d. Collimator

e. Aluminium source holder.

Fig. 3.3. Horizontal cross-section of the source holder.

The sample holder was made of perspex to avoid interfering X-rays from the holder itself. Samples were prepared on membrane filters and could be mounted in a fixed position with the help of a plastic ring pressed against the holder.

The source-sample assembly could be further mounted on a wooden bench which was permanently fixed on a small table. The whole arrangement was such that the distance between the detector and the source-sample assembly could be varied between 2 to 25 cm. The photograph of the entire arrangement is shown in Fig. 3.4.

3.2.2 Electronic systems

In our experiments we have used a lithium-drifted silicon or Si(Li) X-ray detector. It was procured from EG and G Ortec Inc., U.S.A. The diameter and height of the active region of the detector diode were 6.00 mm and 5.08 mm respectively. The diode had a surface barrier contact of gold (thickness \approx 200 \AA) as the front surface. The dead layer in silicon itself was mentioned to be less than 0.1 μm . The detector diode was sealed in a port with a beryllium window of thickness 50 μm . Distance between the beryllium window and detector diode was 7.00 mm. The detector was also provided with a low noise FET preamplifier. To obtain best resolution, the detector was always kept at liquid nitrogen temperature.

A lithium-drifted silicon detector is a solid state ionization device. The detector diode has a p-i-n

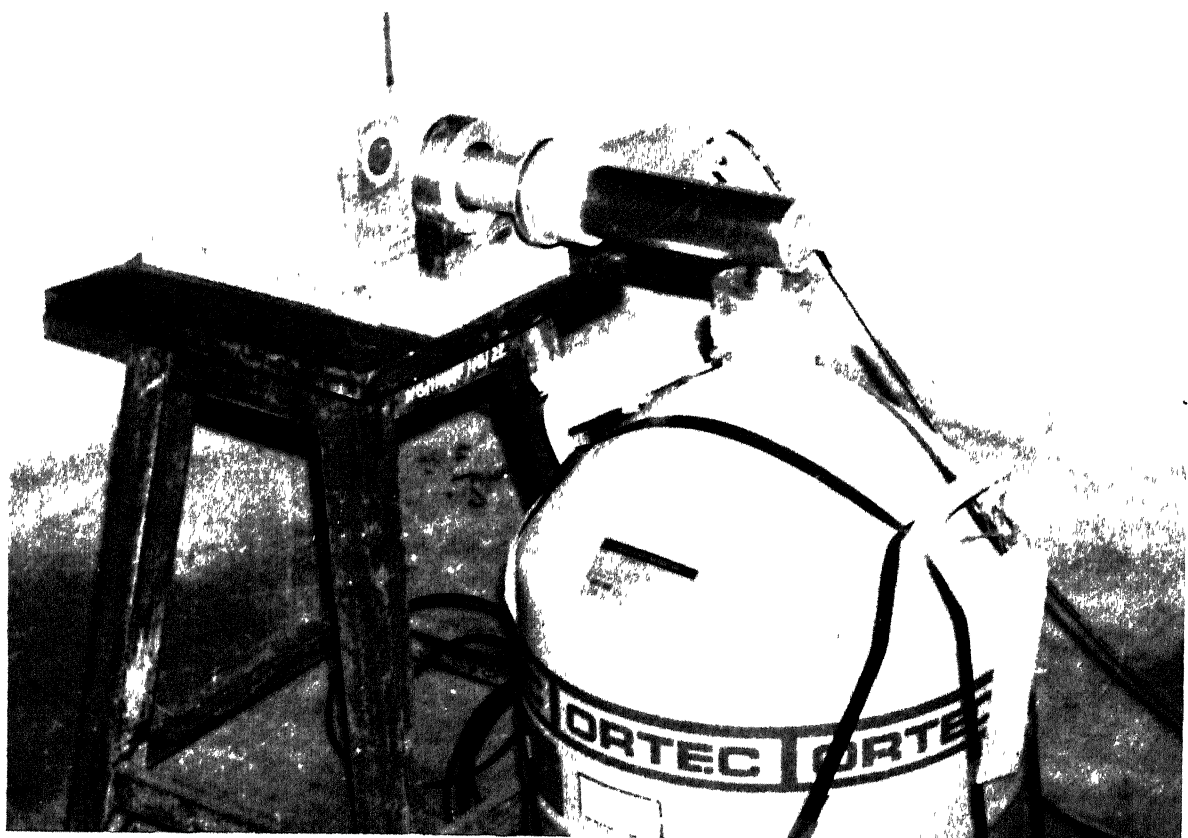


Fig. 3.4. Experimental arrangement for mounting the source and sample in front of the detector.

structure. It is made from a p-type silicon with n-type lithium diffused on the outside of the crystal and drifted towards a central core under a strong electric field. During this process the excess of p-type impurities originally present in silicon is precisely compensated and a region of high resistivity called the intrinsic region is produced. Thus there is a p-type contact on the entry side followed by the intrinsic active volume and the lithium-diffused n-contact. When reverse bias is applied to the device the drifted region acts as an insulator with an electric field throughout its volume. At liquid nitrogen temperature it exhibits very low leakage current and signals produced by radiation-induced ionization are directly proportional to the energy of the absorbed radiation.

Interactions of photons with the matter in the intrinsic region of the detector produce high-speed electrons. The three processes involved in the interaction of the photon with the matter are the photoelectric effect, Compton scattering and pair production. In XRF experiments only the first two processes are relevant. Electrons produced by any of these processes lose their kinetic energy in ejecting electrons from one of the shells of the Si atom creating a vacancy which is filled by the emission of Si characteristic X-rays or an Auger electron. When all the energy of the electron and that of secondary radiation is absorbed in the sensitive region of the detector a charge signal proportional to the energy of the electron is

produced.

In general the observed spectrum, for a monochromatic radiation, consists of a Gaussian peak centered at the energy and a continuous background below that energy. The observed line width of the Gaussian peak is much greater than the natural line width of a X-ray lineshape. We also know that the intensity function for atomic emission lines is a type of Lorentzian [3].

The Gaussian lineshape is due to the pulse shaping done by the electronic system, mainly the linear amplifier. The large full width at half maximum (FWHM) is because of the statistical fluctuation (R_d) in the number of ion pairs produced for a given energy E . The electronic noise due to preamplifier, amplifier and the detector leakage current also contributes to the width of the peak. Let this contribution be R_n . Then, FWHM can be expressed as [4]

$$R = \sqrt{R_n^2 + R_d^2} \quad (3.1)$$

where

$$R_d = 2.355\sqrt{(\varepsilon F)} \quad (3.2)$$

ε is the average energy required to produce an electron-hole pair and F is the Fano factor. For a Si(Li) detector $\varepsilon = 3.8$ eV and $F = 0.125$. It is possible to estimate the contribution due to electronic noise in FWHM by plotting Energy vs. FWHM. The intercept at zero energy will be equal to the noise contribution due to the electronics used.

In Fig. 3.5 we have shown an energy resolution spectrum obtained with our set-up. A radioactive source of ^{57}Co was used for this purpose. The observed resolution is 181 eV at 6.403 keV and matches well with the warranted resolution (180 eV). The observed full width at 1/10th of peak height (FWTM) is 343 eV. For a Gaussian peak $\text{FWTM} = 1.83 \text{ FWHM}$. So the Gaussian shape obtained with our spectrometer has no tailing effect. We have measured resolution (FWHM) as a function of energy using a ^{241}Am source. In Fig. 3.6 we have plotted FWHM as a function of energy for various energies. It can be seen from the figure that the electronic noise contribution to FWHM in our set-up is approximately 100 eV.

Some of the mechanisms in the detector which contribute significantly to the spectrum background are discussed by Goulding [5]. These are : (i) escape mechanisms and (ii) poor charge collection. Escape mechanisms in the detector could involve both the escape of photoelectrons produced in the detector and the emission and escape of bremsstrahlung photons produced by these electrons. The escape of photoelectrons produced in the detector will give rise to a small spurious peak below the main peak.

Malm et al. [6] have discussed the effect of the presence of surface channels on detectors. These produce distortion in the electric field pattern in the detector in such a way that collection of charge produced by X-rays

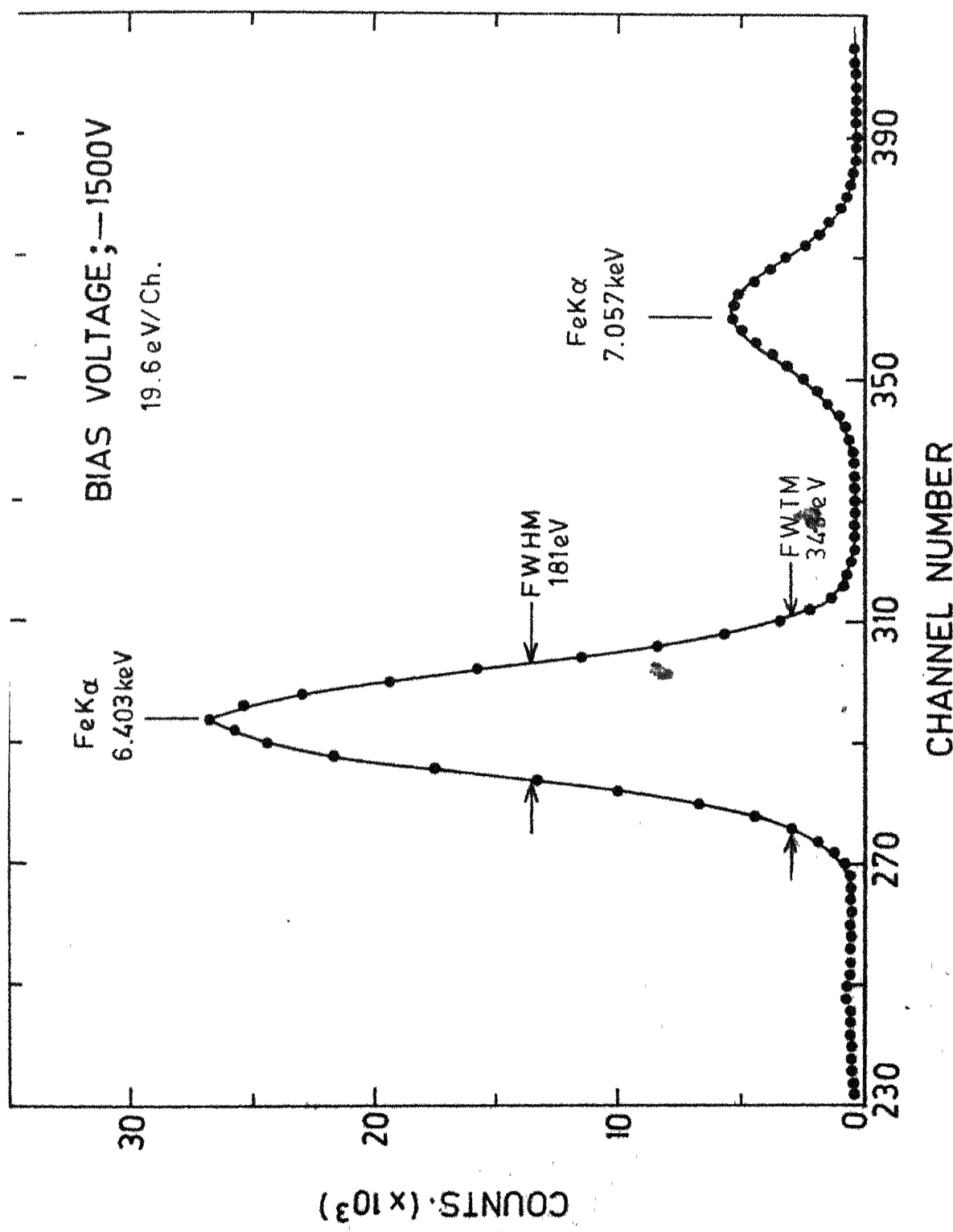


Fig. 3.5. Energy resolution spectrum using radioactive ^{57}Co source.

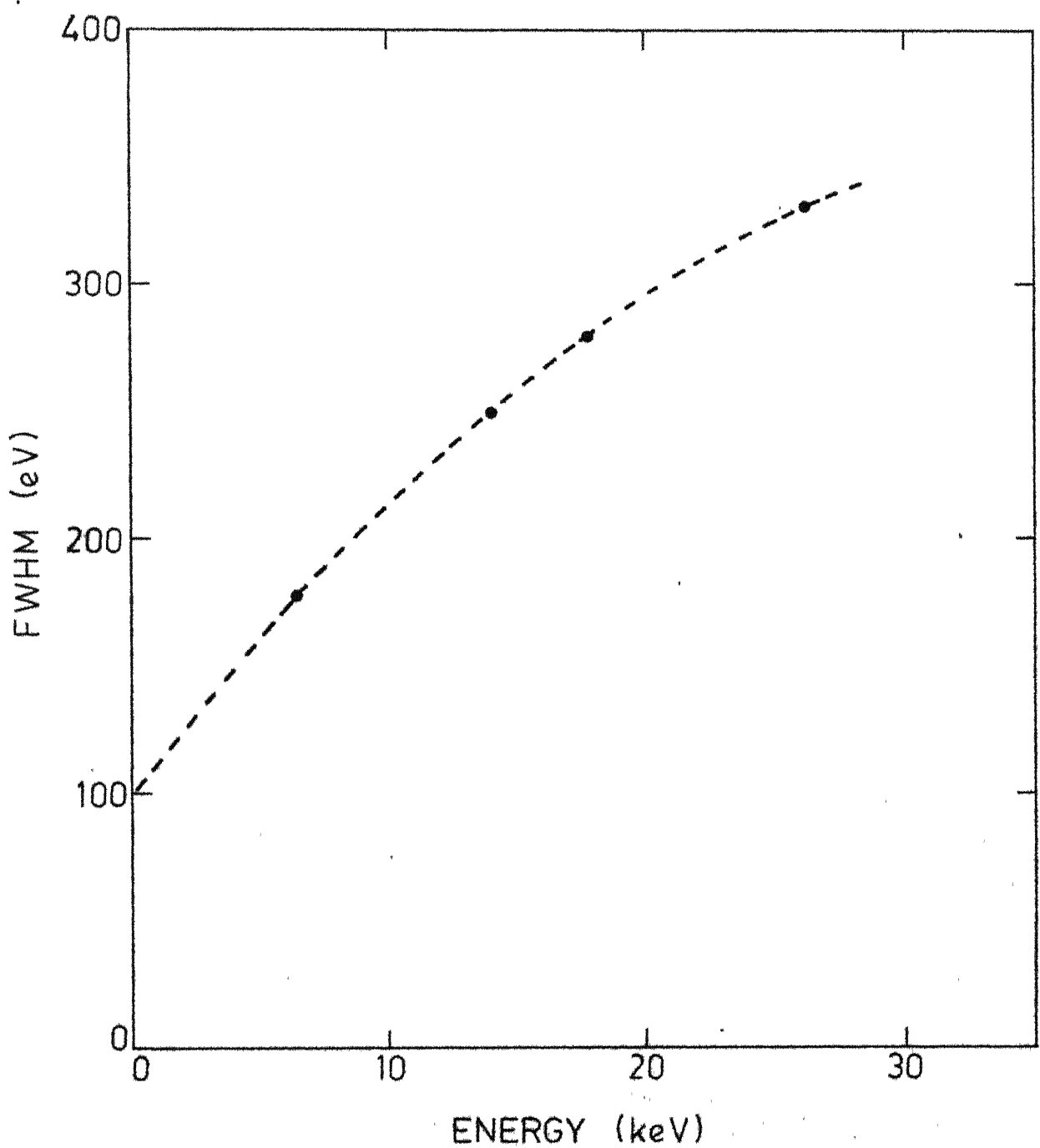


Fig. 3.6. Plot of FWHM vs Energy.

interacting in some parts is via the surface layers. This causes a loss of charge resulting in smaller signals. These signals contribute significantly to the spectrum background. This effect can be reduced by collimation of incident radiation or by using a guard-ring detector suggested by Goulding [7].

Incomplete charge collection can also be due to thick dead layers at the entry surface of the detectors. A thickness of 0.3 to 0.4 μm is reported by many workers [8,9]. This may be due to the diffusion of some electrons into the surface layer before being collected by the electric field. By simple diffusion analysis Goulding [5] has estimated the dead layer thickness to be approximately 0.3 μm . This seems to be an inherent limitation in minimizing the background contribution due to the detector.

The other electronic systems used in our experiments were: Spectroscopy amplifier (Model No. 571) or a Research amplifier (Model No. 450) and a high voltage power supply (Model No. 459) from EG and G Ortec Inc., U.S.A. Multi-channel analyzer used was either of the following three analyzers : (i) Nuclear Data Model ND-60 (ii) Nuclear Data Model ND-6600 (iii) Canberra Series-80. Typical block diagram of the experimental set-up is shown in Fig. 3.7.

The primary requirements of the electronic system in a XRF experiment are (i) good energy resolution (ii) excellent gain stability (iii) essentially zero drift in

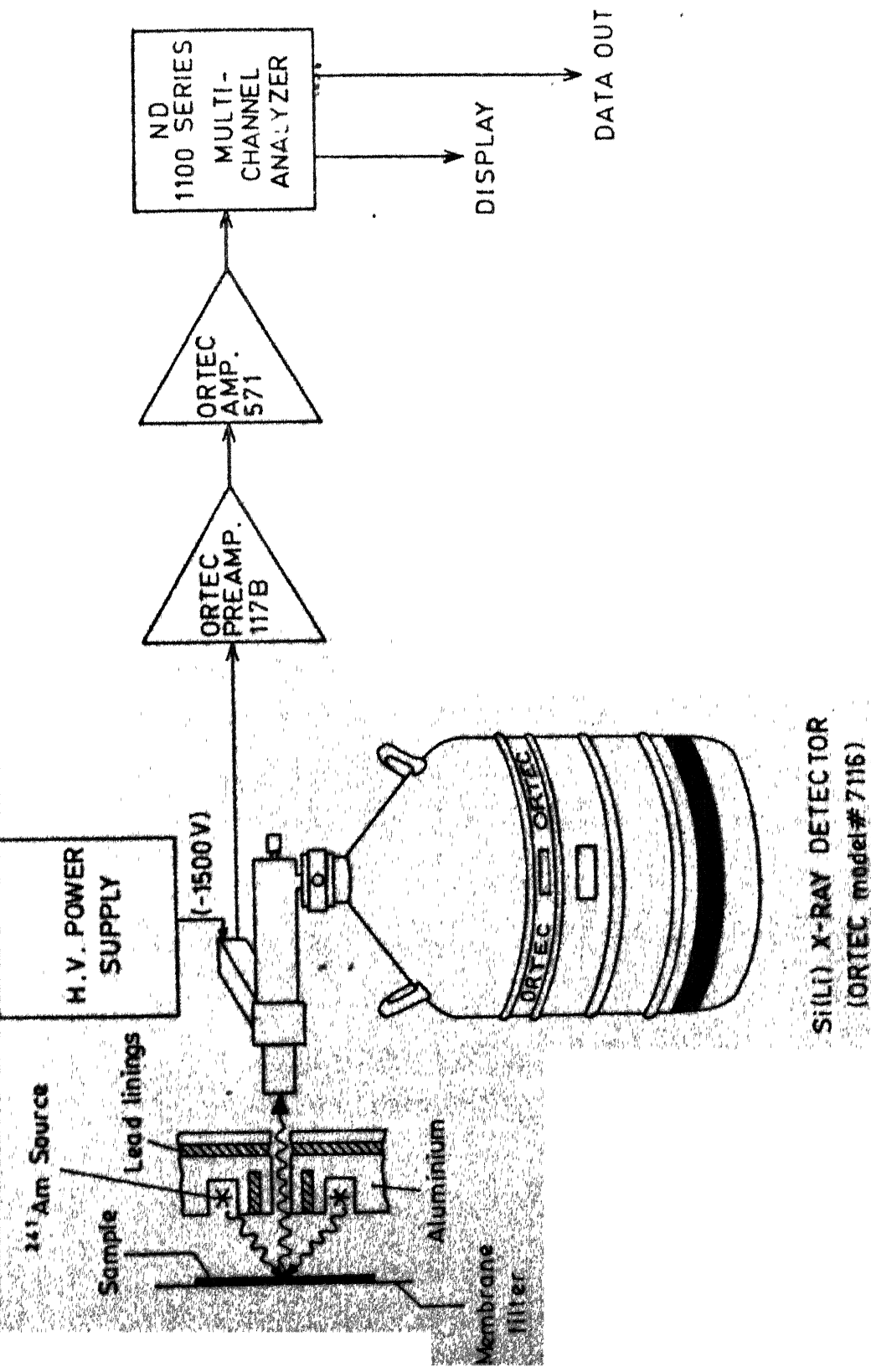


Fig. 3.7. Typical block diagram of the experimental set-up.

the baseline of signals and (iv) capacity to handle large count rates.

Amplifiers used in X-ray spectrometry are provided with active filter circuits for pulse shaping. To optimise the resolution there are various adjustments like baseline restorer (BLR), pole-zero adjustment and pile-up-rejection. We shall discuss each one of these in brief.

Sometimes the unipolar output pulse of a linear amplifier shows an undershoot of the baseline at the completion of the pulse. When the count rate is high, a second pulse may occur before the undershoot has returned to baseline. Then the apparent amplitude of the second pulse will be decreased. This undershoot causes a baseline shift. It can be cancelled by addition of one resistor to the differentiating circuit and is called pole-zero cancellation. After pole-zero adjustment, the remaining baseline shift is compensated by BLR circuits. This restores the signal quickly to the baseline when an undershoot occurs.

The upper limit for allowable count rate is determined by the phenomenon called pile-up. Since the output pulses of a processing system have a finite duration, there is a possibility that two such pulses will be superimposed either fully or partly on one another, in which case their true height will not be seen by the pulse height analyzer.

Best electronic resolution and high count rates are conflicting requirements. Resolution improves with increase in shaping time for the pulse. But the count rate that can be handled decreases. So adjustments have to be made according to specific requirements.

In our experiments, a negative bias of -1500 V DC was applied to the detector. The shaping time used was 10 μ sec as the count rates were not very high. A spectrum obtained with our spectrometer is already shown in Fig. 3.5. The ^{241}Am source spectrum given in Fig. 3.2 compares well with the one reported by Elad et al. [11]. The additional peaks have energies corresponding to Am L X-rays. These may be due to some stable americium isotope present in the source. Its intensity is small and does not affect our calibration method. Gain stability of the system is checked by frequent calibration runs and by peak positions of prominent peaks in sample spectra. We have found that the position of a peak is same over a measurement period of a couple of months. A calibration spectrum of energy vs. channel number is shown in Fig. 3.8. It shows the good linearity of the spectrometer over the energy range of interest.

3.3 Calibration of Our Spectrometer

3.3.1 Method

The relation between fluorescent intensity and elemental concentration depends on the form and composition

Slope = 0.018 keV/ch
Intercept = 0.696 keV

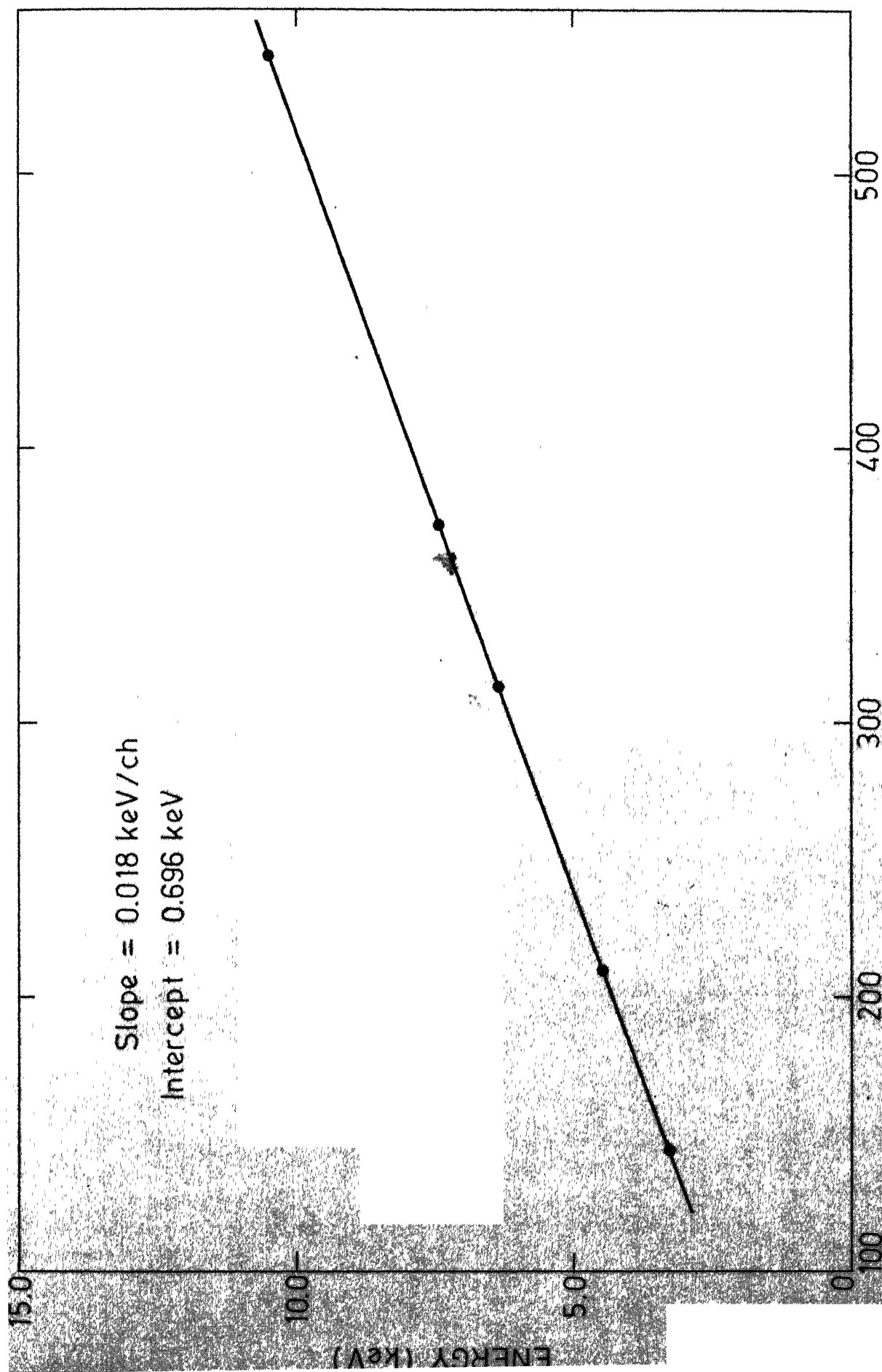


Fig. 3.8. An energy calibration curve.

of the specimen and host matrix effects. Thin film method proposed by Giaque et al. [12] is by far the most widely used method in the analysis of biological and air particulate samples. The outline of the derivation of this method is given below.

The method is applicable to thin homogeneous specimen of uniform thickness for which the enhancement effects are negligibly small. When a monochromatic radiation is used as a source of excitation, the probability of exciting the K X-rays of energy E_j from element j in the thickness dx and then detecting them is given by

$$P = P_1 P_2 P_3 \quad (3.3)$$

where P_1 , the probability that the primary radiation will reach a depth x , is given by

$$P_1 = G_1 \exp(-\mu_1 \rho x \cosec \theta_1); \quad (3.4)$$

P_2 is the probability that element j will absorb the primary radiation in the thickness dx and emit a K X-ray of energy E_j and is given by

$$P_2 = \tau_j \rho_j \cosec \theta_1 \left[1 - \left(\frac{1}{J_K} \right) \right] \omega_j f_j dx, \quad (3.5)$$

and P_3 is the probability that the K X-ray (of energy E_j) reaching the detector will be detected. It is given by

$$P_3 = G_2 \exp(-\mu_2 \rho x \cosec \theta_2) A_j \epsilon_j \quad (3.6)$$

The meaning of various symbols used in eq. (3.3) to eq. (3.6) is as follows:

G_1 and G_2 are geometry factors.

μ_1 and μ_2 are the total mass absorption coefficients (cm^2/gm) of the sample for exciting and the fluorescent radiation.

ϕ_1 and ϕ_2 are the angles formed by the exciting and the fluorescent radiations with the sample surface.

ρ is the density (gm/cm^3) of the sample.

ψ_j is the density of element j within the sample considering the entire sample distribution.

τ_j is the photoelectric mass absorption coefficient of element j for the primary radiation.

J_k is the ratio between the photoelectric mass absorption coefficient at the top and the bottom of the K absorption edge; $[1-(1/J_k)]$ is the fraction of the photoelectric events which occur in the K shell.

ω_j is the fluorescent yield for the K X-rays from element j .

f_j is the fraction of the K X-rays of energy E_j with respect to the total K X-rays emitted.

$\hat{\epsilon}_j$ is the absorption of energy E_j in the air path between the sample and the detector.

ϵ_j is the detector efficiency for X-rays of energy E_j .

The values of μ_1 , μ_2 , τ_j , J_k , ω_j and f_j can be obtained from literature [13-16]. The values of ϵ_j can be measured experimentally.

If the intensity of the incident radiation is I_0 , then the X-ray intensity due to the element j at a depth x is

$$dI = I'_0 G K_j [\exp(-a \hat{\epsilon} x)] \hat{\epsilon}_j dx \quad (3.7)$$

where $I'_0 = I_0 \operatorname{Cosec} \phi_1$

$$G = G_1 G_2$$

$$K_j = \tau_j \left(1 - \frac{1}{J_k}\right) \omega_j f_j A_j \epsilon_j$$

$$a = \mu_1 \operatorname{Cosec} \phi_1 + \mu_2 \operatorname{Cossec} \phi_2$$

Integrating over the sample thickness d and multiplying the numerator and denominator by d one obtains from eq. (3.7)

$$I_j = I'_0 G K_j C_j m_j \quad (3.8)$$

where

$$C_j = \frac{1 - \exp(-a \hat{\epsilon} d)}{a \hat{\epsilon} d} \quad (3.9)$$

and $m_j = \hat{\epsilon}_j d$ is the concentration of element j which is to be determined. For very thin samples C_j is negligible. Then eq. (3.7) will reduce to

$$I_j = I'_0 G K_j m_j \quad (3.10)$$

Theoretical values of K_j can be calculated for various X-ray lines and for constant intensity of the exciting radiation involving fixed geometry. The value of $I'_0 G$ can be determined from a standard specimen (consisting of a thin film containing a single element) for which absorption effects are negligible. The experimental X-ray fluorescent yield data are in disagreement by several percent with the theoretical fluorescent yield data used in the calculations [17]. To obtain higher accuracy in the analysis, thin film standards for each of the elements of interest can be prepared by various methods described by Giaque et al. [18]. The standard specimens should be thin enough such that the absorption effects are negligible. Using this procedure the values of $I'_0 G K_j = S_j$ can be determined empirically for individual elements of interest. Then

$$I_j = S_j m_j \quad (3.11)$$

where I_j = the intensity (counts/sec) of the characteristic X-ray line for an element j .

$S_j = I'_0 G K_j$ is the sensitivity in counts/sec/ $\mu\text{g}/\text{cm}^2$ for an element j .

m_j = the mass of element j ($\mu\text{g}/\text{cm}^2$) in the thin specimen of element j .

This is one of the methods recommended by Giaque et al. [18] for the analysis of environmental samples which are thin.

We have used this method to calibrate our spectrometer for the analysis of air particulate matter.

3.3.2 Preparation of the standards of pure elements

Thin specimens used for the calibration of the spectrometer were prepared by one of the following two methods:

(i) Filtration method : A weighed amount of fine powder (300 mesh) of the chosen element or its insoluble salt was placed in suspension in a known volume of distilled water. A few drops of digol was added to the solution. A uniform suspension was obtained by agitating the solution with an ultrasonic vibrator. The thin specimens were prepared on Sartorius membrane filters (dia. = 47 mm, pore size = 0.45 μm) using the filtration assembly shown in Fig. 3.9. It consisted of a filter holder, a reservoir, a 37 mm circular sintered disk and a metal clamp. The filter paper was kept on the moist sintered disk and the filter holder was clamped on it. A known volume of the solution was filtered using adequate suction. The filter paper was later dried under IR lamp. An aluminum ring with a circular hole, just slightly larger than the deposition area was kept on the filter paper to avoid curling of the filter paper during drying. Depositions of varying mass were obtained by filtering different volumes of the solution. Deposition area was 10.18 cm^2 . The membrane filters were weighed before and after filtration under identical conditions. A

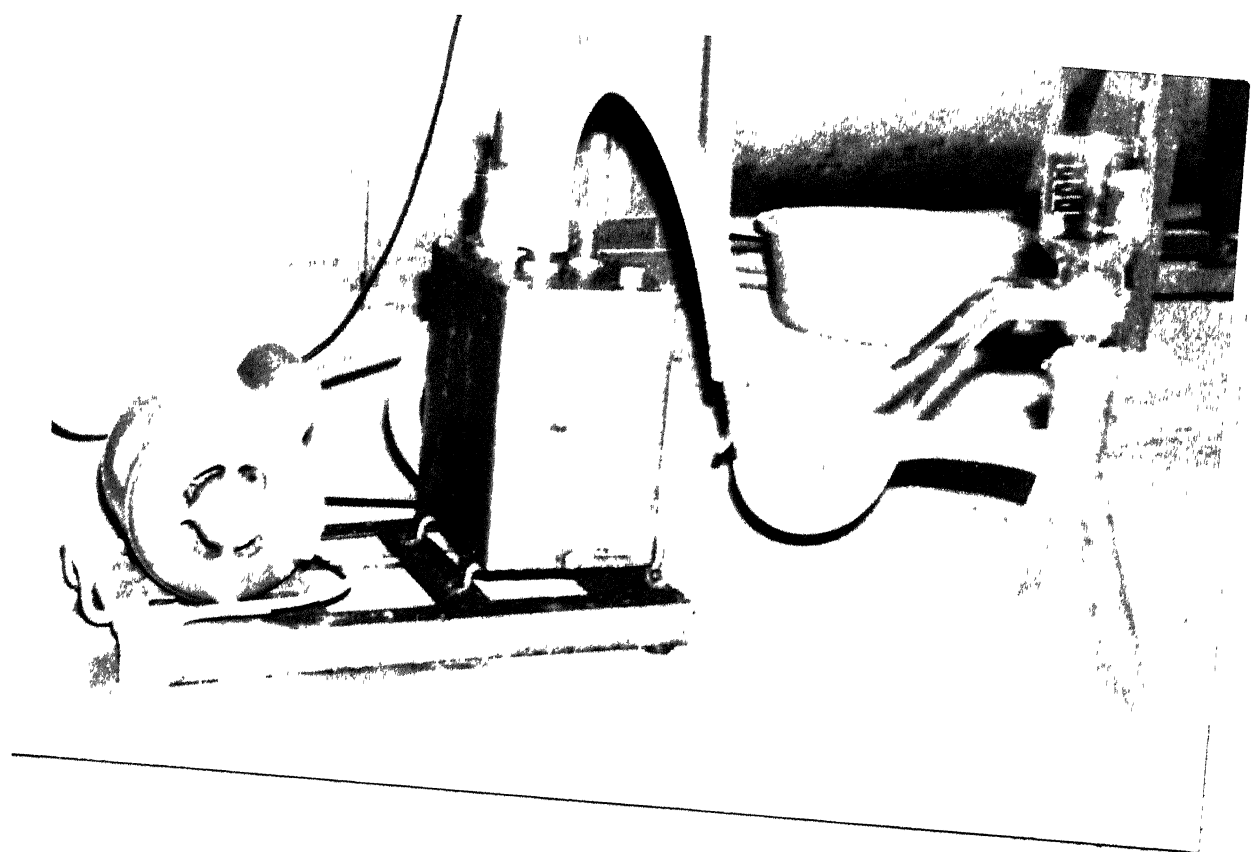


Fig. 3.9. The filtration assembly used for thin element sample preparation.

few blank filters were also weighed during preweighing and postweighing of the filters to avoid any error in adjusting the balance each time. All the weighing was done on a semi-micro balance with a least count of 10 μg . Using this method 5 to 7 standard specimens of TiO_2 , V_2O_5 , Fe, ZnO and PbO_2 with a thickness in the range $10\text{-}600 \mu\text{g/cm}^2$ were prepared.

(ii) Nebulizer method : A locally made nebulizer shown in Fig. 3.10 was used to generate a very fine mist from a standard solution of an element. This was collected on a preweighed filter paper pressed between two mylar sheets with a central hole of diameter 37 mm in the centre. A distance of approximately 1 ft. was maintained between the nebulizer and the filter. It was observed that the less glossy surface of the filter absorbs the depositions with greater penetration into the filter material. Therefore the more glossy surface of the filter material was always used for deposition. Standard solutions of Cr, Mn, Ni, Cu, Pb and Ba were prepared using $(\text{NH}_4)_2\text{Cr}_2\text{O}_7$, $\text{MnSO}_4 \cdot \text{H}_2\text{O}$, $\text{NiSO}_4 \cdot 5\text{H}_2\text{O}$, $\text{Pb}(\text{NO}_3)_2$, $\text{Ba}(\text{CH}_3\text{COO})_2$ compounds. Using these solutions a number of thin specimens for each element were prepared. The weight of the element of interest was in the range of 10 to 500 $\mu\text{g/cm}^2$.

3.3.3 XRF analysis of the standards of pure elements

In order to obtain maximum sensitivity we used X-rays and gamma rays from the radioactive source ^{241}Am to excite

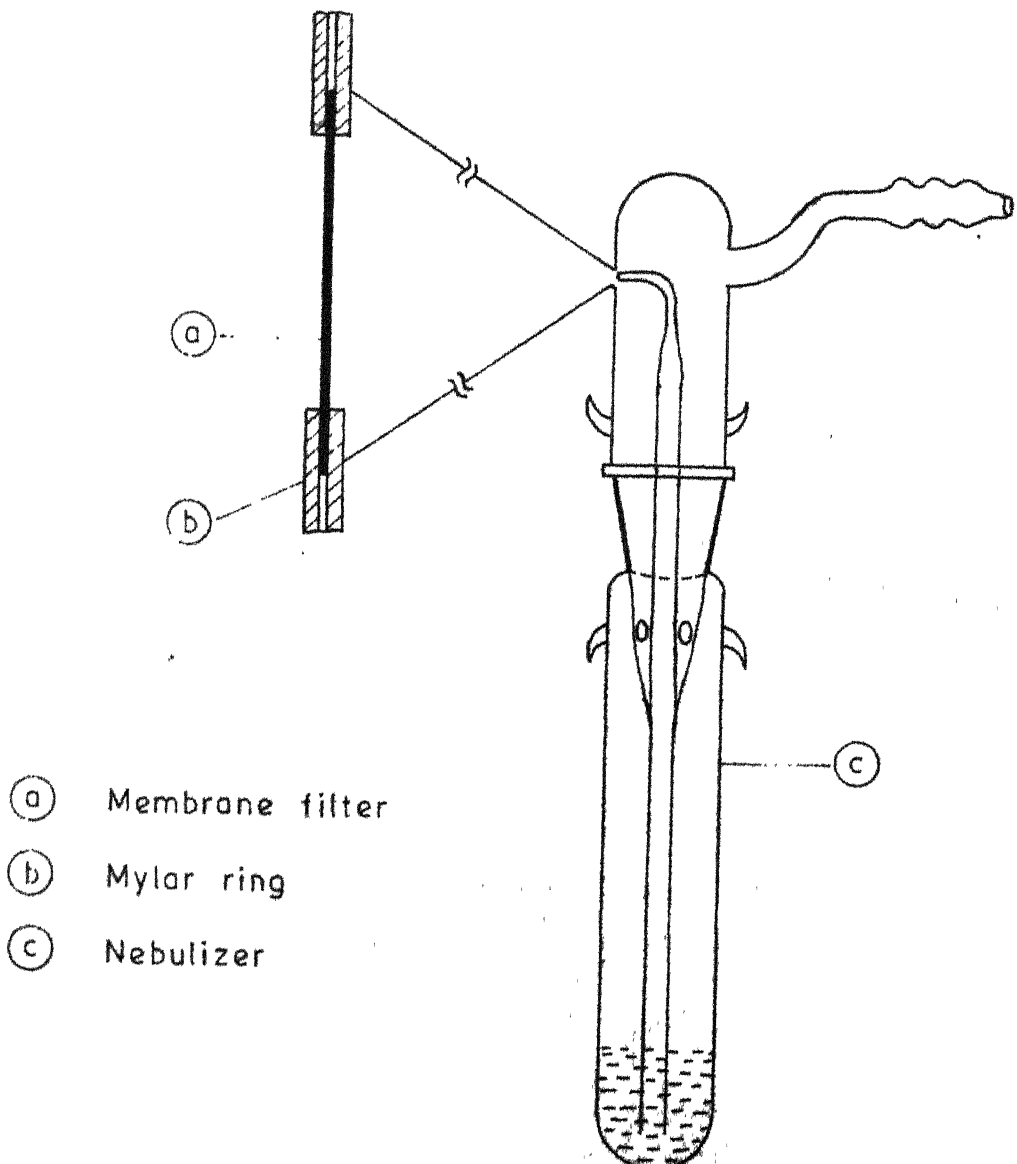


Fig. 3.10. Arrangement showing the preparation of thin samples from solutions using a nebulizer.

fluorescent radiation in the samples. To obtain maximum counting rate we varied the distance between the sample and the source holder noting the counting rate for $Fe K_{\alpha}$ at each position. The graph of distance vs. peak area is shown in Fig. 3.11. Distance between the sample and the source holder for maximum peak area was found to be 13 mm. Source holder was kept as near to the detector as possible. The experimental arrangement used in the present work is shown in Fig. 3.4.

XRF experiments were carried out in the above geometry for all pure elemental standards. The standard samples were irradiated and their gamma-ray spectra were recorded. The excitation period for each sample was such that the statistical error (standard deviation) in the peak area of interest was less than 0.1 %.

Area analysis was done by non-linear least square fitting method. A Gaussian function for the peak and a quadratic function for the background was used to perform curve-fitting of the data. Sensitivity and detection limit are the two quantities used to characterise a XRF spectrometer. Sensitivity for an element was determined from the graphs of peak intensity (counts/sec) vs. deposition ($\mu g/cm^2$) for the element. We used K_{α} lines for all elements except Pb where L_{α} line was used to determine the peak intensity. In Fig. 3.2 we have shown the graphs of intensity (counts/sec) vs. deposition ($\mu g/cm^2$) for Pb and Cr. Similar lines

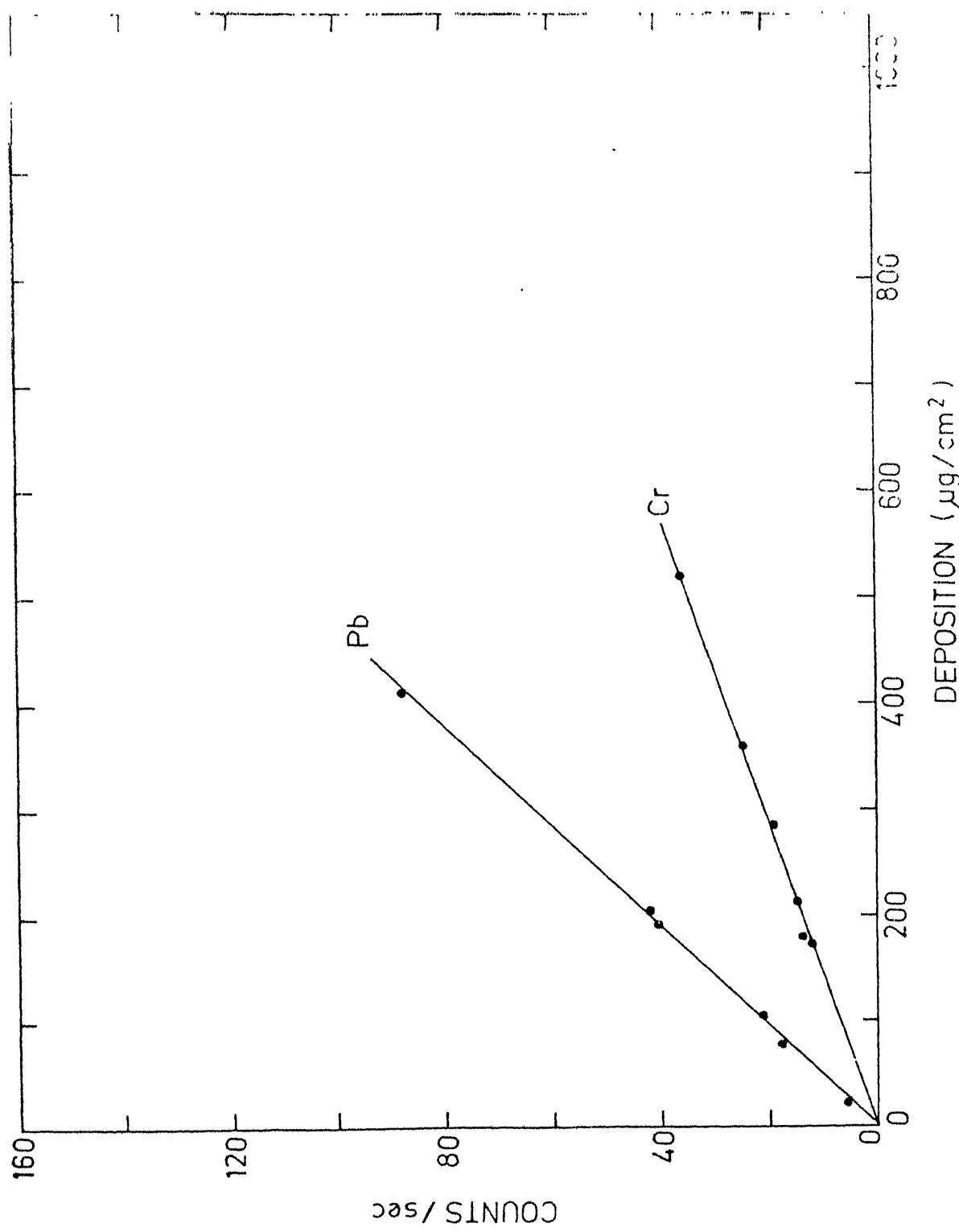


Fig. 3.12. A plot of deposition vs intensity for Pb and Cr.

were obtained for other elements of interest. Slope of the line gives sensitivity in (counts/sec)/($\mu\text{g}/\text{cm}^2$). All the data were fitted with a straight line by the method of least squares. Correlation coefficients obtained between intensity and deposition for various elements were between 0.95 to 0.99. In Table 7.2 we have given the values of sensitivities and standard deviations for different elements. Sensitivity for K and Ca was determined using XRF analysis of NIM standards (described in Section 3.3.4), while pure element standards were used for all other elements. An interesting feature of the sensitivity is the sudden increase in its value for Ni, Cu and Zn. This may be due to the sudden fall in the background (arising from the Compton edge of higher energy radiation) after the iron peak which occurs at 6.4 keV. Compatibility between two methods of sample preparation was checked by preparing standards for Pb by using both methods. The agreement between the values of sensitivity obtained was 5 %.

The detection limit is a measure of the performance of a X-ray fluorescence spectrometer. We use the definition given by Birks [19] i.e. the detection limit is the concentration of an element that gives, in a specified time, a number of counts (above the background) which is equal to three times the standard deviation of the background. It is given by

$$\text{Detection limit} = \text{D.L.} = \frac{3}{S} \sqrt{\frac{B}{t}} \quad (3.12)$$

Table 3.2

Sensitivities for Different Elements for the XRF Spectrometer Used in the Present Work.

Element	Sensitivity (<u>counts/sec</u>) $\mu\text{g/cm}^2$
K	0.0059 ± 0.0004
Ca	0.0140 ± 0.0003
Ti	0.0484 ± 0.0045
V	0.0588 ± 0.0002
Cr	0.0713 ± 0.0005
Mn	0.0852 ± 0.0085
Fe	0.0992 ± 0.0001
Ni	0.2283 ± 0.0009
Cu	0.2176 ± 0.0006
Zn	0.2979 ± 0.0003
Ba	0.0830 ± 0.0083
Pb	0.2126 ± 0.0002

where S is the sensitivity, B is the background count rate, and t is the real counting time. If background and the sample spectra are recorded for same time then

$$D.L. = \frac{3}{S} \sqrt{\frac{B_T}{t}} \quad (3.13)$$

where B_T is the background below the peak. In Table 3.3 the values of detection limits for various elements are given. These were calculated using XRF analysis of a typical air particulate sample which is described in Chapter 4. The pure element detection limits will be generally lower than the values given in Table 3.3.

In Table 3.4 we have also given the values of K_β/K_α ratio determined by us. These were determined using the XRF spectra for thin samples of pure elements. Our results compare well with those obtained by Slivinsky et al. [20], after correcting for air-absorption and the detector efficiency.

3.3.4 Accuracy

The various sources of errors in XRF method have been discussed by Currie [21]. The total error in a measurement using an analytical method is the sum of systematic and random errors. Random error is mainly due to the counting statistics and can be reduced to some extent by increasing counting time. Various sources of systematic errors are : i) sample preparation method ii) impurities in blank filter paper iii) spectral interferences like overlap of K_α and K_β

Table 3.3

Detection Limits for Different Elements Calculated from a XRF Spectrum of a Typical Air Particulate Sample Collected by us.

Element	Detection Limit $\mu\text{g}/\text{cm}^2$
K	3.314
Ca	1.485
Ti	0.378
V	0.323
Cr	0.214
Mn	0.227
Fe	0.225
Ni	0.063
Cu	0.066
Zn	0.043
Pb	0.045
Ba	0.072

Table 3.4

K_{β}/K_{α} Ratios for Some Elements.

Element	K_{β}/K_{α}	
	Our work	Slivinsky [20]
Ti	0.1332 ± 0.0024	0.1319 ± 0.0017
V	0.1344 ± 0.0019	0.1339 ± 0.0011
Cr	0.1326 ± 0.0019	0.1344 ± 0.0011
Fe	0.1380 ± 0.0019	0.1366 ± 0.0011
Ni	0.1380 ± 0.0019	0.1385 ± 0.0011
Zn	0.1398 ± 0.0019	0.1418 ± 0.0011

iv) improper calibration and v) matrix effects. Currie et al. [22] have discussed the methods of obtaining systematic error bounds. Limits of systematic error may be arrived at in two different ways. They may be estimated by comparing an experimental result with the certified value for a standard sample. The second approach is to evaluate the systematic error through detailed analysis. We checked the systematic errors involved in the calibration method by analysing NIM rock samples obtained from South African Bureau of Standards. The NIM rock samples were prepared for XRF analysis by filtration method described in Section 3.3.2. The deposition obtained from different samples was in the range of 0.7 to 2.8 mg/cm^2 . Reproducibility of the method was checked by taking spectra of two samples from the same NIM rock powder. The method of analysis of these spectra is similar to that of air particulate samples and is described in Section 4.5. The results obtained are shown in Table 3.5. Agreement between the determined values and NIM values is within 5 % for major constituents. Greater deviation was found for small concentrations and for elements Cu and Pb. We have found Cu and Pb impurity in the blank filters and variability in their concentration may be one of the reasons for greater deviation for Cu and Pb. The other source of error is the significant statistical error involved in determining small concentrations. Considering the standard deviation in sensitivity and the agreement

Table 3.5

Analysis of NTM Samples (Concentration values are given in parts per million (ppm)).

Element	Mn	Fe	Ni	Cu	Zn	Pb
NIM-G^a						
Determined ^c	197 \pm 31	14425 \pm 650	-	8 \pm 2	61 \pm 2	53 \pm 1
Certified ^f	160	14300	-	12	50	40
NIM-L^b						
Determined ^c	6263 \pm 88	70859 \pm 304	-	162 \pm 25	376 \pm 14	98 \pm 1
Certified ^f	6000	70190	-	13	395	43
NIM-C^c						
Determined	1401 \pm 80	65059 \pm 100	90 \pm 30	61 \pm 8	48 \pm 15	-
Certified	1400	59262	120	14	66	-
NIM-P^d						
Determined ^c	1670 \pm 72	91657 \pm 263	598 \pm 59	-	-	-
Certified ^f	1700	88401	555	-	-	-

^aNIM-G Granite

This reference material is a granite rock-type which consists mainly of quartz and K-feldspar, and has smaller amounts of mica and Na-feldspar [23].

^bNIM-L Lujavrite

This rock type is a lujavrite and undersaturated igneous rock which consists of nepheline, sphene, aegerene, magnetite and some feldspar [23].

^cNIM-N Norite

This rock type is a norite which consists of orthopyroxene, plagioclase, magnetite, ilmenite, and clinopyroxene and minor amounts of quartz and alteration products [23].

Table 3.5 (Continued)

^dNIM-P Pyroxenite

This rock type is a pyroxenite which consists of orthopyroxene, clinopyroxene, and plagioclase and minor amounts of olivine and chromite [23].

^eResults determined by us.

^fCertified values by supplier. Blanks in table indicate concentration values below the detection limit.

between experimental and certified values for NIM samples, an accuracy of 10-15 % can be obtained using the present calibration method.

REFERENCES

1. C.M. Lederer, J.K. Poggenburg, F. Asaro, J.O. Ramussen and J. Perlman, Nucl. Phys., 84, 481 (1966).
2. T. Yamazaki and J.M. Hollander, Nucl. Phys., 84, 505 (1966).
3. A. Hoyt, Phys. Rev., 40, 477 (1932).
4. F. Adams and R. Dams, Applied Gamma-Ray Spectrometry, Pergamon Press, (1976), p. 192.
5. F.S. Goulding, Nucl. Instrum. Methods, 142, 213 (1977).
6. H.L. Malm and R.J. Dinger, IEEE Trans. Nucl. Sci., NS-24, 76 (1977).
7. F.S. Goulding, J.M. Jaklevic, B.V. Jarrett and D.A. Landis, Advan. X-ray Anal., 15, 470 (1972).
8. R.H. Pehl, F.S. Goulding, D.A. Landis and M. Leslinger, Nucl. Instrum. Methods, 59, 45 (1968).
9. R.G. Bushet and W. Bauer, Nucl. Instrum. Methods, 109, 543 (1973).
10. F.S. Goulding and J.M. Jaklevic, Nucl. Instrum. Methods, 142, 313 (1977).
11. E. Elad and M. Nakamura, Nucl. Instrum. Methods, 42, 316 (1966).
12. R.D. Giaque, F.S. Goulding, J.M. Jaklevic and R.H. Pehl, Anal. Chem., 45, 671 (1973).
13. G.L. Simons and J.H. Hubbell, NBSIR 73-241, (1973).
14. E. Sturm and H.I. Israel, Nucl. Data Tables A7, 565 (1970).
15. E.H.S. Burhop and W.N. Assad, Adv. in Atomic and Mol. Phys. 8, 269 (1972).
16. J.H. Scofield, Nucl. Data Tables, 14, 121 (1974).
17. R.W. Fink, R.C. Jopson, N. Mark and C.D. Swift, Rev. Mod. Phys., 38, 513 (1966).

18. R.D. Giaque, R.B. Garrett and L.Y. Goda X-ray Fluorescence Analysis of Environmental Samples, ed. T.G. Dzubay, Ann Arbor Science Publishers, Michigan (1977) p. 153.
19. L.S. Birks X-ray Spectrochemical Analysis, Wiley-Interscience, New York, (1969), p. 54.
20. V.W. Slivinsky and P.J. Ebert, Phys. Rev. A5, 1581 (1972).
21. L.A. Currie, X-ray Fluorescence Analysis of Environmental Samples, ed. T.G. Dzubay, Ann Arbor Science Publishers, Michigan (1977), p. 289.
22. L.A. Currie and J.R. Devoe, Validation of the Measurement Process, ACS (1977) p. 117.
23. Catalogue of Certified Reference Materials, South African Bureau of Standards, (1979).

Chapter 4

SAMPLE COLLECTION AND XRF ANALYSIS OF THE SAMPLES

4.1 Sampling Plan

4.1.1 Area description

Kanpur claims importance as the largest city within the largest state (Uttar Pradesh) of India. With a population of about 1.7 million in 1981 it is the eighth most populous city in India. It is an old industrial city and is the second largest metropolis of northern India.

Geographically Kanpur is situated on the right bank of the river Ganges. It has latitude and longitude of $25^{\circ} 26' N$ and $80^{\circ} 22' E$ respectively. It is about 900 km. north-west of Bay of Bengal and about 950 km. north-east from the Arabian sea coast. It lies beyond the tropics and is about 350 km. north of the tropic of cancer. Kanpur is in the semi-arid area of Uttar Pradesh and there are no hills in the surroundings. The soil in Kanpur is grey and brown typical of the Gangetic basin and is impregnated with salts.

The climate of Kanpur is typical of northern India with dry hot ($\sim 45^{\circ}C$ maximum) summer which changes into a warm humid (95 % maximum) season during monsoon (July-September). The winter is severe, with temperatures becoming low ($\sim 5^{\circ}C$ minimum) in the night. Duststorms are a common feature in the summer and due to the dry climate dust gets lifted up in the atmosphere readily. The daytime heating

produces intense vertical and horizontal mixing of the air mass. In winter intense night time radiational cooling results in the development of shallow and stable inversions. Contrary to the normal weather pattern there was no rainfall during the period of our study. The winds follow a prevailing east-west direction pattern in the summer, switching over to west-east direction in winter.

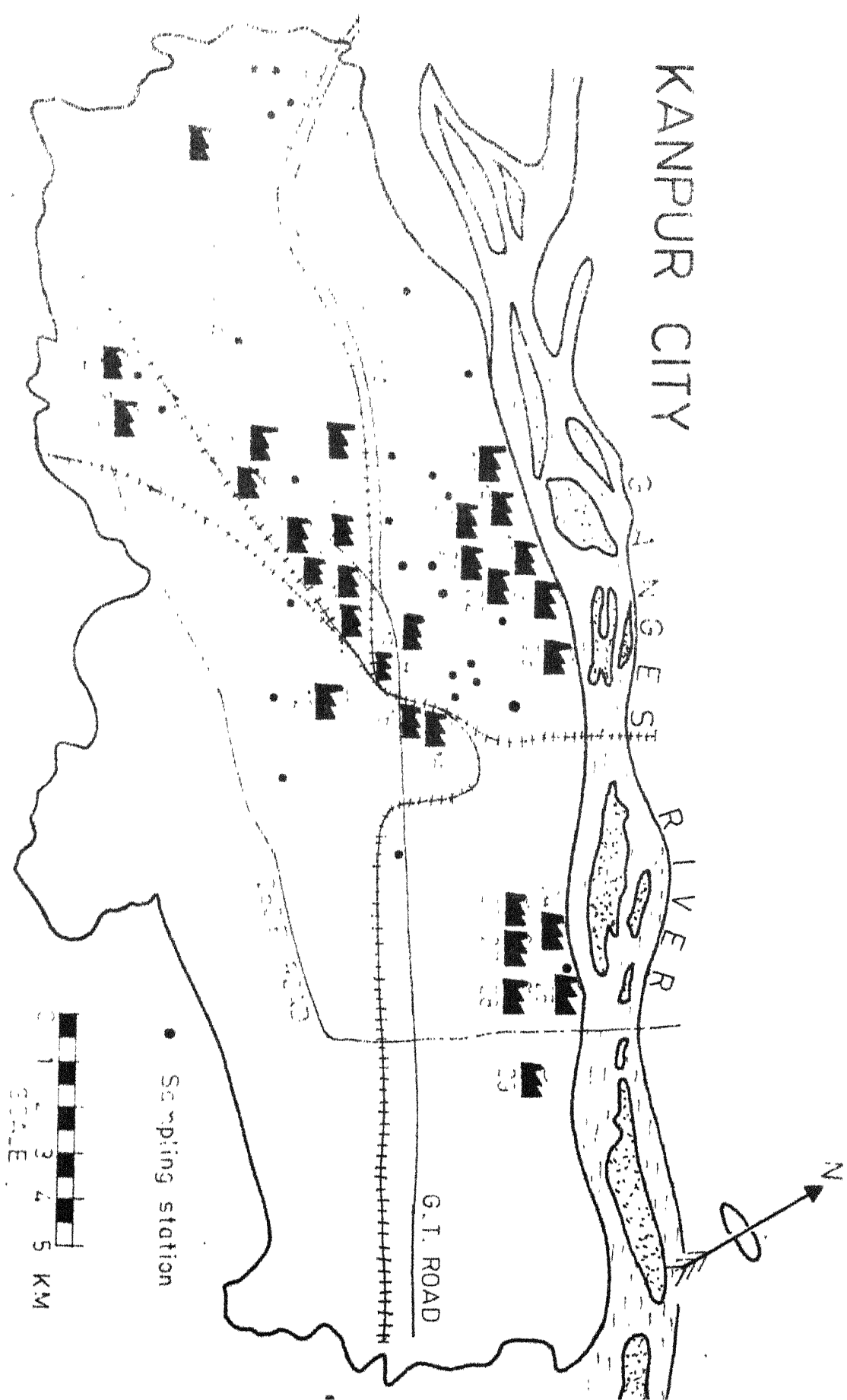
Kanpur is also an important transport node. The Grand Trunk Road and the railway routes link it with Calcutta in the east and Delhi in the west, Bombay in the south west and Gauhati in the north east. Kanpur being a junction of the Northern, Central and North-Eastern railways also make it a very busy center of railway traffic. The transportation system, consisting of mostly railways and heavy trucks, is a major source of pollution due to the consumption of considerable amount of coal and diesel oil.

Over the years Kanpur has been a big industrial centre because of the availability of water, raw materials, other resources, human labour and facilities for communication. The important industries of the city are textiles, woollens, tanning and leather, oil and flour mills, armaments, small and heavy engineering and rolling mills. Recently modern industrial units like Hindustan Aeronautics, Indian Explosives Limited (production of chemicals and fertilizers), two major thermal power plants etc. have also come up.

The industrial development as well as the urban growth of the city is totally unplanned and haphazard and this has confounded the problem of pollution. Some idea of these problems can be obtained from Fig. 4.1. In Table 4.1 we have provided the list of major industries shown in the map of Kanpur in Fig. 4.1. Most of the industries are located in the central region with some pockets on the outskirts of the city. Industries in Kanpur are mainly labour oriented. The living conditions for the majority of the population are very poor. Most of the houses use wood and coal for cooking purposes. Since the industrial and residential areas are intermixed, pollution in the area is high and is expected to show unusual pattern. Total area of the city is 57,000 acres though only about 16,000 acres are now in urban use. Nearly two thirds of the area is in agricultural use.

4.1.2 Station locations

For the purpose of air particulate sampling to study the elemental composition of total suspended particulates (TSP) of Kanpur city, the first task was to choose a number of sampling locations in the city which could not only provide representative samples but also reflect overall pollution pattern. A few general guidelines are listed by Ludwig [1] and Morgan et al. [2]. The concept of spatial representativeness provides a useful basis for classifying stations and the uses to which their data are put. Furthermore, the concept of representativeness has a physical basis that can serve to



Sampling stations, showing important industries and main roads.

Table 4.1

List of the Big Industries in Kanpur Shown in Fig. 4.1.

Site Number. on the map (Fig. 4.1)	Name of the Industry
1.	Panki Thermal Power Station
2.	Indian Explosives Limited (IEL)
3.	Other factories like steel etc.
4. }	Ordnance Factories
5. }	
6.	J.K. Sugar and Veg-oil Mills
7.	Laxmi Ratan Cotton Mills
8.	J.K. Iron and Steel
9.	J.K. Plastics and many other factories and foundries
10.	J.K. Jute Mills
11.	Singh Engineering Works and many others (like chrome factory etc.)
12.	Swadeshi Cotton Mills
13. }	Textile Mills
14. }	
15.	Ganges Flour Mill
16.	Rolling Mill and foundries
17.	Tanneries
18.	River-side Thermal Power Station

Continued

Table 4.1

List of the Big Industries in Kanpur Shown in Fig. 4.1.

19.	Elgin Mill No. 1	Textile Mills
20.	Victoria Mill	
21.	Lal Imli Mill (Woollen Mill)	
22.	Muir Mill (Textile Mill)	
23.	Small Arms Factory	
24. to 28.	Tanneries	
29.	J.K. Rayon	
30.	TAFCO (Leather Industry)	

defining station characteristics. Urban-wide conditions cannot be specified with a single station representing a neighbourhood, but when the sampling at several locations is done, it is not necessary to find the ideal urban-wide location. Siting criteria also must be such that exposures of the population to pollutants will be realistically represented. Alipy et al. [3] have suggested that the larger sizes of particles are dominated by relatively innocuous minerals and that the smaller sizes contain most of the lead compounds, sulfates and nitrates. Taking into account the health motivations of the air quality regulations routine, TSP monitoring should be conducted at sites where the aerosol concentrations are representative of smaller, somewhat more toxic fraction. The smaller particles tend to be related more to primary anthropogenic sources rather than resuspended natural and unnatural dusts.

We divided the Kanpur city into three different zones for TSP monitoring to study the air quality of Kanpur city. The zone-wise distribution of sampling stations is shown in Fig. 4.2 and is described in Table 4.2. Zone A is a heavily populated region in the centre of Kanpur city. It has significant commercial and industrial influence. The region is also marked with heavy traffic density. Zone B is a less populated area surrounding the densely populated and industrial zone. In this zone the extent of pollution due to man-made activities is expected to be less. In zone C the sampling stations were selected in the vicinity of various

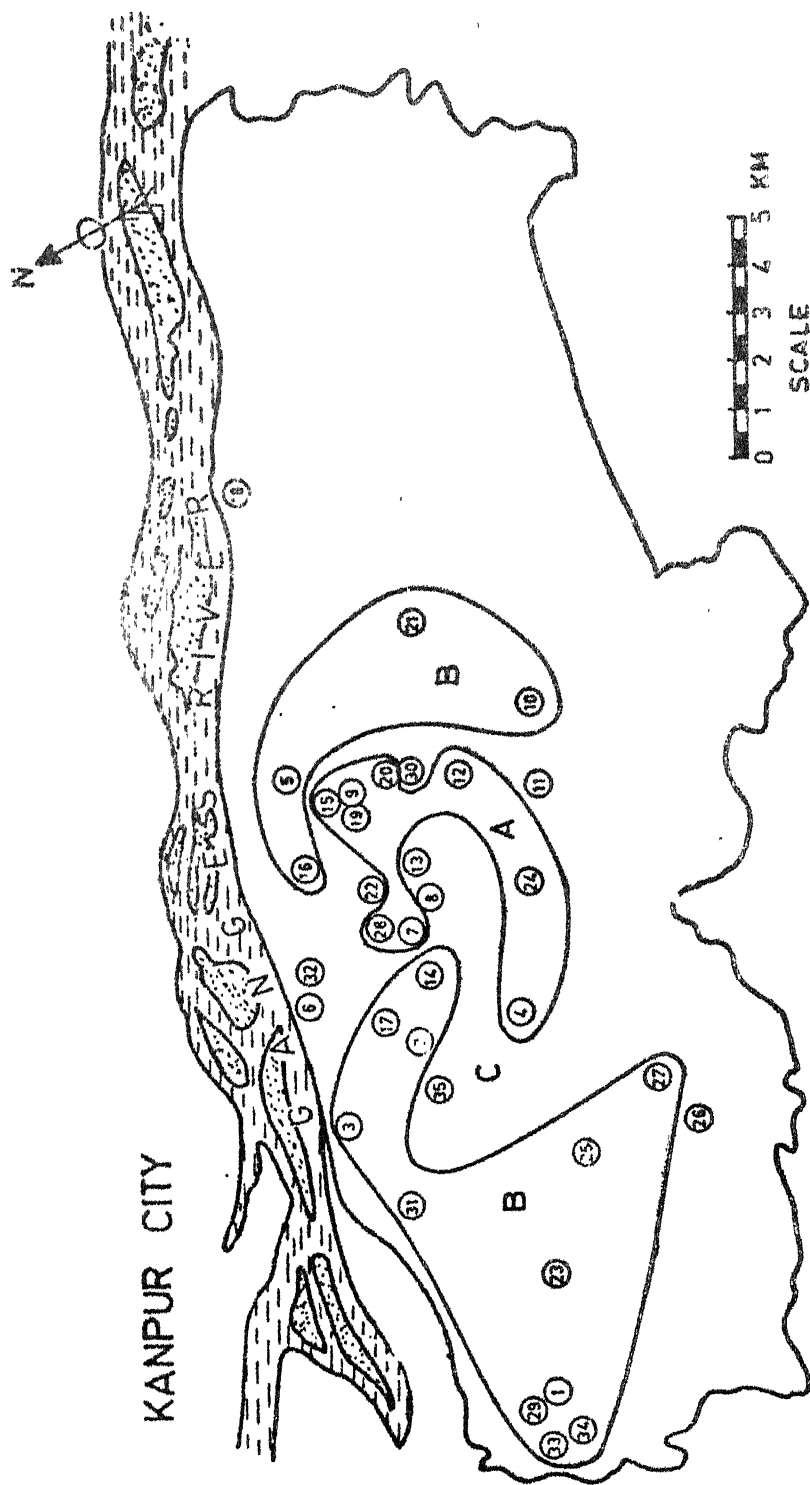


Fig. 4.2. Map of Kanpur city showing sampling locations for air particulate samples.

Table 4.2

Description of the Sampling Stations Shown in Fig. 4.2.

Zone A		Zone B		Zone C	
Mainly Thickly Populated	Mainly Less Populated	Mainly Industrial	Name of the Location	No.*	Name of the Location
Mainly Thickly Populated	Mainly Less Populated	Mainly Industrial			
No.*	Name of the Location	No.*	Name of the Location	No.*	Name of the Location
(4)	Shastri Nagar	(1)	I.I.T.	(6)	Souter Ganj
(7)	Gandhi Nagar	(29)	I.I.T.	(8)	Jareeb Chowk.
(9)	Ghantaghar	(33)	I.I.T.	(11)	Juhi Labour Colony
(12)	Transport Nagar	(34)	I.I.T.	(13)	Anwar Ganj
(15)	General Ganj	(2)	Swaroop Nagar	(18)	Jajmau
(19)	Dhan Kutty	(3)	Azad Nagar	(22)	Chaman Ganj
(20)	Rail Bazar	(5)	Phool Bagh	(26)	IEL
(24)	Govind Nagar	(10)	Kidwai Nagar	(30)	Harris Ganj
(28)	Bajariya Police Station	(14)	Ashok Nagar		
		(16)	Naveen Market		
		(23)	Kalyanpur		
		(25)	Armapur		
		(27)	Dada Nagar		

*The number indicates the label number of the site in the map shown in Fig. 4.2.

industries and represent industrial influence on the neighbourhood. Zone boundaries are not rigid and certain amount of intermixing can be expected. Zone-wise selection of sampling locations helps in understanding the pollution pattern in Kanpur city.

Besides air quality monitoring, study of dust suspended on the roadways has gained significant importance in recent years due to high levels of toxic elements present in the roadway dust [4,5]. To study the extent of pollution in TSP along the busy roads, we selected a few sampling stations at some busy road crossings in the city. The air particulate samples at these locations are expected to show considerable influence of auto-exhaust. These locations are shown in Fig. 4.3 and are listed in Table 4.3. All the crossings involved heavy traffic and large scale human activity.

To study the extent of heavy metal pollution inside various factories we conducted air quality monitoring inside a few factories. The factories selected were iron and steel factory, leather processing factory and paints manufacturing factory. Various sections inside the factory were selected for the air particulate sampling to study the effect of different kinds of industrial activities on the inside atmosphere.

4.2 Sample Collection

4.2.1 Selection of the sampling sites

In selecting a particular sampling site at a given location it is necessary that the sampler be situated to yield data representative of the location and yet it should

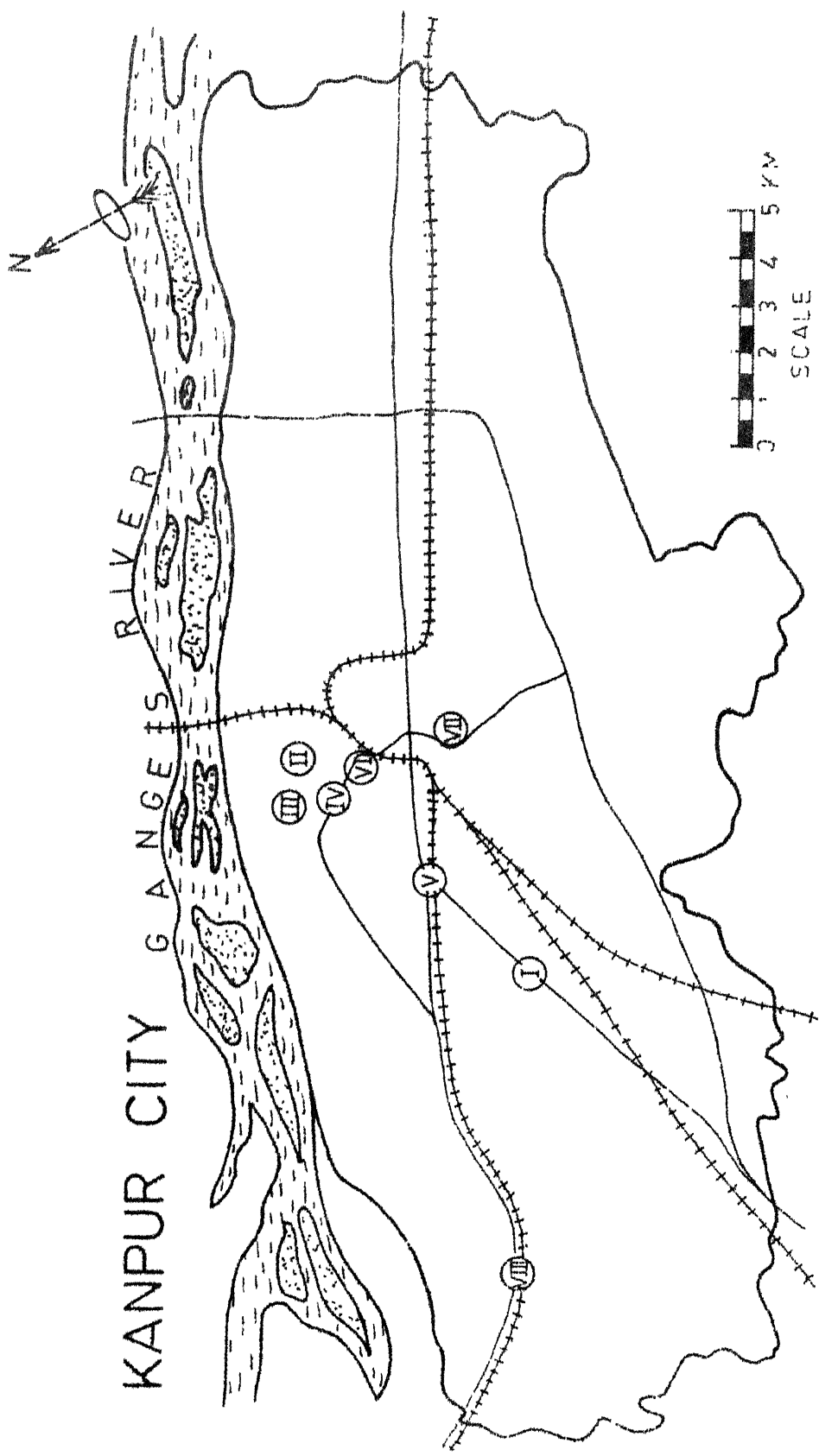


Fig. 4.3. Map of Kanpur city showing some busy crossings where air particulate samples were collected at breathing level.

Table 4.3

List of the Sampling Sites Shown in Fig. 4.3.

Label on the Map (Fig. 4.3)	Name of the Crossings
I	Vijay Nagar Crossing
II	Phool Bagh Crossing
III	Bada Chowrah
IV	Mool Ganj Crossing
V	Jareeb Chowky
VI	Ghantaghar
VII	Transport Nagar
VIII	Kalyanpur

not be unduly influenced by the immediate surroundings. Environmental Protection Agency (EPA) recommends [6] a minimum distance of 25 meters from the nearest traffic lane and a height of 2 to 15 meters for air particulate sampling. We selected a sampling site at a particular location according to the EPA criteria. As far as possible constraints to the air flow from any direction was avoided in choosing a site.

4.2.2 Sampling equipment

To collect total air particulate matter suspended in air following equipment and materials are needed ;(a) a filter paper to collect the deposition of the TSP, (b) a filter holder assembly, (c) a flow meter to calculate the volume of air drawn, (d) a suction pump to draw air through the filter paper.

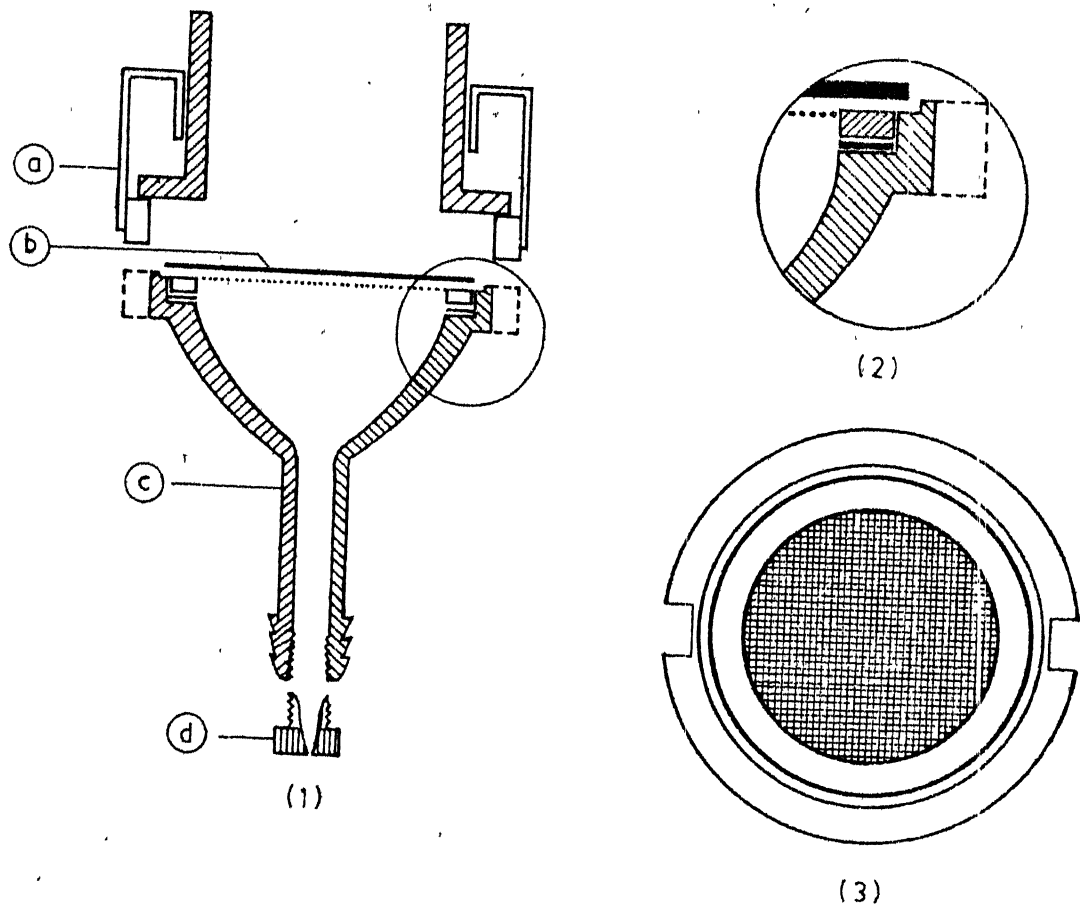
(a) Filter paper : The filter for collecting TSP should meet several requirements like low hygroscopicity, absence of impurities that might interfere with the analysis and a very high collection efficiency for particulates of different sizes.

Glass fibre filters, polystyrene filters and membrane filters are generally used for sample collection. Oikawa [7] has summarized physical and chemical properties of various filters and also their applicability in collecting atmospheric particulates. Nitro-cellulose and cellulose acetate membrane filters are best suited for low volume air sampler and instrumental method of analysis. In our experiments we used nitro-cellulose Sartorius (Type: SM) membrane filters of 47 mm diameter and 0.47 μm pore size.

(b) Filter holder assembly : This is shown in Fig. 4.4 and consists of a fine mesh of diameter of 3.6 cm, a place to fix the filter and a 2.5 cm hood of diameter 3.6 cm. The limiting orifice shown is to restrict the rate of air-flow coming into the device. The filter holder and the limiting orifice set were obtained from Millipore Corporation Inc., U.S.A.

(c) Flow meter : The devices widely used for flow measurement are the float area flow meter, orifice flow meter and gas meter. In our experiment we used a rotameter to check the flow rate fixed by limiting orifice. A rotameter consists of a float mounted in a vertical tapered tube. As air enters the lower end of the tube, its flow is obstructed by the float and a pressure difference arises between the front and rear of the float. Then the float is lifted up by the resultant upward force, and comes to rest at a point where the pressure is balanced by its effective weight. The distance of float movement is correlated to the flow volume. Calibration of the rotameter is commonly done using a wet test meter, which can give volume measurements with an error of about 0.1 - 0.5 % .

(d) Suction pump : To sample suspended air particulate matter it is desirable that the suction pump provides high vacuum, has a large flow volume and is easily portable. Generally rotary vacuum pumps and blower motors are used for this purpose. A portable GEC vacuum-pressure pump (1/6 HP motor) was used to collect the TSP in our experiments.



(1) Filter holder assembly
 (a) Top cover with hood
 (b) Membrane filter
 (c) Filter holder base
 (d) Limiting orifice.

(2) Magnified view of circled region.
 (3) Top view of the filter holder base showing stainless steel mesh.

Fig. 4.4. A schematic diagram of the filter holder.

4.2.3 Collection of air particulate samples

The procedure for collecting suspended particulate matter consisted of the following steps :

- (i) Filter weighing before collection : A number of filters were weighed on a semimicro balance with a precision of $\pm 10 \mu\text{g}$. Some filters were marked as control filters to be weighed along with the sample deposited filters to avoid instrumental error. Weighing was done at 20°C and 75 % relative humidity.
- (ii) Collection of particulate matter : Sample holder was cleaned and a weighed filter was fixed in it. The 14 litre/min. limiting orifice was fixed and the whole assembly was connected to the vacuum port of the suction pump through a rotameter. The experimental arrangement is shown in Fig. 4.5. The filter holder was always pointed downwards to avoid big size particles settling on filter paper under gravity. Power was switched on and the pressure head was adjusted to give the specified flow rate. The samples were usually collected during day time, but some samples were also collected overnight. Normally 10 m^3 of air was passed through the filter. The collection of the TSP for air quality studies was done at a height of about 5 to 15 meters. Sampling at busy crossings and inside factories was done at breathing level (~ 2 meter). Samples were also collected from a motor-cycle exhaust and from a well maintained car under controlled conditions.

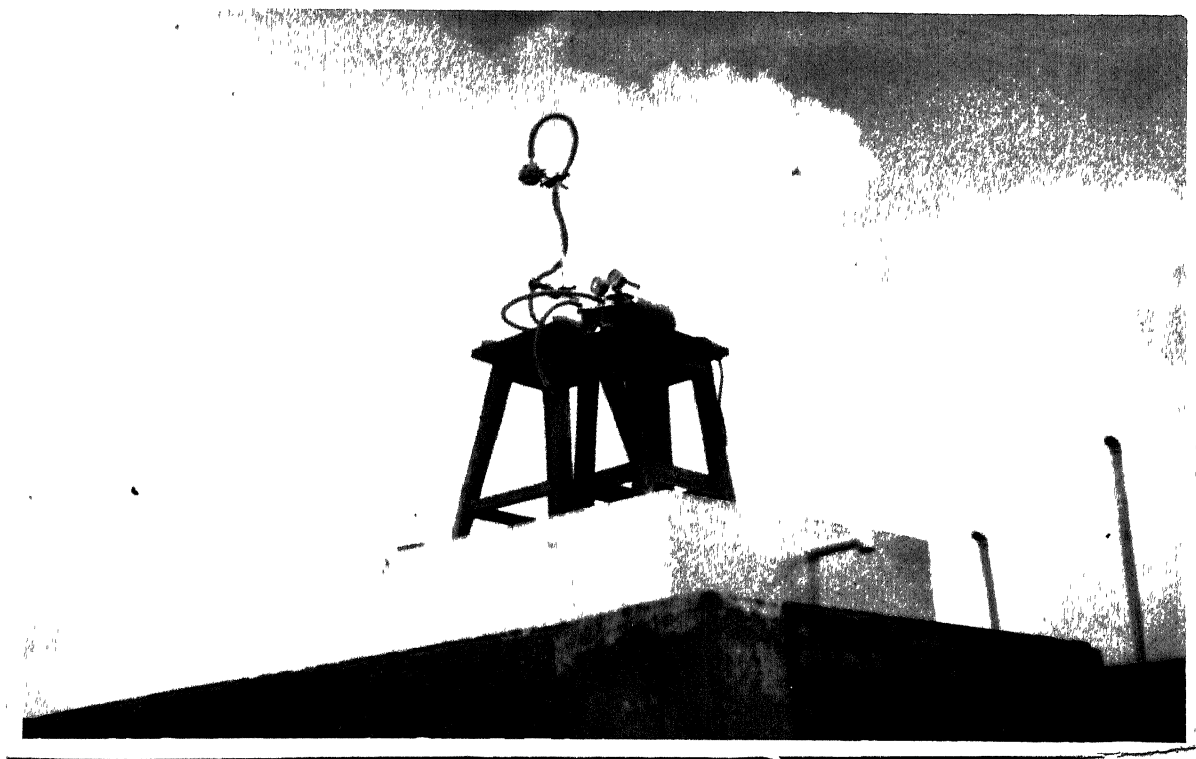


Fig. 4.5. Experimental arrangement for air particulate sampling.

(iii) Weighing of filter after collection : A deposited filter was weighed along with a set of control filters.

(iv) Data to be recorded : The following data were recorded at each sampling location. (1) place, (2) date, (3) filter code, (4) time at the start and at the end of sampling, (5) useful meteorological data (weather condition, temperature, wind direction etc.) and (6) collector's name.

(v) Calculation of the concentration of the TSF : The concentration of TSP in $\mu\text{g}/\text{m}^3$ was calculated from the filter weight and suction flow rate using the following equation

$$\text{TSP } (\mu\text{g}/\text{m}^3) = \frac{W_e - W_s}{V_{\text{NTP}}} \times 10^3 \quad (4.1)$$

where W_e is the filter weight after sampling (mg), W_s the filter weight before sampling (mg), and V_{NTP} is the air volume (m^3) at normal temperature and pressure (NTP).

Calculation of V_{NTP} was done as follows. The limiting orifice was calibrated using a wet test meter. The flow rate was measured before and after sampling. Average flow rate was found to be 13 litres/min. Knowing the total time of sampling the volume of the air sucked was calculated. To calculate the volume of the air at NTP the following formula was used

$$\frac{V_{\text{NTP}}}{V_t} = \frac{F_t}{F_{\text{NTP}}} \quad (4.2)$$

where, V_{NTP} - is the volume of air at NTP.
 V_t - is the volume of air at $t^{\circ}\text{C}$.
 ρ_t - is the density of air at $t^{\circ}\text{C}$.
 ρ_{NTP} - is the density of air at 25°C .

Values of the dry air density as a function of temperature are given [8] by

$$\rho_t = \frac{0.001293}{1 + 0.00367 t} \frac{H}{76} \text{ g/ml} \quad (4.3)$$

where, H - is the pressure in cm of Hg.
 t - is the temperature in $^{\circ}\text{C}$.

Substituting for ρ_t from eq. (4.3) in eq. (4.2) we have

$$V_{NTP} = V_t \frac{1.09175}{1 + 0.00367 t} \quad (4.4)$$

Concentration of the TSP was then calculated using eq. (4.1). A precision of $\pm 10 \mu\text{g}$ in weighing results in a precision of $1 \mu\text{g}/\text{m}^3$ for a sample volume of 10 m^3 .

Following the above method a large number of samples were collected in different zones during June 1979 to August 1979. Few samples were collected in each zone during November-December 1979 to study the effect of seasonal variation on the concentration of air particulate matter. Different kinds of deposition obtained is shown in Fig. 4.6. Sampling inside the factories and at busy crossings was also done during 1979. All samples were kept in air-tight plastic

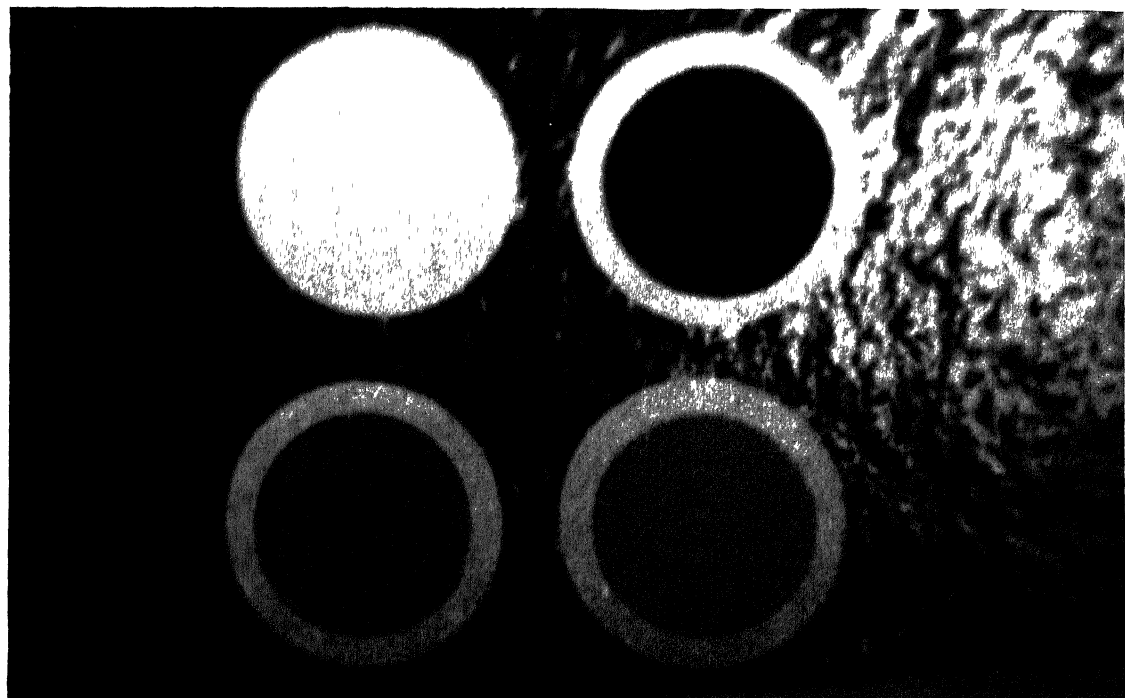


FIG. 4.6. Photograph of some air particulate samples collected on the filter paper.

boxes which were preserved in desiccators for elemental analysis. A total of about 70 samples were collected. The relevant data on sample collection will be presented and discussed in Chapter 5.

4.3 XRF Analysis

4.3.1 Data acquisition

The experimental arrangement to record the XRF spectra of air particulate samples is the same as that used for single element standards and is already described in Sec. 3.3. The gain of the amplifier was set to record an energy spectrum from 0 to 35 keV. Characteristic X-ray peaks generally obtained in the spectra are shown in Fig. 4.7. Each spectrum was collected in a 2048-channel multichannel analyzer for 15 to 20 hrs. In between the measurements of two samples an energy calibration run was made using a multi-element sample with known elements. Spectra were recorded for about 60 air particulate samples of different kinds. XRF spectra for five blank membrane filters were recorded to obtain the background due to impurities. We found that the elements Fe, Cu, Pb and Sn were present in the XRF spectra of blank filter papers.

4.3.2 Method of analysis

All the spectra were manually plotted and analyzed by following the steps outlined below. A computer program for curve-fitting was also developed and applied to some spectra,

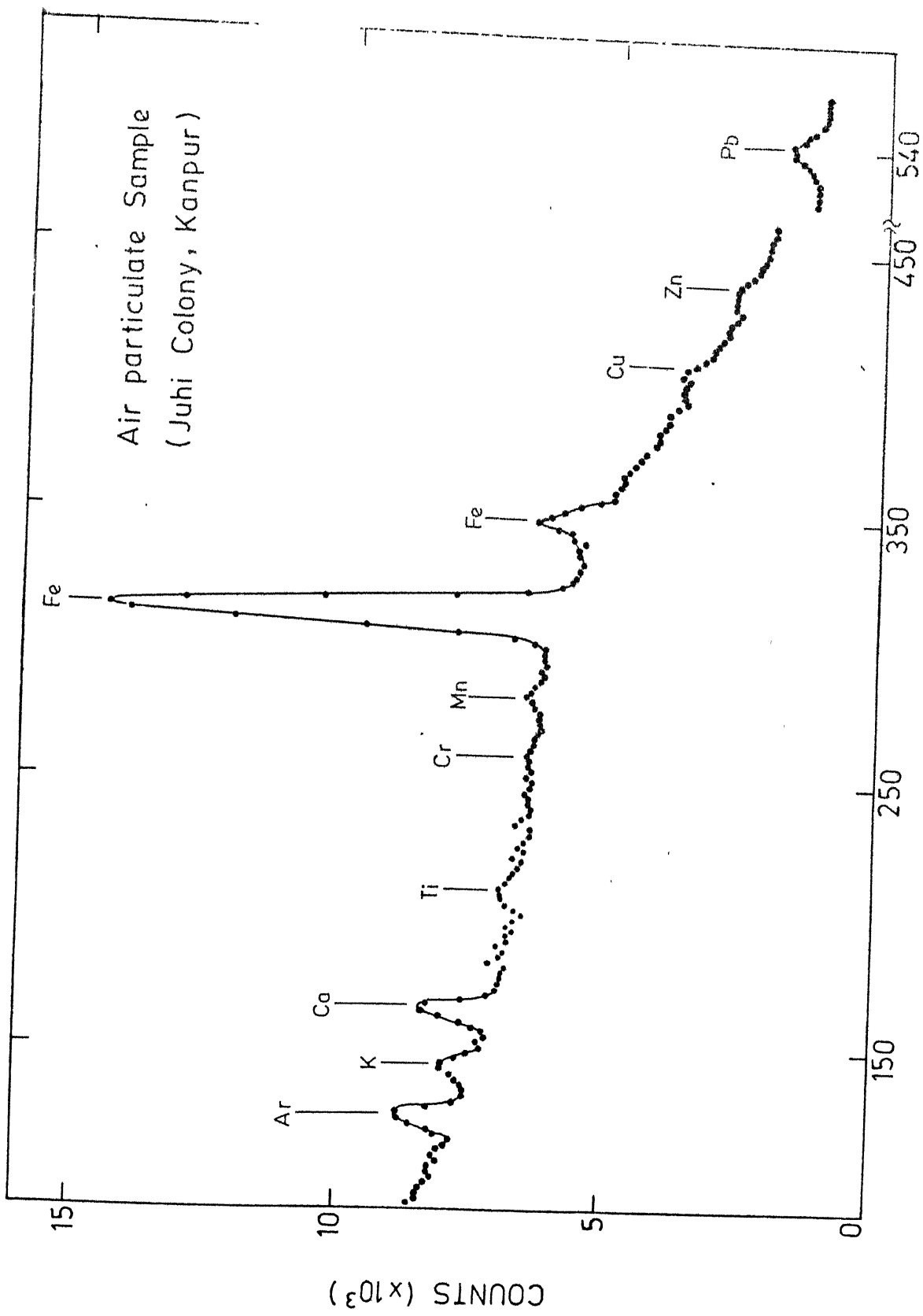


Fig. 4.7. A typical XRF spectrum of an air particulate sample.

to assure overselves of the consistency of the procedure used. A Gaussian function was used for the peak while the background was fitted to a function of the type $Y = A_1 x^2 + A_2 x + A_3 + (1/(1 + e^{(x-A_4)A_5}))$. The parameters A_1 to A_5 were found by a non-linear least square fitting method described by Bevington [9].

(i) Identification of elements :

The prominent peaks in the spectra were identified and their energies were calculated using energy calibration curve. Wherever necessary a three-point smoothening of the data was made for peak identification. Various elements were identified by their K_α X-ray energies. However, Pb was identified by L_α X-ray energy.

(ii) Calculation of the peak area :

The total area under different peaks was determined by summing the counts in the channels of the peaks. Background area was determined from the counts in the channels on each side of the peak and was subtracted from the total area to give net peak area. Number of counts per second (CPS) in the peak area was calculated by dividing the net peak area by the live time of spectrum collection. For elements from K to Fe it was necessary to correct for the spectral overlap of K_β and K_α lines of neighbouring elements. The K_β contribution was subtracted from the K_α line of neighbouring element by using experimentally determined K_β/K_α ratios. Another possible interference was the overlap of TiK_α with

BaL_α and experimental value of K_α/L_α for Ba was used whenever both the elements were present. For elements Fe, Cu, Pb it was necessary to correct the CPS for the impurities present in the background.

(iii) Matrix effects :

Matrix effects generally encountered in the XRF analysis are of two types (i) enhancement effect (ii) absorption effect. Enhancement effects are found to be negligible for thin specimens [10]. Rhodes et al. [11] defined a thin specimen as a mass m (g/cm^2) $< 0.1/\mu$, where μ (cm^2/g) is the sum of the specimen mass absorption coefficients for the excitation and fluorescent radiations. Such a mass would experience less than 5 % attenuation effect. For example, the critical value calculated for FeK_α X-rays excited in a deposition consisting of 95 % sand is $1600 \mu\text{g}/\text{cm}^2$. All the NIM samples and also air particulate samples had values of deposition well below thin specimen criteria. Hence these two effects were neglected. In addition to this two more effects viz. (i) particle size effects (ii) effects due to penetration of material in the filter paper, may cause serious errors in the concentration of low Z element upto Ca [12] in case of air particulate samples. Rhodes et al. [11] estimated the combined error due to these two sources to be less than 10 %. In our experiments we minimized these errors by using membrane filters (in which case penetration will be

small) and by avoiding collection of heavy particles.

(iv) Estimation of concentrations :

For thin specimens the concentration is directly proportional to the intensity. Concentration for all the elements were calculated using the equation

$$I_j = S_j M_j \quad (4.5)$$

where,

I_j - CPS corresponding to j th element.

S_j - is the sensitivity for j th element and is given in Table 3.2.

The conversion of m_j ($\mu\text{g}/\text{cm}^2$) to $\mu\text{g}/\text{m}^3$ was done using the equation

$$q_j = \frac{m_j A}{V_{NTP}} \quad (4.7)$$

where,

A - is the area of the deposition.

V_{NTP} - volume of the air in m^3 sucked at NTP.

m_j ($\mu\text{g}/\text{cm}^2$) was converted to ppm by using the equation

$$M_j = \frac{m_j}{x} \times 10^3 \quad (4.8)$$

where x is the deposition of the air particulate matter in mg/cm^2 .

v) Error analysis :

The statistical uncertainty in the peak areas is the

REFERENCES

1. F.L. Ludwig, Environ. Sci. Technol., 7, 774 (1978).
2. G.B. Morgan and G. Ozolins, Introduction to the Scientific Study of Atmospheric Pollution, D. Reidel Publishing Company, Dordrecht-Holland (1971), p. 152.
3. G.M. Hidy and S.K. Friedlander, Proc. 2nd IUAPPA Clean Air Congr., (1971), p. 391.
4. K.A. Rahn and R.P. Harrison, Proc. of the Conference on Atmosphere Surface Exchange of Particulate and Gaseous Pollution, CONF-740921, NTIS (1974), p. 557.
5. R.N. Solomon and J.W. Hartford, Environ. Sci. Technol., 10, 773 (1976).
6. Federal Register 44, (92) : 27557 (May 10, 1979).
7. K. Oikawa, Trace Analysis of Atmospheric Samples, John Wiley and Sons, (1977), p. 22.
8. C.D. Hodgman, ed., Hand Book of Chemistry and Physics, Chemical Rubber Publishing Co., (1962), p. 2163.
9. P.R. Bevington, Data Reduction and Error Analysis for the Physical Sciences, McGraw-Hill Inc., New York (1969), p. 204.
10. R.D. Giaque, F.S. Goulding, J.M. Jaklevic and R.H. Pehl, Anal. Chem., 45, 671 (1973).
11. J.R. Rhodés, A.H. Pradzynski, R.D. Sieberg, CSI Internal Report No. 116 (1972).
12. T.G. Dzubay and R.O. Nelson, Advan. in X-ray Anal., 18, 619 (1975).

Chapter 5

RESULTS AND DISCUSSION

5.1 Analysis of the Air Quality Data of Kanpur City

5.1.1 Introduction

Accounting for the elemental composition of air particulate matter has been the long term objective in the investigations of the atmospheric aerosol. The measured levels of heavy metals can serve as an index of the extent of pollution and can be used to compare environmental pollution in different areas. The elemental concentration data can be of help in foreseeing and preventing possible health hazards. Further analysis of elemental data by various methods like calculation of the enrichment factor, correlation analysis and determination of the weightage factors by factor analysis can give information about the sources of pollution. We performed the following analysis of the data in order to gather maximum information about the inter-relationships among the various elements with an aim to identify the processes which influence the concentration and distribution of atmospheric particulate species.

The first step in the analysis is a comparison of the levels of total suspended particulates(TSP) and the concentrations of other elements in Kanpur city with those in the other cities of the world (including Bombay). Contribution from the elements of soil origin and from

anthropogenic sources to the TSP is estimated. A zone-wise analysis of the air quality data is performed to understand the level of pollution in each zone. Some observations about the distribution of the levels of the TSP and elements according to month, wind direction and season are also made. These results are presented in Section 5.1.2.

In Section 5.1.3 we calculate the enrichment factors (EF) for all elements to determine the relative importance of natural and anthropogenic sources of pollution. EFs for various elements in Kanpur are compared with those for other polluted areas and also with those found in natural aerosols. Zone-wise analysis of EFs is made.

The method of calculation of correlation coefficients is discussed and the correlation coefficient matrices for all possible element pairs and the TSP in zone A, B and C are presented in Section 5.1.4. The correlations among various elements point out clusters of elements of same origin or similar behaviour in the atmosphere.

In Section 5.1.5 the application of factor analysis method to the air quality data is discussed. We have first outlined the method of computing factor loadings starting from the correlation matrix. The factor patterns obtained for zone A, B and C help in understanding the nature of sources of various pollutants in these zones.

Results of XRF analysis of air particulate matter collected at breathing level at various busy crossings are

presented and discussed in Section 5.2. Here also analysis of the data is performed in terms of EFs, correlation coefficients and factor analysis. Comparison of the data is done with the air quality data obtained at nearby locations.

In Section 5.3 we have compared the levels of various elements obtained in work-room atmosphere of various factories with the recommended maximum values.

The summary of the present work, its major findings and the conclusions drawn are given in Section 5.4.

5.1.2 Levels of TSP and amounts of trace elements in Kanpur city

Normally TSP and metal concentrations follow a log-normal distribution [1] and air quality data are presented in terms of the geometric mean. A few workers have also reported air quality data in terms of arithmetic averages [2,3]. In our analysis the levels of TSP and trace metals in Kanpur city appeared to follow a log-normal distribution. In Table 5.1 we have reported the values of TSP and metal levels obtained for Kanpur city in the present work as well as similar data reported for other cities. These data are given in terms of the values for the geometric mean and the standard deviation over the entire set of data collected during June 1979 to September 1979 and during November and December 1979. Arithmetic averages for the concentration data are also calculated and these results are given in Table 5.2. From Table 5.1 it can be seen that the TSP

Table 5.1

Geometric Mean and Standard Deviation for Metals and TSP Concentration ($\mu\text{g}/\text{m}^3$) in Kanpur and Some Other Cities.

Place Method Used Element	Kanpur, India [Present Work] XRF	Bombay, India INAA	Rio de Janeiro, Brazil [1] AA	New York J.S.A. [6] AS	Tel-Aviv, Israel [7] -
TSP	279 \pm 3	-	-	103 \pm 0.002	52.5
K	18.591 \pm 0.002	-	-	1.504 \pm 0.002	0.099
Ca	14.117 \pm 0.003	-	-	-	-
Ti	2.466 \pm 0.002	-	-	-	-
V	0.626 \pm 0.002	-	-	0.031 \pm 0.001	0.0388
Cr	0.966 \pm 0.002	-	-	0.022 \pm 0.002	0.0085
Mn	0.769 \pm 0.002	-	-	0.055 \pm 0.002	0.019
Fe	9.038 \pm 0.003	6.606 \pm 0.003	-	2.467 \pm 0.001	1.012
Ni	0.219 \pm 0.002	-	-	0.016 \pm 0.002	0.0352
Cu	0.147 \pm 0.003	0.451 \pm 0.002	-	0.025 \pm 0.002	0.0439
Zn	0.336 \pm 0.003	0.557 \pm 0.002	-	0.298 \pm 0.002	0.293
Pb	0.357 \pm 0.002	0.287 \pm 0.002	-	0.518 \pm 0.002	1.074
					0.370

Table 5.2

Arithmetic Mean Values and Standard Deviation ($\mu\text{g}/\text{m}^3$) of TSP and Elemental Concentration in Kanpur and Some Other Cities.

Place Method Element	South U.S.A. AAS	Arizona, U.S.A. [3]	Kellog, Idaho U.S.A. [2] INAA and XRF	Boston U.S.A. [4] INAA	Kanpur, India (Present Work) XRF
TSP	111 \pm 72.9	148 \pm 47	-	-	443 \pm 457
K	2.6 \pm 2.1	1.110	-	-	23.933 \pm 17.204
Ca	5.3 \pm 3.4	0.583	-	-	22.758 \pm 25.425
Ti	0.39 \pm 0.30	0.0957	-	-	4.101 \pm 7.276
V	-	0.002	0.725 \pm 0.50	0.805 \pm 0.531	-
Cr	0.0040 \pm 0.0034	0.0068	0.0034 \pm 0.0055	1.391 \pm 1.402	-
Mn	0.055 \pm 0.044	0.071	0.027 \pm 0.019	0.977 \pm 0.666	-
Fe	2.9 \pm 2.1	1.835	1.09 \pm 1.0	15.516 \pm 18.268	-
Ni	0.0060 \pm 0.0036	-	-	-	0.255 \pm 0.124
Cu	0.19 \pm 0.07	0.186	-	-	0.214 \pm 0.181
Zn	0.17 \pm 0.11	4.620	0.190 \pm 0.220	0.554 \pm 0.556	-
Pb	0.69 \pm 0.45	10.800	-	-	0.553 \pm 0.772

*A large standard deviation is due to the average over a large number of sites covered in the present study.

concentration in Kanpur is comparable to that in Tel-Aviv, Israel but is very high compared to New York, U.S.A. and Rio de Janeiro, Brazil. This value is also high compared to other cities in the U.S.A. like Chicago ($86.5 \mu\text{g}/\text{m}^3$), Cincinnati ($74.3 \mu\text{g}/\text{m}^3$), Philadelphia ($58.5 \mu\text{g}/\text{m}^3$), Washington, D.C. ($56.3 \mu\text{g}/\text{m}^3$) [8]. The elemental values in Kanpur for K, Ca, Ti, V, Cr, Mn, Fe, Ni, and Cu are very high compared to those in other places. The averages shown for Cr, V, Ni and Mn in Kanpur are on the higher side because these elements were present in amounts below the detection limit at some locations. For Zn the value obtained at Kanpur is comparable with that at Rio de Janeiro and New York. The concentration of Pb in Kanpur as well as in Bombay are lower than at Rio de Janeiro and New York but is comparable with the value at Tel-Aviv. Concentration of Cu and Zn appear to be higher in Bombay than in Kanpur indicating high level of pollution due to industrial emission in Bombay. From Table 5.2 except for Pb, Cu and Zn all the values obtained at Kanpur are higher than at South Arizona, U.S.A. [3], Kellog, Idaho, U.S.A. [2] and Boston, Massachusetts, U.S.A. [4]. Very high values of Zn and Pb at Kellog are due to a lead smelting complex nearby. Values of Cu in Kanpur, South Arizona and Kellog are comparable.

The concentration of the TSP obtained in the present work compares well with the earlier results reported by Yennawar et al. [9] ($488 \mu\text{g}/\text{m}^3$) and Sharma et al. [10] ($490 \mu\text{g}/\text{m}^3$) obtained in the year 1968 and 1970 to 1971

respectively. Very high concentrations of elements like K, Ca, Ti and Fe originating in the soil appear to be one of the reasons for high value of the TSP. Another reason may be high content of the organic matter in TSP. The very high value of the TSP in Kanpur may be due to the totally uncontrolled and unplanned development of Kanpur city. The dusty traffic roads as well as the climate of Kanpur city could also play an important part in this characteristic. In deciding the air quality criteria for TSP in India it seems necessary that a background level of the TSP should be fixed first and it should be based on studies in different parts of the country. The level of pollution should be measured with respect to the background level.

Assuming that the observed concentration of K, Ca, Ti and Fe are mainly due to soil dispersion source, we calculated the percentage (%) of these elements in the TSP concentration. It was found that the TSP in Kanpur had the highest contribution due to these elements (15 %) whereas in Kellogg, Idaho, U.S.A. it was only 2.4 %. Percentage of Cu, Mn and Pb in the concentration of TSP was found to be the highest in New York (2.6 %) whereas in Kanpur it was 0.3 %. To further estimate the influence of natural sources on TSP and elemental levels, we have calculated EPs and the results are discussed in next section.

Monthly analysis of the TSP data indicates that during the period of our observation maximum concentrations

occur in the month of November. For elements K, Ti, Zn and Pb highest concentration occurred in December whereas for Fe and Ca it occurred in November. This may be due to the greater fuel (fossil and coal) consumption and also because of the increased frequency of temperature inversions during those months. Similar observation is also made by McDonald et al. [11] for the atmosphere of Glasgow, U.K. We also noticed that still weather and westerly winds are generally associated with high concentrations of the TSP.

5.1.3 Zone-wise analysis of Kanpur air quality results

Tables 5.3(a), 5.3(b) and 5.3(c) give the description of the TSP data collected at different locations in Kanpur city. Fig. 5.1 shows the concentration of TSP at different locations by a colour code which is explained in the figure. Tables 5.4(a), 5.4(b) and 5.4(c) show the elemental concentrations at different locations in zone A (mainly thickly populated), zone B (mainly thinly populated) and zone C (mainly industrial). The numbers in the brackets in Tables 5.4 are the statistical errors in the peak area and the blanks indicate a value below the detection limit. The actual error in the measurement will be larger than the statistical error mentioned because of the spectral overlap and also because of the systematic error bounds (10-15 %). In our experiments we find that the statistical errors are quite large and can be reduced with further refinement of the technique. The data on elemental concentration is also

Table 5.3(a)

Information about the Air Particulate Samples Collected in Thickly Populated Zone A.

Site No. in Fig. 5.1	Place	Date	Deposi- tion μg/m ³	Tempe- rature °C	Wind Direction
4	Shastri Nagar	17.6.79 and 18.6.79	264	35.1	E → W
7	Gandhi Nagar	30.6.79	352	34.2	W → E
7	Gandhi Nagar	17.11.79	566	36.4	E → W
9	Ghantaghar	13.7.79	644	36.0	Still
9	Ghantaghar	23.11.79	1136	31.4	Still
12	Transport Nagar	20.7.79	628	32.4	Still
12	Transport Nagar	24.8.79	1306	34.9	W → E
12	Transport Nagar	22.11.79	971	30.8 35.3	Still E → W
15	General Ganj	2.8.79	71	35.3	E → W
15	General Ganj	15.11.79	2204	36.6	E → W
19	Dhan Kutty	18.8.79	118	34.0	W → E
20	Rail Bazar	19.8.79	101	34.0	W → E
24	Govind Nagar	11.9.79 and 12.9.79	234	32.0	W → E
24	Govind Nagar	8.12.79 and 9.12.79	433	28.0	Still
28	Bajaria Police Station	17.11.79	636	36.0	Still

Table 5.3(b)

Information about the Air Particulate Samples Collected in Thinly Populated Zone B.

Site No. in Fig. 5.1	Place	Date	Depo- sition µg/m ³	Tempe- rature °C	Wind Direction
1	I.I.T.	8.6.79 and 9.6.79	876*	34.0	E --> W
1	I.I.T.	1.9.79	36	33.4	W ---- E
29	I.I.T.	24.11.79 and 25.11.79	320	31.0	W --> E
33	I.I.T.	21.12.79	138	18.2	W ---- E
33	I.I.T.	22.12.79	85	13.3	Still
33	I.I.T.	22.12.79	77	21.3	Still
34	I.I.T.	26.12.79	143	25.0	W ----> E
2	Swaroop Nagar	12.6.79 and 13.6.79	242	32.5	NE ----> SW
3	Azad Nagar	15.6.79	237	32.1	E --> W
5	Phool Bazar (LIC)	19.6.79 and 20.6.79	249	42.6	E --> W
10	Kidwai Nagar	19.7.79	103	31.4	E --> W
14	Ashok Nagar	12.11.79	66	33.5	E --> W
14	Ashok Nagar	12.11.79	573	36.0	Still
16	Naveen Market	3.8.79	56	35.3	E --> W
16	Naveen Market	13.11.79	631	36.8	Still
17	Swaroop Nagar	6.8.79	86	35.8	E --> W
21	Defence Lab.	22.8.79 and 23.8.79	97	35.8	W ----> E
23	Kalyanpur	3.9.79	231	36.1	W ----> E
23	Kalyanpur	4.9.79	163	34.6	W ---- E
25	Armapur	12.9.79 and 13.9.79	139	31.8	NW ----> SE
31	H.B.T.I.Qrts.	12.12.79	198	25.0	Still

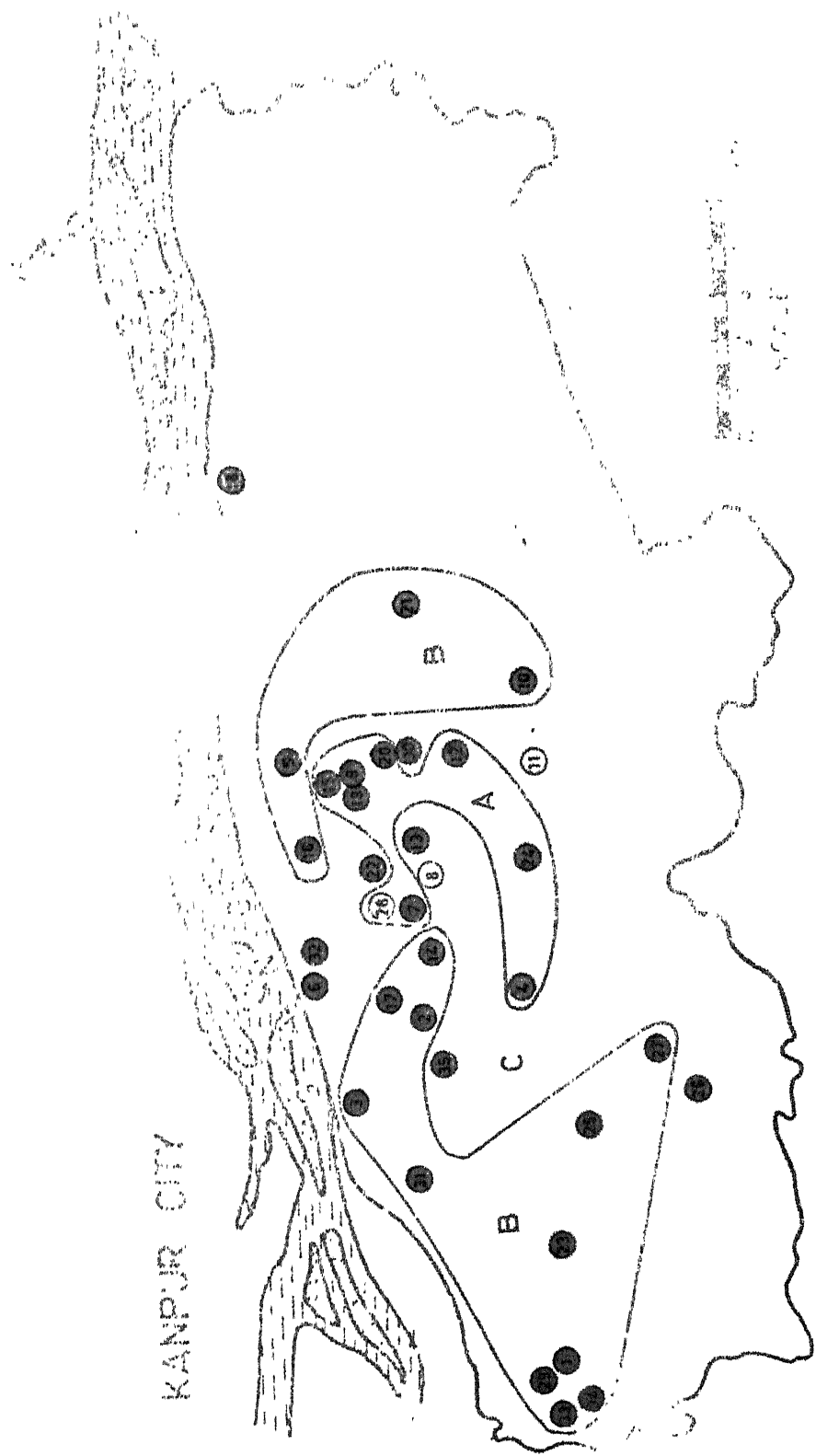
*This large value is perhaps due to the smoke and soot from Panki Thermal Power Station.

Table 5.3 (c)

Information about the Air Particulate Samples Collected in Industrial Zone C.

Site No. in Fig. 5.1	Place	Date	Depo- sition μg/m ³	Tempe- rature °C	Wind Direction
6	Souter Ganj	26.6.79 and 27.6.79	89	39.2	E \dashv W
6	Souter Ganj	5.12.79	207	35.2	EW \dashv WS
32	Souter Ganj	16.12.79	159	25.0	N \dashv S
8	Jareeb Chowky	7.7.79 and 9.7.79	389	36.0 and 28.5	NW \dashv SE and E \dashv W
8	Jareeb Chowky	14.11.79	1069	36.6	Still
11	Juhu Labour Colony	19.7.79	326	31.4	S \dashv W
11	Juhu Labour Colony	21.11.79	799	32.8	Still
13	Anwar Ganj	30.7.79	236	33.0	E \dashv W
18	Jajmau	7.8.79	173	34.0	E \dashv W
22	Chaman Ganj	30.8.79 and 31.8.79	327	36.6	W \dashv E
22	Chaman Ganj	18.11.79	545	33.8	Still
26	IEL	13.9.79	33	34.7	Still
27	Dada Nagar	14.9.79	233	35.1	E \dashv W and W \dashv E
30	Harris Ganj	10.12.79	1648	25.0	E \dashv W
35	Rawatpur	27.12.79	465	25.0	W \dashv E

KANPUR CITY



- Between 500 - 800 $\mu\text{g}/\text{m}^3$
- Above 800 $\mu\text{g}/\text{m}^3$
- Below 200 $\mu\text{g}/\text{m}^3$
- Between 200 - 500 $\mu\text{g}/\text{m}^3$

Fig. 5.1. Map of Kanpur city showing levels of air particulate matter at various locations. The levels are indicated by a colour code

Table 5.4(a)

TSP and Elemental Concentrations ($\mu\text{g}/\text{m}^3$) at Various Locations in Thickly Populated Zone A.

Location	Site No. in Fig. 5.1	TSP	K	Ca	Ti	V	Cr
Shastri Nagar	4	272	-	10.823 (6.7)	1.322 (19.7)	-	-
Gandhi Nagar	7	363	-	2.006 (68.6)	2.908 (13.2)	-	-
Gandhi Nagar	7	589	27.262 (8.7)	22.889 (4.3)	1.981 (13.8)	-	4.072 (4.4)
Ghantaghar	9	663	30.100 (6.8)	35.135 (2.4)	4.736 (5.6)	1.111 (12.2)	0.743 (18.0)
Ghantaghar	9	1160	47.764 (3.6)	51.001 (2.7)	5.111 (5.3)	-	-
Transport Nagar	12	644	26.834 (8.9)	36.928 (2.8)	2.064 (13.5)	-	-
Transport Nagar	12	1350	37.717 (4.6)	56.646 (2.0)	2.551 (12.4)	-	2.193 (9.1)
Transport Nagar	12	990	24.588 (10.9)	70.031 (1.9)	2.554 (13.0)	-	1.485 (15.3)
General Ganj	15	73	-	5.873 (12.5)	-	-	-
General Ganj	15	2290	96.201 (2.4)	133.417 (0.8)	9.369 (2.9)	1.847 (7.6)	1.201 (10.1)
Chan Kutty	19	121	-	12.968 (4.5)	-	-	-
Rail Bazar	20	104	-	8.500 (9.8)	-	-	-
Govind Nagar	24	240	24.428 (9.6)	15.709 (6.1)	2.328 (8.6)	-	-
Govind Nagar	24	437	23.123 (8.2)	15.906 (4.8)	2.836 (7.5)	-	-
Bajaria Police Station	28	659	22.601 (9.3)	13.641 (6.1)	2.646 (9.1)	-	1.04 (16.)

Continued

Table 5.4(a)

Elemental Concentrations ($\mu\text{g}/\text{m}^3$) at Various Locations in Thickly Populated Zone A.

Location	Site N ^o . in Fig. 5.1	Mn	Fe	Ni	Cu	Zn	Pb
Shastri Nagar	4	-	9.009 (1.3)	-	-	0.684 (3.5)	0.295 (9.2)
Gandhi Nagar	7	1.276 (16.2)	9.835 (1.8)	-	0.339 (9.9)	0.713 (5.6)	0.293 (11.4)
Gandhi Nagar	7	0.963 (14.2)	18.836 (0.9)	-	0.259 (28.8)	2.233 (1.4)	0.288 (8.7)
Ghantaghar	9	2.439 (5.1)	27.376 (0.5)	-	0.083 (11.4)	0.649 (4.0)	0.518 (4.9)
Ghantaghar	9	2.509 (4.5)	35.082 (0.4)	-	0.125 (10.7)	0.786 (3.8)	0.643 (4.2)
Transport Nagar	12	1.199 (13.3)	24.074 (0.6)	0.353 (14.1)	0.463 (7.2)	0.424 (7.1)	0.211 (11.9)
Transport Nagar	12	1.458 (9.4)	27.023 (0.4)	0.332 (14.8)	0.135 (13.8)	0.531 (5.9)	1.149 (2.9)
Transport Nagar	12	0.873 (17.9)	22.804 (0.8)	0.415 (14.4)	0.216 (10.4)	0.371 (9.7)	0.419 (7.7)
General Ganj	15	-	1.428 (3.1)	0.502 (6.5)	0.185 (8.9)	0.197 (10.7)	0.286 (7.8)
General Ganj	15	2.265 (6.6)	88.987 (0.2)	0.232 (18.8)	0.333 (7.9)	1.813 (1.7)	1.590 (2.1)
Dhan Kutty	19	-	6.302 (1.2)	-	0.084 (11.0)	1.390 (1.6)	0.289 (8.3)
Rail Bazar	20	-	9.114 (1.6)	0.158 (27.7)	0.088 (13.0)	0.128 (21.2)	0.238 (9.3)
Govind Nagar	24	-	10.870 (1.0)	-	0.061 (15.4)	0.330 (17.4)	1.715 (1.6)
Govind Nagar	24	0.322 (34.1)	13.603 (0.9)	-	0.187 (10.5)	0.315 (6.7)	0.430 (5.2)
Bajaria Police Station	28	1.108 (10.9)	22.239 (0.6)	-	0.295 (7.8)	1.372 (2.1)	2.284 (1.4)

Table 5.4(b)

TSP and Elemental Concentrations ($\mu\text{g}/\text{m}^3$) at Various Locations in Thinly Populated Zone B.

Location	Site No. in Fig. 5.1	TSP	K	Ca	Ti	V	Cr
Swaroop Nagar	2	248	4.416 (24.0)	6.174 (9.6)	0.858 (16.9)	-	-
Azad Nagar	3	243	9.898 (12.2)	26.283 (2.3)	0.976 (17.4)	-	0.499 (22.9)
Phool Bagh	5	264	11.547 (11.2)	6.960 (6.8)	1.328 (12.4)	0.204 (28.8)	0.312 (30.3)
Kidwai Nagar	10	105	18.840 (25.1)	11.665 (14.5)	-	0.247 (30.7)	0.394 (33.5)
Ashok Nagar	14	68	-	6.253 (20.4)	-	-	-
Ashok Nagar	14	596	28.664 (5.5)	24.886 (2.6)	7.111 (7.9)	0.824 (15.3)	0.499 (21.3)
Navcen Market	16	58	-	9.610 (13.7)	-	-	-
Navcen Market	16	656	32.452 (5.5)	34.936 (2.2)	2.080 (10.5)	-	0.344 (17.5)
Swaroop Nagar	17	89	-	8.626 (8.77)	-	-	-
Defense Lab.	21	97	3.962 (26.8)	14.179 (3.6)	0.572 (23.5)	0.477 (27.5)	0.430 (23.4)
I.I.T.	1	37	14.754 (7.4)	39.421 (1.3)	0.597 (26.6)	-	0.369 (28.5)
Kalyanpur	23	239	21.088 (6.8)	24.385 (2.5)	1.815 (10.1)	-	1.076 (11.3)
Kalyanpur	23	169	10.344 (17.2)	4.784 (9.6)	-	-	-
Armapur	25	142	2.327 (23.8)	4.322 (6.1)	1.211 (19.6)	-	-
I.I.T.	29	326	8.447 (23.3)	5.557 (14.3)	4.049 (6.4)	-	6.054 (2.8)
H.B.T.I. Qrts.	31	198	31.872 (4.2)	12.068 (4.2)	-	-	-
I.I.T.	34	143	1.655 (54.4)	-	-	-	-

Continued

Table 5.4(b)

Elemental Concentrations ($\mu\text{g}/\text{m}^3$) at Various Locations in Thinly Populated Zone B.

Location	Site No. in Fig. 5.1	Mn	Fe	Ni	Cu	Zn	Pb
Swaroop Nagar	2	-	7.064 (1.1)	-	0.055 (12.7)	0.083 (17.3)	0.089 (15.0)
Azad Nagar	3	0.393 (21.1)	11.726 (1.4)	-	0.122 (13.6)	0.307 (8.9)	0.174 (12.3)
Phool Bagh	5	1.007 (7.8)	10.033 (0.8)	-	0.007 (13.9)	0.069 (26.1)	0.099 (12.6)
Kidwai Nagar	10	0.255 (37.8)	9.823 (3.1)	-	0.485 (16.0)	0.480 (12.3)	0.446 (14.1)
Ashok Nagar	14	2.079 (5.6)	1.273 (3.3)	-	0.071 (12.7)	0.228 (10.2)	0.278 (7.0)
Ashok Nagar	14	0.773 (12.9)	14.024 (0.7)	-	0.168 (10.0)	0.564 (3.7)	0.285 (6.5)
Naveen Market	16	-	1.109 (4.3)	-	0.050 (16.0)	-	-
Naveen Market	16	0.514 (21.0)	31.072 (0.4)	-	0.525 (6.0)	0.443 (5.1)	0.543 (4.1)
Swaroop Nagar	17	-	3.352 (2.2)	-	0.014 (16.0)	0.027 (17.0)	0.200 (8.5)
Defence Lab.	21	-	6.989 (1.0)	-	0.944 (9.2)	-	0.268 (5.3)
I.I.T.	1	0.232 (28.4)	5.136 (1.6)	-	0.063 (10.4)	0.126 (9.4)	0.228 (5.1)
Kalyanpur	23	0.271 (26.7)	13.122 (0.8)	0.225 (13.3)	-	0.135 (14.6)	0.205 (8.1)
Kalyanpur	23	-	7.529 (1.3)	-	-	-	0.232 (10.7)
Armapur	25	0.270 (15.5)	0.753 (2.3)	0.057 (20.8)	0.157 (4.8)	0.070 (10.8)	0.165 (5.1)
I.I.T.	29	-	6.686 (1.6)	0.119 (23.6)	-	0.161 (13.3)	0.142 (10.3)
H.B.T.I. Qrts.	31	-	4.359 (1.7)	-	0.062 (9.0)	-	0.338 (7.9)
I.I.T.	34	-	3.828 (2.6)	-	0.396 (0.7)	0.257 (10.8)	0.148 (14.9)

Table 5.4(c)

TSP and Elemental Concentrations ($\mu\text{g}/\text{m}^3$) at Different Locations in Industrial Zone C.

Location	Site No. in Fig. 5.1	TSP	K	Ca	Ti	V	Cr
Souter Ganj	6	93	-	3.280 (20.0)	-	-	-
Souter Ganj	32	159	-	7.001 (13.7)	-	-	-
Jareeb Chowky	8	509	24.802 (8.8)	22.610 (3.3)	1.163 (25.0)	-	0.882 (19.1)
Jareeb Chowky	8	1112	31.831 (7.5)	51.064 (2.2)	4.579 (6.7)	-	-
Juhu Colony	11	333	10.226 (15.7)	5.124 (12.5)	-	-	1.067 (12.2)
Juhu Colony	11	820	24.934 (8.7)	16.595 (5.1)	2.496 (10.5)	-	2.710 (19.2)
Anwar Ganj	13	242	6.798 (31.0)	13.953 (6.6)	-	-	-
Jajmau	18	178	43.696 (3.5)	19.919 (3.3)	-	-	-
Chaman Ganj	22	340	18.933 (7.1)	21.927 (2.5)	2.115 (7.2)	-	-
Chaman Ganj	22	565	40.310 (6.7)	31.269 (3.5)	3.335 (8.9)	0.927 (24.3)	1.417 (14.9)
JEL	26	34	-	4.943 (13.0)	-	-	1.03 (14.9)
Dada Nagar	27	241	-	3.535 (13.8)	-	-	-
Harris Ganj	30	1648	112.27 (2.0)	97.600 (1.0)	41.248 (0.8)	-	-
Rawatpur	35	465	17.791 (9.5)	14.820 (4.8)	2.992 (7.4)	-	-

Continued

Table 5.4(c)

Elemental Concentrations ($\mu\text{g}/\text{m}^3$) at Different Locations in Industrial Zone C.

Location	Site No. in Fig. 5.1	Mn	Fe	Ni	Cu	Zn	Pb
Souter Ganj	6	0.348 (25.0)	2.148 (2.6)	0.106 (28.7)	-	0.128 (14.7)	0.160 (10.3)
Souter Ganj	32	-	0.935 (3.8)	0.320 (13.9)	0.149 (11.0)	0.163 (17.2)	0.391 (7.5)
Jacob Chowky	8	0.772 (24.9)	19.766 (0.8)	-	0.142 (13.1)	0.538 (5.0)	0.429 (6.0)
Jacob Chowky	8	1.049 (14.2)	46.617 (0.4)	-	0.352 (8.2)	1.066 (3.3)	0.527 (5.4)
Juhu Colony	11	-	3.175 (2.2)	-	0.160 (9.5)	0.363 (6.3)	1.138 (2.3)
Juhu Colony	11	0.753 (15.6)	17.691 (0.7)	0.139 (28.0)	0.171 (10.1)	0.283 (9.9)	0.500 (5.2)
Anwar Ganj	13	-	8.188 (1.4)	-	-	0.200 (12.8)	0.179 (12.5)
Jajmau	18	-	5.291 (1.5)	-	0.046 (10.6)	0.022 (8.3)	0.117 (17.1)
Chaman Ganj	20	0.427 (18.1)	14.960 (0.6)	0.295 (14.4)	0.165 (8.7)	1.363 (1.3)	0.226 (6.2)
Chaman Ganj	20	0.795 (17.2)	18.781 (0.9)	0.315 (16.4)	0.366 (8.1)	0.459 (7.3)	0.642 (5.4)
IEL	26	-	2.373 (2.3)	-	-	-	0.319 (6.4)
Dada Nagar	27	0.640 (13.1)	9.507 (1.0)	-	-	0.211 (8.8)	0.539 (3.6)
Harris Ganj	30	1.399 (8.9)	86.340 (0.3)	-	0.445 (5.7)	2.147 (1.5)	4.751 (1.0)
Rawatpur	35	-	13.518 (0.8)	-	0.220 (7.5)	0.904 (2.9)	0.462 (4.9)

represented by a colour code in Figs. 5.2 to 5.12 for the elements K, Ca, Ti, V, Cr, Mn, Fe, Ni, Cu, Zn and Pb. Usually the concentration levels were divided into four classes, viz. i) below detection limit : This class consists of those sampling sites where a particular element could not be detected, ii) below a certain minimum concentration level ($x \mu\text{g}/\text{m}^3$), iii) between x and an intermediate concentration y , iv) above $y \mu\text{g}/\text{m}^3$.

In zone A the sites 9, 12 and 15 show maximum values for TSP, the sites 4, 7, 24 and 28 have intermediate TSP concentrations whereas the sites 19 and 20 show low value of the TSP. The locations 9, 12 and 15 involve very high traffic density in addition to a large population density. The levels of K, Ca, Ti and Fe are high at these locations compared to those at other locations; but the levels of Cu, Zn and Pb are comparable with those at 7 and 28. This may be due to the fact that K, Ca, Ti and Fe are found mainly on large particles [12] whereas Cu, Zn and Pb are found in small particles and are dispersed over larger areas.

In zone B the sites 1, 2, 3, 14, 16, 27, 29 and 5 have TSP values between 200 to $500 \mu\text{g}/\text{m}^3$ while at other sites the TSP values are less than $200 \mu\text{g}/\text{m}^3$. The level of pollution is lower than that in zones A and C. An interesting feature in this zone is the variation in elemental and TSP concentrations at different locations (1, 29, 34) in IIT. (Site 33 is not included in the analysis because air particulate sampling was done for very small time). This

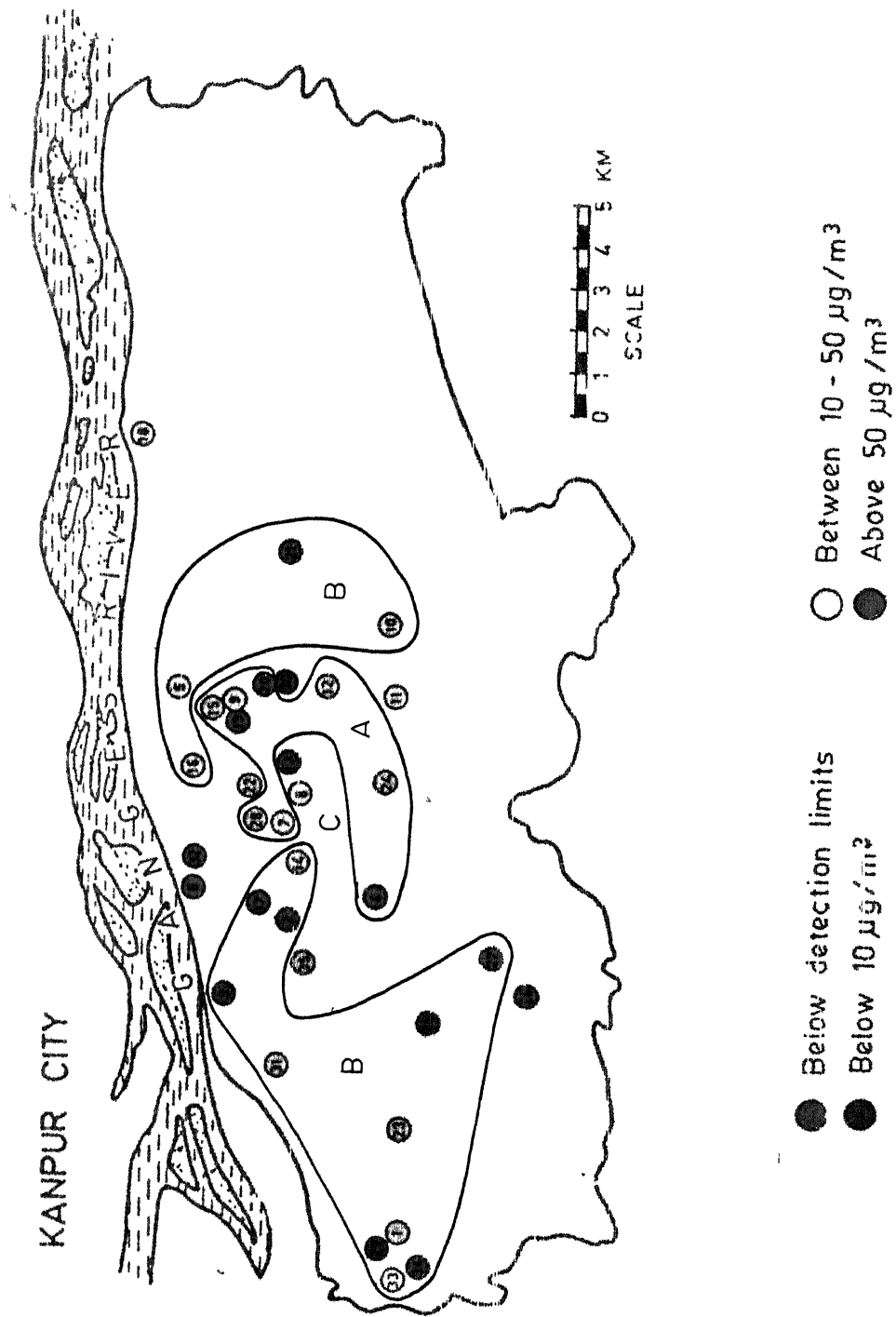


Fig. 5.2. Map of Kanpur city showing level of Potassium detected in air particulate samples at various locations. The levels are indicated by colour code.

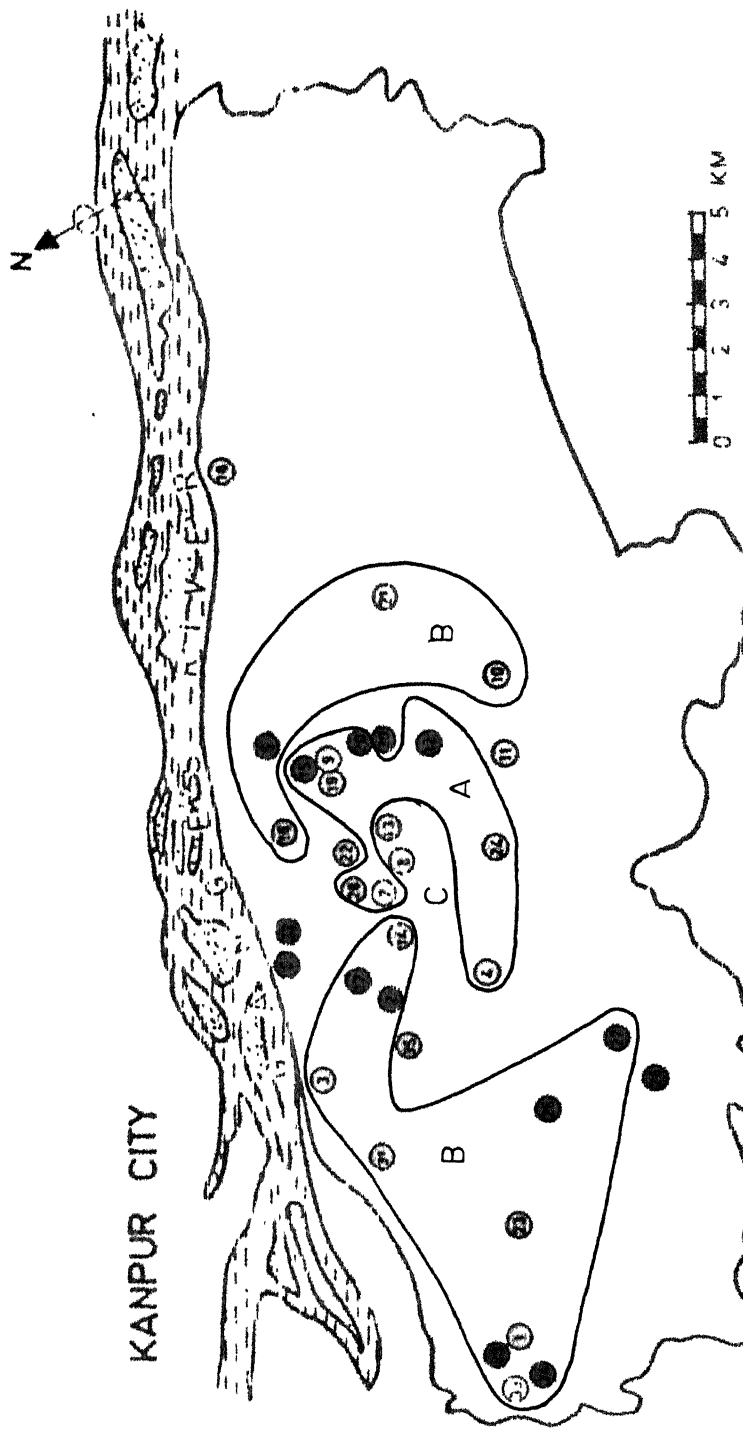


Fig. 5.3. Map of Kanpur city showing level of Calcium detected in air particulate samples at various locations. The levels are indicated by a colour code

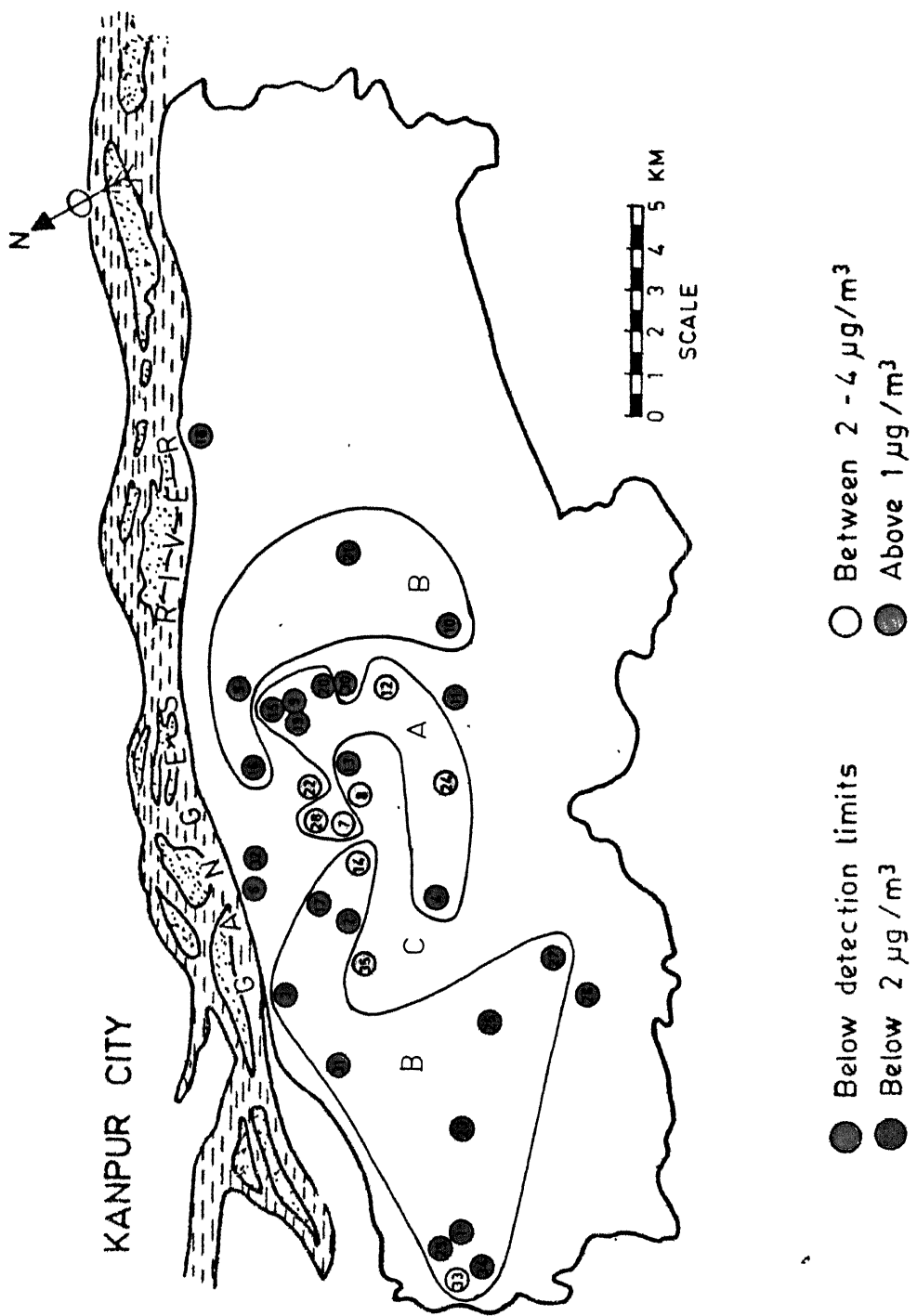


Fig. 5.4. Map of Kanpur city showing level of Titanium detected in air particulate samples at various locations. The levels are indicated by a colour code.

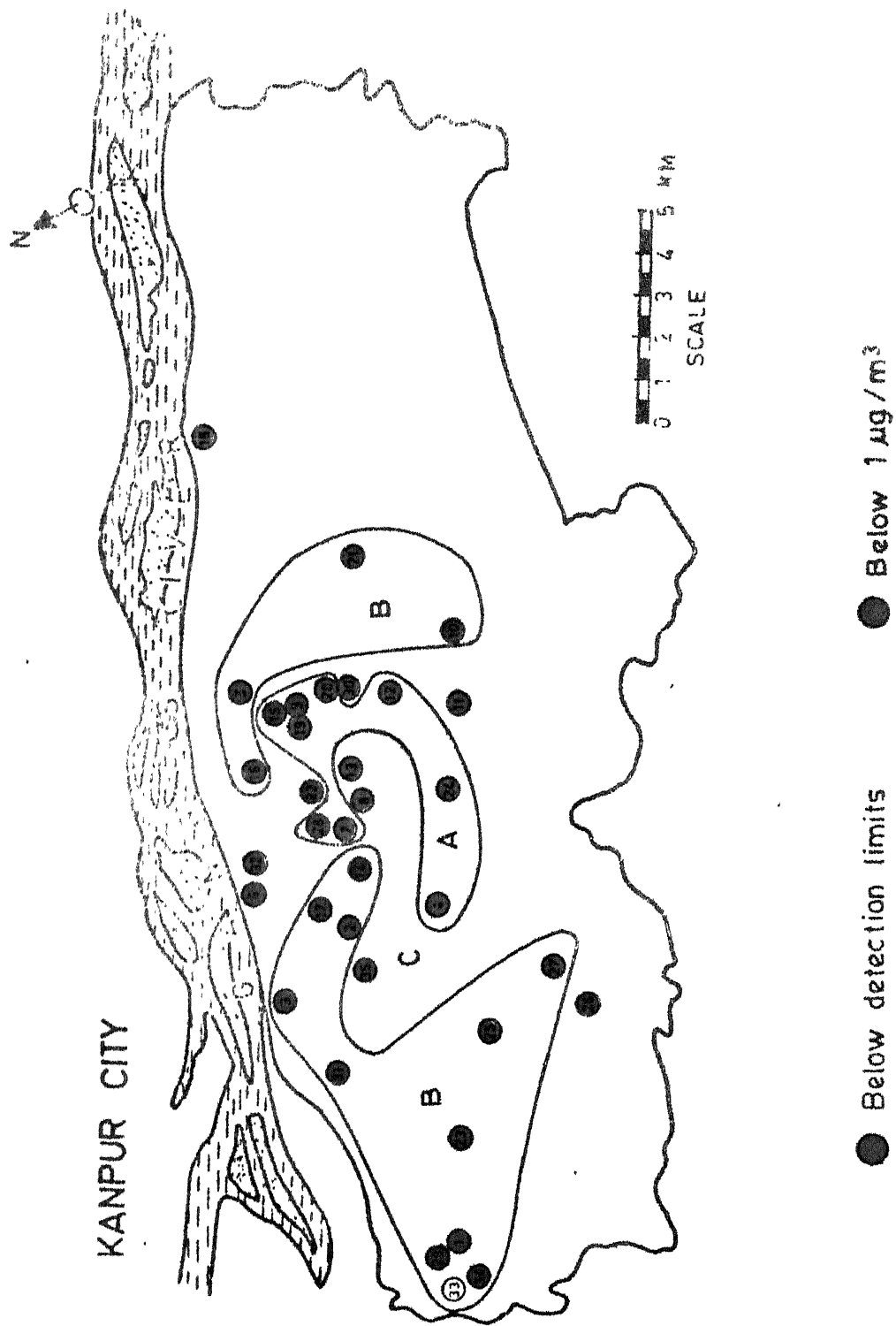


Fig. 5.5. Map of Kanpur city showing level of Vanadium detected in air particulate samples at various locations. The levels are indicated by a colour code.

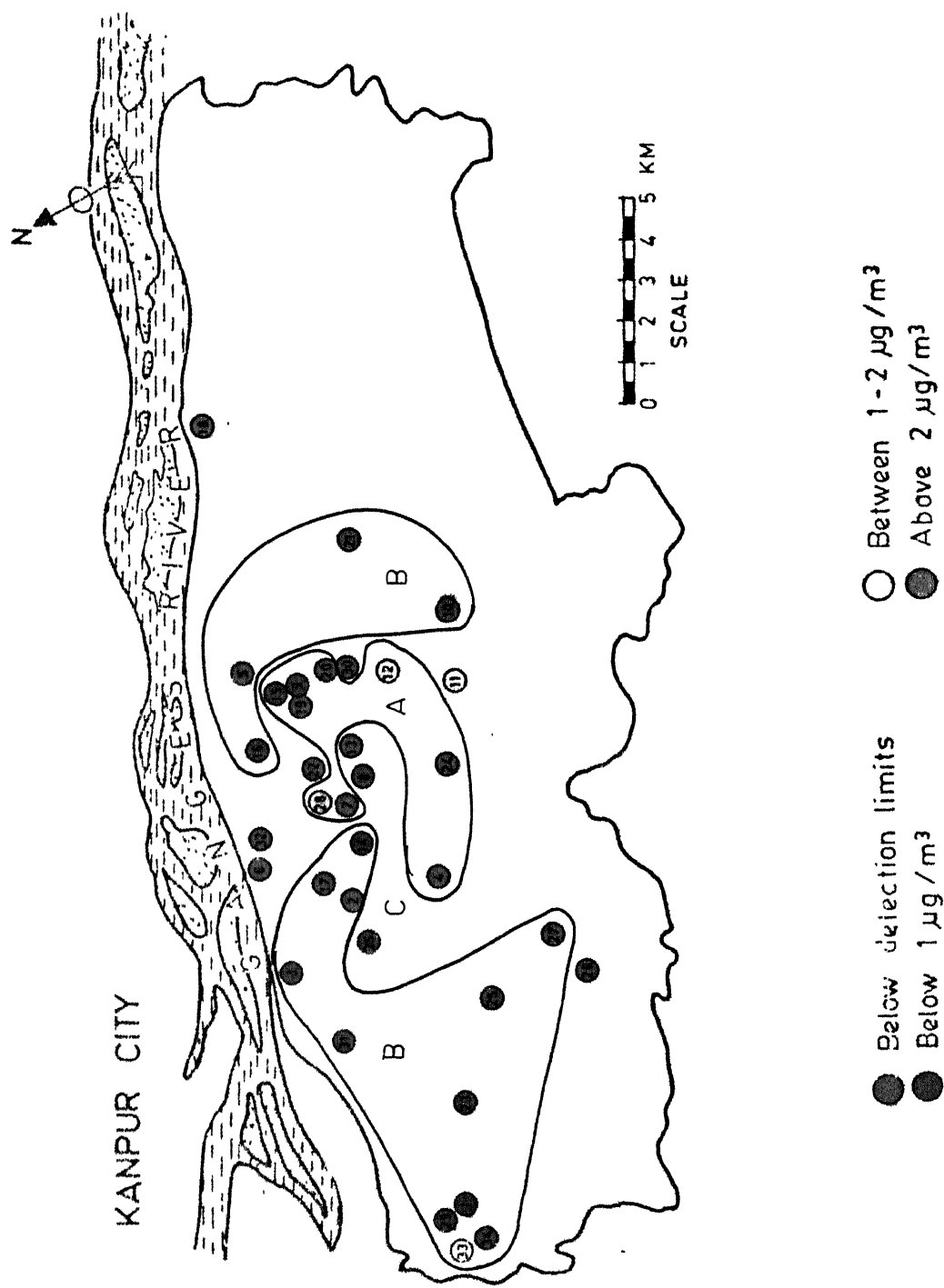


Fig. 5.6. Map of Kanpur city showing level of Chromium detected in air particulate samples at various locations. The levels are indicated by a colour code.

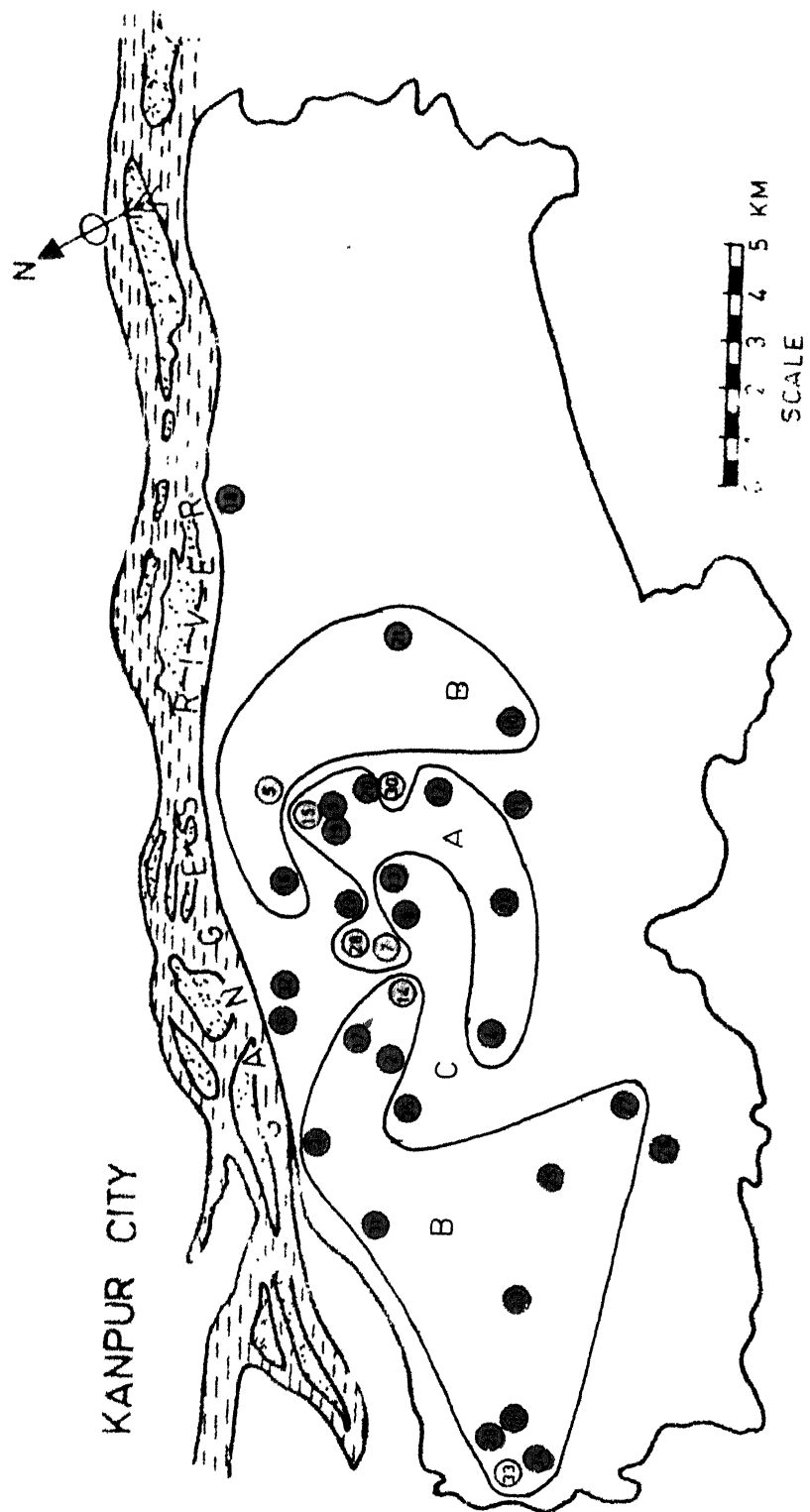


Fig. 5.7. Map of Kanpur city showing level of Manganese detected in air particulate samples at various locations. The levels are indicated by colour code.

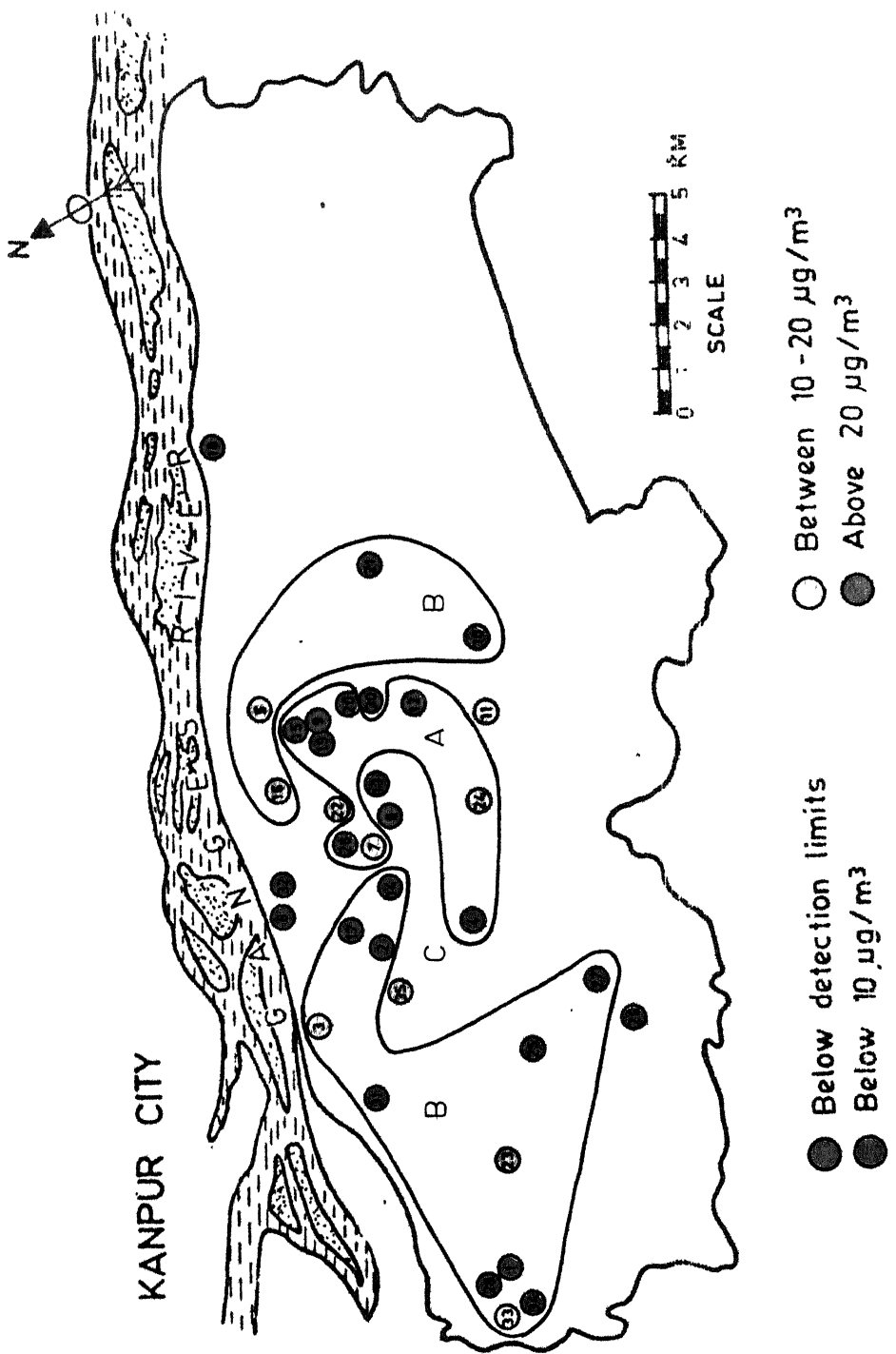


Fig. 5.8. Map of Kanpur city showing levels of Iron detected in air particulate samples at various locations. The levels are indicated by a colour code.

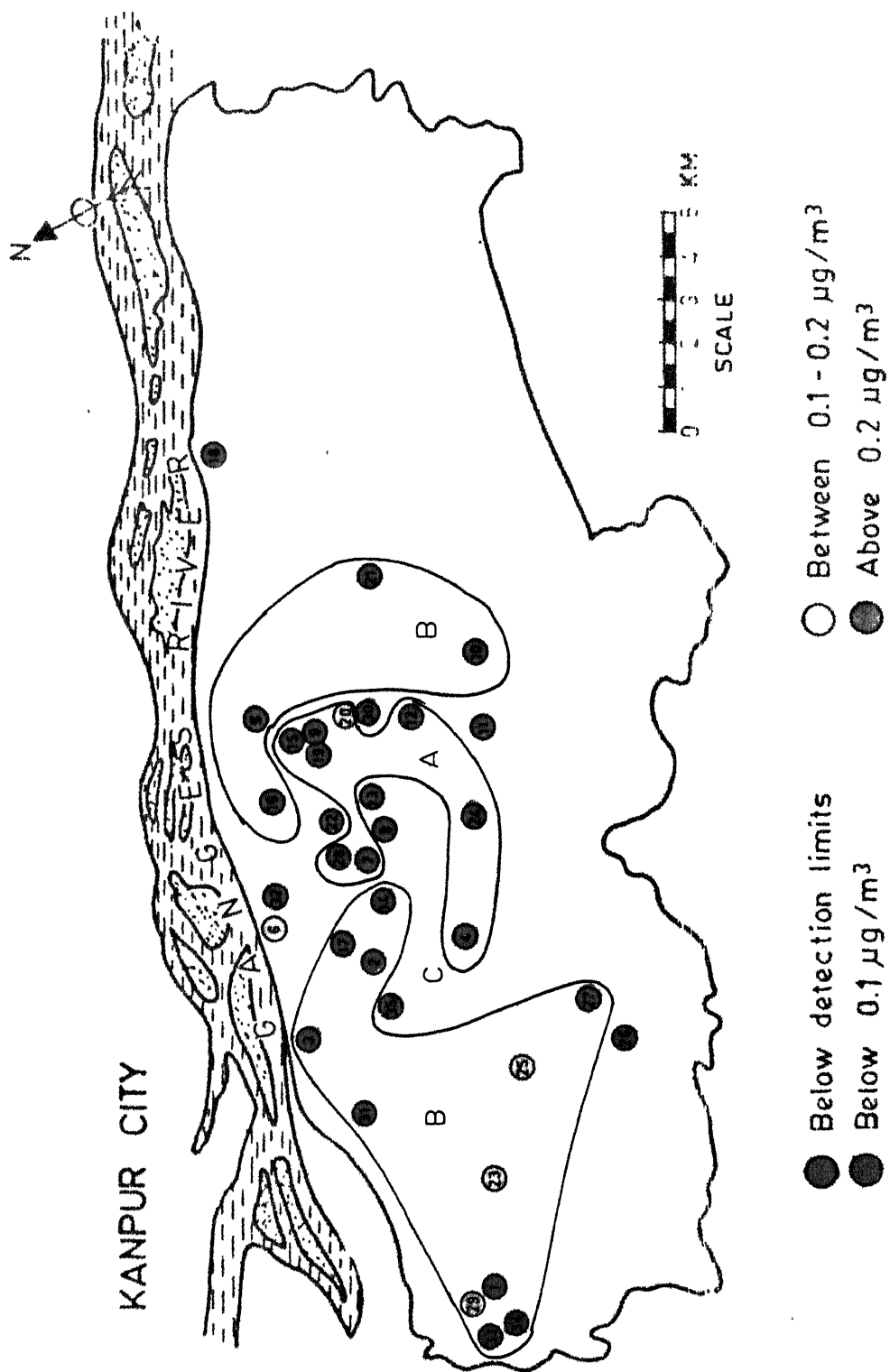
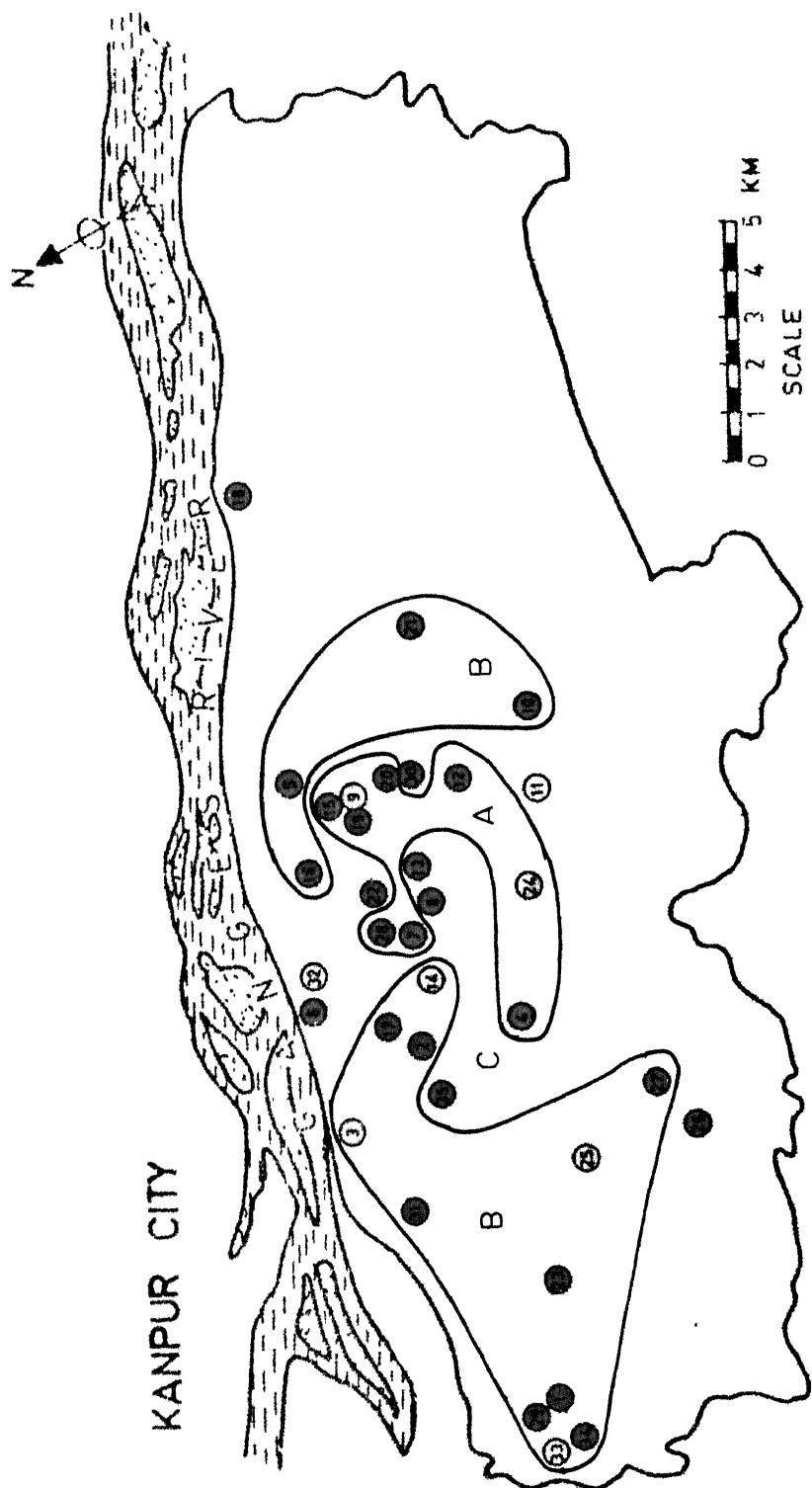


Fig. 5.9. Map of Kanpur city showing levels of Nickel detected in air particulate samples at various locations. The levels are indicated by a colour code.



● Below detection limits

● Below $0.1 \mu\text{g}/\text{m}^3$

○ Between $0.1 - 0.2 \mu\text{g}/\text{m}^3$

● Above $0.2 \mu\text{g}/\text{m}^3$

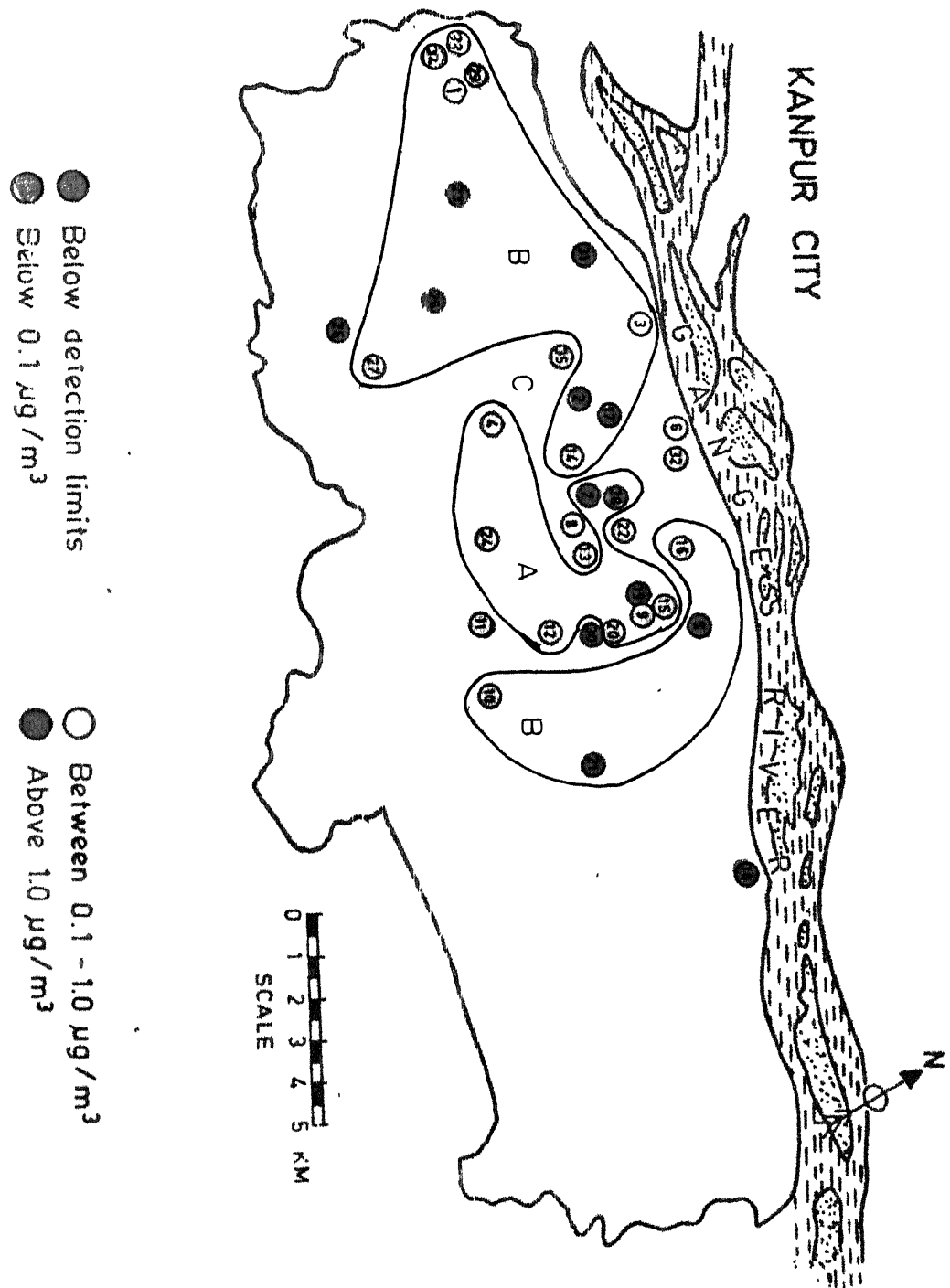


Fig. 5.11. Map of Kanpur city showing levels of Zinc detected in air particulate samples at various locations. The levels are indicated by a colour co-

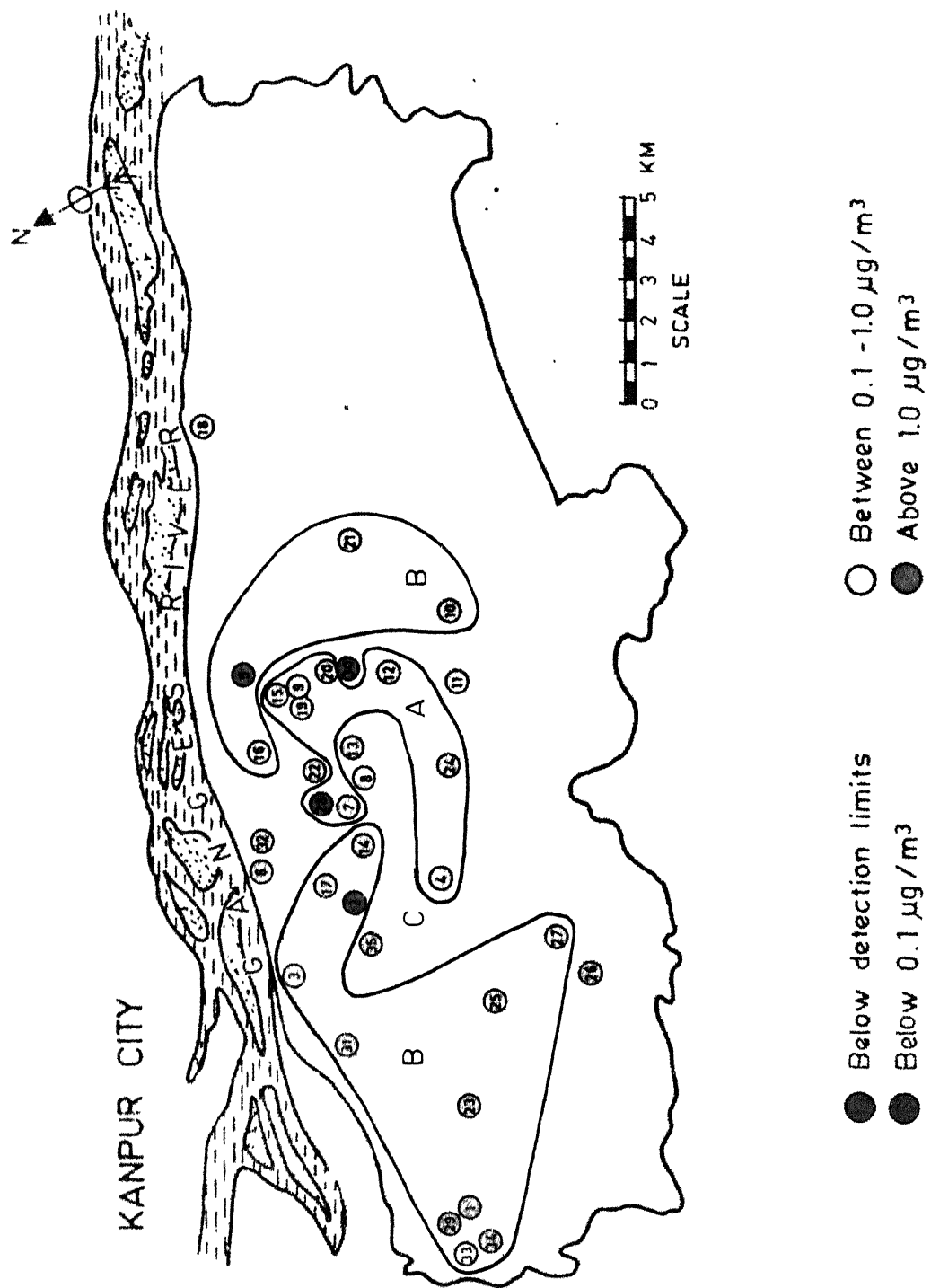


Fig. 5.12. Map of Kanpur city showing level of Lead detected in air particulate samples at various locations. The levels are indicated by a colour code

may be due to the influence of local activities and nearby brick kiln. Site 29 is in a residential colony near the brick kiln activity whereas site 34 is in a residential colony where wood and coal burning is the main source of fuel. The effect of Panki Thermal Power Station (No. 1, Fig. 4.1) may not be very significant as the wind direction was such that the plumes from the Thermal Power Station dispersed away from the site. When the plumes were directed towards the site 1 we obtained a concentration of $876 \mu\text{g}/\text{m}^3$ for the TSP.

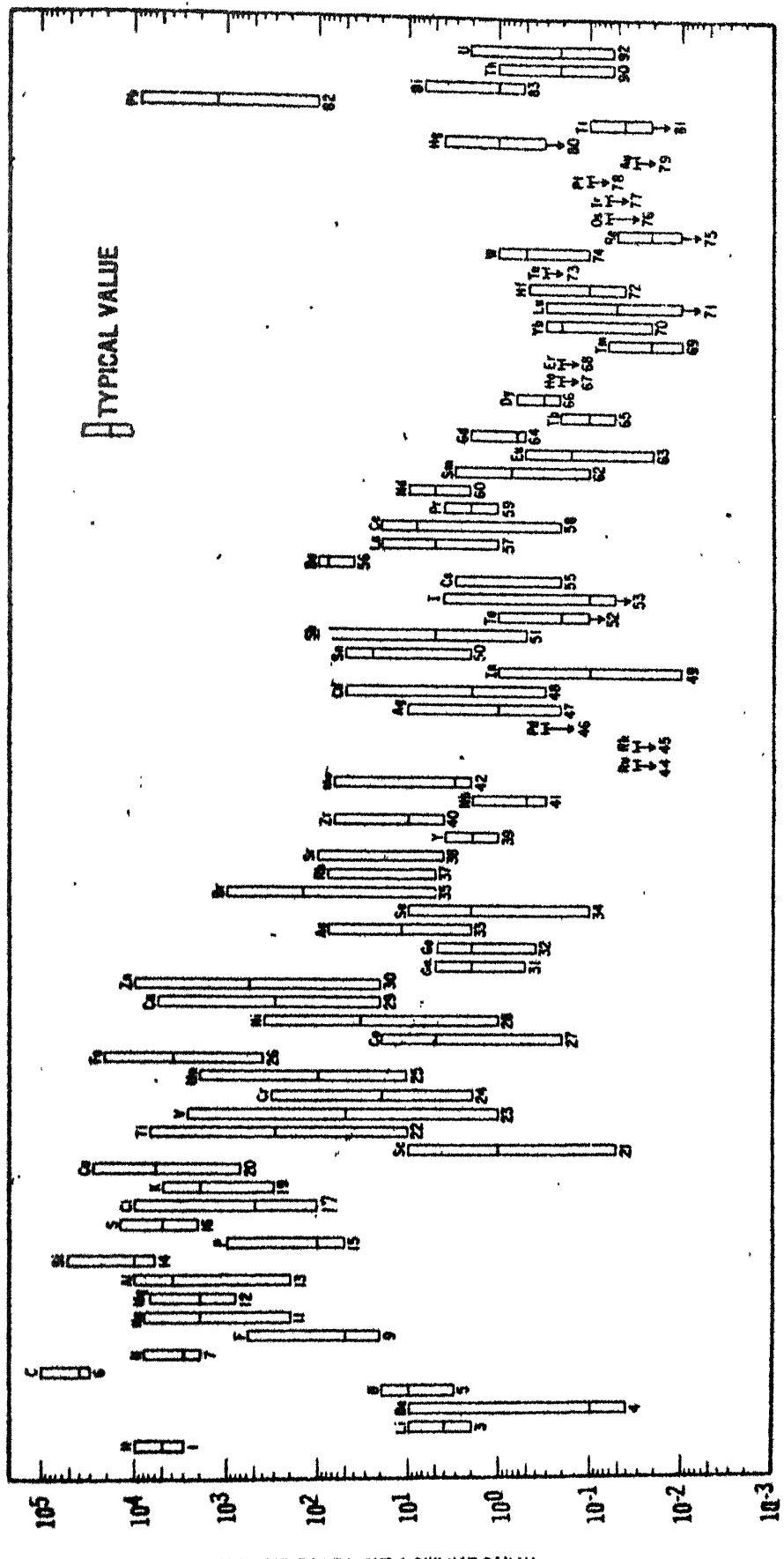
In zone C, the location 30 is highly polluted while 8 and 11 have intermediate values. At location 26 which was inside the IEL area all elements except Cr were present in very small quantities indicating a high level of Cr pollution due to the IEL plant. Site 6 and 32 were very near Riverside Thermal Power Station (No. 18, Fig. 4.1) and textile mills (No. 13, 14, 19, Fig. 4.1). These sources seem to contribute significant amounts of Ni and Zn in the atmosphere. In locations 8 and 13 the main difference was that the traffic density was higher at 8. The elemental values reflect this with high values of concentration for soil-borne elements, whereas elements of industrial origin show similar concentration at both the sites.

Table 5.5 gives the average and range of the concentration values for each zone. The range of values obtained for V, Cr, Mn, Ni, Cu, Zn and Pb lie within the range of values for urban atmosphere compiled by Cooper et al. [13] and shown in Fig. 5.13. At locations the concentrations of K, Ca, Ti and Fe are above the range of values for urban atmosphere shown in Fig. 5.13. The concentration of TSP and other elements except for Cu is

Table 5.5

Range, Geometric Mean and Standard Deviation ($\mu\text{g}/\text{m}^3$) of the TSP and elemental Concentrations in Different Zones of Kanpur.

Element	Zone A		Zone B		Zone C	
	Thickly Populated Range	Average	Thinly Populated Range	Average	Industrial Range	Average
TSP	73-2290	447 \pm 3	58-656	164 \pm 2	34-1648	320 \pm 3
K	22.601-110.081	32.199 \pm 0.005	2.327-32.452	11.623 \pm 0.002	6.798-112.27	19.769 \pm 0.002
Ca	2.006-133.471	23.839 \pm 0.003	0.403-39.241	10.371 \pm 0.002	3.280-97.60	13.976 \pm 0.003
Ti	0.400-9.369	4.689 \pm 0.005	0.597-7.111	1.479 \pm 0.002	1.163-41.248	3.806 \pm 0.003
V	1.111-1.847	1.432 \pm 0.001	0.247-0.824	0.375 \pm 0.002	0.927	0.927
Cr	0.142-4.072	1.521 \pm 0.002	0.344-6.024	0.605 \pm 0.002	0.882-	2.710 1.301 \pm 0.002
Mn	0.332-2.509	1.249 \pm 0.002	0.255-2.079	0.482 \pm 0.002	0.348-	1.399 0.710 \pm 0.002
Fe	1.428-88.987	15.267 \pm 0.002	0.753-29.704	5.585 \pm 0.003	0.935-	86.340 9.224 \pm 0.003
Ni	0.158-0.502	0.310 \pm 0.001	0.057-0.225	0.115 \pm 0.002	0.106-	0.320 0.213 \pm 0.002
Cu	0.061-2.928	0.171 \pm 0.002	0.007-0.525	0.106 \pm 0.004	0.046-	0.445 0.188 \pm 0.002
Zn	0.128-2.233	0.596 \pm 0.002	0.027-0.564	0.164 \pm 0.002	0.022-	1.363 0.354 \pm 0.003
Pb	0.211-2.284	0.513 \pm 0.002	0.089-1.938	0.214 \pm 0.002	0.160-	1.138 0.437 \pm 0.003



5.13 The range and typical values of urban trace element concentrations.

maximum in zone A, intermediate in zone C and minimum in zone B. Figs. 5.1 to 5.12 indicate that zone A contains more number of sites with high elemental levels. The zone A and zone C which form the central part of the city seem to be highly polluted and need more extensive studies with respect to possible health hazards. The values of Pb observed at some places is above the air quality standard for Pb prescribed by Environmental Protection Agency (EPA) in U.S.A. The TSP levels in zones A, B and C showed maximum values in the month of November. It was also found that in each zone the high values of TSP are associated with westerly winds or still weather.

The sampling period was divided into two separate periods viz. summer (June, July and August) and winter (November and December). At few places in each zone like Transport Nagar (site 12 in Fig. 5.1), Ghantaghar (9), Gandhi Nagar (7), Govind Nagar (24), General Ganj (15) in zone A, Naiveen Market (16) and Ashok Nagar (14) in zone B; Juhi Colony (11), Jarceeb Chowky (8), Souter Ganj (6) and Chaman Ganj (22) in zone C, sampling was done in one of the summer months and again in November or December. In zone A at all such places except General Ganj the ratio of the concentration of TSP obtained in winter to that in summer is between 1.5 to 1.8. In zone C the ratio is between 1.7 and 2.5 but in zone B it is quite high i.e. around 10. Similar trend is not noticed in the concentration of various elements. The soil-borne elements like Ca and Fe show more

variability in concentration values than the elements like V, Mn, Ni, Cu, Zn, and Pb. A possible reason is the elements Fe and Ca are found mainly on the largest particles and the dominant source is expected to be dispersion of soil dust.

5.1.4 Enrichment factor calculation

Besides indicating the extent of pollution and the elements involved, the analytical data from the multielemental analysis provide limited information regarding the sources and transportation of pollutants. The data represent contribution from natural as well as anthropogenic sources. In order to differentiate between anthropogenic and natural sources of pollutants many workers [14-17] have discussed their data in terms of enrichment factor, EF, which may be defined as follows:

$$EF = (x/C)_{\text{Air}} / (x/C)_{\text{Source}} \quad (5.1)$$

where x is the concentration of any element of interest and C is the concentration of an appropriate normalizing element which is predominantly of natural origin. The quantity $(x/C)_{\text{Air}}$ is the ratio of concentration of element x to the reference element in air particulate sample while $(x/C)_{\text{Source}}$ is the ratio of the concentration of x to the concentration of the reference element in source material. EF for x is given by the ratio of the above two ratios. Generally the source materials used in such calculations have been earth crust materials such as rock and soil while the reference elements

used most frequently are Al, Sc and Fe. In the studies of marine aerosol, the source material used has been sea water, with Na and Cl as reference elements. A factor significantly greater than unity indicates an influence from sources other than human activity. By comparing EFs for various elements at different places in the world it is possible to estimate the level of pollution due to sources other than soil.

In the present work the enrichment factors were calculated for elemental air quality data assuming Fe as a reference element and average soil composition given by Bowen [18] as the source material. In Table 5.6 enrichment factors calculated for elemental data at various places (Tables 5.1 and 5.2) are given. Enrichment factors for soil origin elements like K, Ca and Ti in Kanpur are comparable with those in South Arizona which has a desert atmosphere. The enrichment factor of Cr for Kanpur is high compared to all other places. For Cu, Zn and Pb which are mainly anthropogenic in origin the values of EFs in Kanpur are quite high but are smaller than at other locations. EF for Pb in Kanpur is comparable with that in Bombay but for Cu and Zn EFs in Bombay are greater than those in Kanpur.

Winchester [19] has discussed the enrichment of various elements in aerosols in natural atmosphere by assuming them to be mainly due to soils from weathering rocks, sea spray and gas to particle conversion processes. It was found that Cu and Zn are enriched by a factor of 10 and the enrichment of Pb is about a factor of 100 at a location in Bolivia which was very remote from industrial sources. Similar enrichments of many of

these elements is found in remote areas of North America [20], Europe [21] and Southpole [22]. Even in India aerosol samples over Arabian sea show an enrichment of about a factor of 50 for Cu whereas for Mn and Cr EF is nearly unity [23]. Since the smelting and other polluting processes are far away from such locations one possibility is the natural crust-to-air fractionation process. The values obtained in Kanpur are comparable with these values but since it is known that nearby anthropogenic pollution sources exist, the contribution of natural processes to the enrichment of Cu, Zn and Pb seems to be much less than at remote places like Europe, North America etc. In this context it would be interesting to study the levels of these elements in some remote corners of India. This may help in differentiating the importance of natural processes and long range transport of pollutants in increasing the concentrations of Cu, Zn and Pb at remote areas. Winchester [19] has also pointed out that the ratios Ti/Fe and Pb/Zn do not vary significantly over the major rock types and hence in natural aerosols similar behaviour of these ratios can be expected. Therefore if these ratios do not vary significantly in the observed air quality data then their origin may be in one of the natural processes. We calculated these ratios and it was found that Ti seems to be mainly due to soil dispersion source whereas variability in the Pb/Zn ratio was large indicating an anthropogenic source.

The zone-wise analysis of enrichment factors is given in Table 5.7. Contrary to the pattern of distribution of elemental concentration most of the elements now appear to have slightly higher enrichment factors in zone C than in zone A and zone B. Zone C is an industrial zone and hence it is natural that the EFs should be higher for zone C. But the levels of enrichment in zone A and B are quite close to zone C indicating that the pollutants due to anthropogenic sources are uniformly distributed in most of the zones.

Enrichment factor analysis at each site helps in pointing out locations with higher enrichment of certain elements. In zone A, site 15 was found to be enriched in Ni, Cu, Zn and Pb whereas 28 and 24 are enriched in Pb only. In zone B, sites 31, 14 and 25 are more enriched in Cu, Zn and Pb than at other sites. In zone C, site 32 is enriched in Ni, Cu, Zn and Pb. This site is very near the Riverside Thermal Power Station. At sites 26 and 11 enrichment of Cr is very high. Site 11 is also enriched in Cu, Zn and Pb. Pb is enriched considerably in location 22. These features are brought out in Table 5.8 where we have grouped sites with high enrichment factors for each element. The EFs for K, Ca, Li and Mn did not vary very widely whereas for other elements the variation was very large. Considering the enrichment in natural aerosols, criteria for enrichment for Zn, Cu and Pb was fixed at higher level whereas for other elements it was fixed at 10.

Thus, it has been possible for us to conclude that the resuspended soil in the atmosphere is a major cause for high

Table 5.7

Enrichment Factors for Different Elements in Various Zones of Kanpur City.

Element	Zone A Thickly Populated	Zone B Thinly Populated	Zone C Industrial
K	3.7	5.7	5.9
Ca	4.4	7.6	5.4
Ti	1.1	2.8	1.4
V	10.2	13.9	16.5
Cr	23.3	56.6	69.6
Mn	2.6	11.6	2.4
Ni	69.4	36.9	87.2
Cu	39.2	83.3	58.9
Zn	44.9	42.6	51.7
Pb	173.6	194.3	347.9

Table 5.8

Identification of Locations with High Level of Pollution due to Sources Other than Soil.

Element	Enrichment Factor (EF)	Site	numbers in Fig. 5.1 to 5.12 with higher EF	
		Zone A	Zone B	Zone C
K	> 10	-	31	18
Ca	> 10	15	1, 14, 16, 25	18, 32
Ti	> 10	-	25	-
V	> 10	9	14	22
Cr	> 10	7, 12, 28	1, 3, 10, 14, 23, 29	8, 22, 26 11
Mn	> 10	-	14, 25	-
Ni	> 10	12, 15, 20	23, 25, 29	6, 22, 32
Cu	> 50	7, 15	10, 14, 16, 25, 34	11, 32
Zn	> 50	4, 7, 15, 28	14, 25, 34	6, 11, 22, 32, 35
Pb	> 100	4, 12, 15, 19, 24, 28	1, 10, 14, 19, 25, 31, 34	6, 11, 22, 26, 27, 30, 32, 35

value of TSP. Two reasons viz. the large scale urban activity on dusty roads and the local climatic conditions appear to be mainly responsible for this. Pollution due to Zn, Pb and Cu is less than that at other industrial cities but is quite high at some locations and needs further investigation. EF analysis has helped us in identifying highly polluted locations in each zone.

5.1.5 Correlation analysis

Correlation analysis is carried out to obtain information about the association between elements in a data set. The use of correlation coefficients allows a quantitative estimate of the similarity of the temporal variation of two elements. Highly correlated elements may come from same primary source or may have been carried together in air.

The linear correlation coefficient for any element pair is obtained by

$$r_{ij} = \frac{\langle x_i x_j \rangle - \langle x_i \rangle \langle x_j \rangle}{\sqrt{\langle (x_i - \bar{x}_i)^2 \rangle \langle (x_j - \bar{x}_j)^2 \rangle}} \quad (5.2)$$

where x_i and x_j denote concentrations of the elements considered, and the bars and brackets indicate averages over the sample set. Using r_{ij} , we can test the hypothesis of no correlation between the elements ($r_{ij} = 0$) by applying Student's t-test [24]. To indicate an interdependence with a specific degree of significance, the value of r_{ij} must exceed a value obtained from the test which depends on the

number of samples included in the set. The t in Student's test is given by

$$t = \frac{r_{ij} \sqrt{(n-2)}}{\sqrt{(1-r_{ij}^2)}} \quad (5.3)$$

where n is the number of samples in the set.

Tables 5.9(a), 5.9(b) and 5.9(c) present linear correlation coefficients for the data collected in zone A, B and C respectively. The correlation coefficients were calculated for all possible pairs over the entire set of data. For concentrations below the detection limit, a value zero was used. The choice of zero became necessary to obtain correlation coefficients for all element pairs over the entire set of data. This will give a lower bound for the correlation coefficients. The values reported in Tables 5.9(a), 5.9(b) and 5.9(c) indicate a statistically significant ($p = 0.05$) relationship. The quantity p is the probability that the two elements may not be significantly correlated. The degree of correlation is improved as the absolute value of the coefficient increases. The following points should be noted from Tables 5.9(a), 5.9(b) and 5.9(c).

The following observations can be made for the zone A :

- 1) TSP, K, Ca, Ti, V, Mn and Fe are highly correlated with each other, 2) Zn and Cr are correlated to a lesser degree. Zn is also correlated with K, Ca and Fe. 3) Cu and Ni do not share significant correlation with any element. The group of elements K, Ca, Ti, V and Mn and the TSP seem to arise mainly

Table 5.9(a)

Linear Correlation Coefficients for Samples in Zone A.

	TSP	K	Ca	Ti	V	Cr	Mn	Fe	Ni	Cu	Zn	Pb
TSP	1.000											
K	0.937	1.000										
Ca	0.950	0.908	1.000									
Ti	0.868	0.912	0.815	1.000								
V	0.672	0.736	0.725	0.813	1.000							
Cr	0.377	a	a	a	a	1.000						
Mn	0.745	0.717	0.626	0.808	0.586	a	1.000					
Fe	0.942	0.956	0.930	0.922	0.830	a	0.713	1.000				
Ni	a	a	a	a	a	a	a	a	1.000			
Cu	a	a	a	a	a	a	a	a	a	1.000		
Zn	0.387	0.418	a	a	a	0.624	a	0.459	a	a	1.000	
Pb	0.442	0.508	a	a	a	a	0.444	a	a	a	1.000	

a - Not significant at 5% level.

Table 5.9(b)

Linear Correlation Coefficients for Samples in Zone B.

TSP	K	Ca	Ti	V	Cr	Mn	Fe	Ni	Cu	Zn	Pb
1.000											
K	0.666	1.000									
Ca	0.396	0.607	1.000								
Ti	0.760	0.407	a	1.000							
V	0.374	a	a	0.633	1.000						
Cr	a	a	a	0.440	a	1.000					
Mn	a	a	a	a	a	a	1.000				
Fe	0.826	0.696	0.619	0.407	a	a	a	1.000			
Ni	a	a	a	a	0.525	a	a	a	1.000		
Cu	a	a	a	a	0.412	a	a	a	a	1.000	
Zn	0.605	0.476	0.416	0.536	0.446	a	0.340	0.590	a	a	1.000
Pb	0.407	0.678	0.443	a	a	a	0.622	a	0.490	0.564	1.000

a - Not significant at 5 % level.

Linear Correlation Coefficient for Samples in Zone C.

	TSP	K	Ca	Ti	V	Cr	Mn	Fe	Ni	Cu	Zn	Pb
TSP	1.000											
K	0.841	1.000										
Ca	0.921	0.936	1.000									
Ti	0.828	0.897	0.910	1.000								
V	a	a	a	a	1.000							
Cr	a	a	a	a	a	1.000						
Mn	0.844	0.680	0.777	0.660	a	a	1.000					
Fe	0.956	0.884	0.978	0.914	a	a	0.834	1.000				
Ni	a	a	a	a	0.510	a	a	a	1.000			
Cu	0.847	0.742	0.807	0.661	0.407	a	0.687	0.785	a	1.000		
Zn	0.805	0.748	0.847	0.808	a	a	0.649	0.863	a	0.761	1.000	
Pb	0.726	0.816	0.786	0.956	a	a	0.556	0.800	a	0.581	0.709	1.000

a - Not significant at 5 % level.

from the soil sources. Zn seems to arise from two sources (See (2) above). One may be a soil source and the other one may be a distant pollution source. Correlation of Cr and Zn indicates a common source or common mode of transportation. Pb is correlated to some degree with TSP, K and Fe indicating its soil component. Cu and Ni appear to come from independent sources of pollution. The influence of high level human activity in zone A is reflected by the strong correlation in the soil origin elements.

We can make the following observations for the zone B :

i) TSP, K, Ca, Ti, V and Fe are highly correlated with each other. Absence of Mn in this group is to be noted. ii) Pb is correlated with Zn and Cu but Zn and Cu are not correlated among themselves. Zn and Pb are correlated with TSP, K, Ca and Fe. Mn and Ni appear to be from independent sources though they show correlation with Zn and Cr. Correlation of Zn and Pb in zone B is notable because in zone A these elements are not correlated. This may indicate that in the zone B, Zn and Pb may be mainly due to natural processes like crust-to-air fractionation.

The main characteristic of the zone C is high correlation among all elements except among V, Cr and Ni. V is correlated with Ni and Cu but Ni and Cu are not correlated. Cr and Cu seem to be from independent sources of pollution.

Thus, with the help of correlation analysis it has been possible to group highly correlated species and also to isolate uncorrelated elements in each zone. Further analysis

of the correlation coefficient matrix is carried out to identify the sources of pollution and it is described in the next section.

5.1.6 Factor analysis method

Examination of correlation coefficients has enabled us to find out group of correlated elements, totally uncorrelated elements and elements having correlation with elements in different groups. Further analysis is done using the method of factor analysis, to determine the number of major influences each element and to identify them.

Factor analysis is a multivariate statistical technique and is widely used in the natural and social sciences. Since the air particulate data is subjected to a large number of natural variations, factor analysis can be applied to deduce the interrelationships between element concentrations and the sources responsible for them. It has been applied for the analysis of the pollution problems by many researchers [25, 26].

In order to perform the statistical analysis, the data are transformed into a standard form

$$z_j = \frac{x_j - \bar{x}_j}{\sigma_j}, \quad (5.4)$$

where z_j is the standardized value of the j^{th} variable, x_j is the value determined for the variable in the sample, \bar{x}_j is the mean value of the j^{th} variable of all of the samples and σ_j is the standard deviation of the distribution of values of this variable. Each standardized variable has a mean value

zero and a standard deviation of one.

In the factor analysis method each standard variable (Z_j) is expressed as a linear combination of m factors (F_i 's) common to all variables and a unique factor U_j as follows:

$$Z_j = a_{j1}F_1 + a_{j2}F_2 + \dots + a_{jm}F_m + d_jU_j \quad (5.5)$$

The coefficients a_{jk} in the above equation are called loadings. By noting which elements have high loadings on a particular factor, it may be possible to assign a physical interpretation to that factor. The factors are the hypothetical variables chosen so that the correlation among the observed variables can be reproduced.

The purpose of factor analysis is to determine a number of such common factors to account for an acceptable amount of the variance in the observed data. The variables have been standardized so that the variance for each variable is one. The total system variance is n . The variance for each variable consists of the common factor variance, specific variance and the error. The specific variance and error are contained in the unique factor. The common and specific variance represent variation in the system because of variation in the causal factors. Common factors can account for varying amounts of the total variance. The communality of a variable is the amount of variance that is accounted for by the common factors. The communality for a variable is equal to the sum of the squares of the factor loadings and is given by

$$h_j^2 = \sum_{i=1}^m a_{ji}^2 \quad (5.6)$$

If the common factors account for the total variance of the variable in the system, then the communality would be one.

The major advantage of factor analysis is that no data on the source emission rates are needed to identify various sources. There are also some assumptions implicit in the use of factor analysis for atmospheric particulate study. All the major influences on particulate composition should be reflected in the correlation matrix. It is further assumed that the major influences are different enough in their effects on the correlation matrix to produce factors which represent only one influence and not combinations of several influences. One limitation of the factor analysis lies in the interpretation of the loadings. Interpretations of factor is based on the magnitudes of the loadings but they also rely on previous knowledge and common sense.

The methods of factor analysis are discussed by Harman [27]. Of the various methods of factor analysis, we have used principal factor analysis model in which the factors are orthogonal to one another and the loadings are also correlation coefficients between the observed variable and the factor. We have performed factor analysis of the data following the principal factor method outlined by Hopke et al. [4]. The first step in the factor analysis is the calculation of the linear correlation coefficients for each of the possible pairs of variables. Thus if there are n variables, an $n \times n$ matrix

of correlation coefficients is obtained. In principal factor method, the matrix of correlation coefficients is modified so that the ones on the principal diagonal are replaced by estimated values of communalities. The matrix is then called a communality matrix. The estimation of communality is done by various methods. The usual methods are to use the highest correlation coefficient for each variable, the squared multiple correlation (SMC), or average of all correlations of a given variables with the other. In our analysis, SMCs have been used as estimated communalities. The SMCs are found from the inverse of the correlation matrix by the formula,

$$SMC_i = 1 - \frac{1}{r_{ii}} \quad (5.7)$$

where, r_{ii} is the diagonal element in the inverse correlation matrix for the i^{th} variable. It has the property of being a lower bound for the communality. The factor analysis program then diagonalizes the communality matrix and determines the eigenvalues and eigenvectors corresponding to each eigenvalue.

One of the major problems of factor analysis is the decision as to the number of factors m to be retained. The factors should retain as much common variance as is possible and should still provide an interpretable pattern. Normally, four to six eigenvectors of the communality matrix corresponding to the largest eigenvalues are used as the factor axes. These orthogonal factor axes are then rotated using orthogonal varimax rotation. The purpose of rotation is to point a

factor at a cluster of variables so that the factor may be easy to interpret. The method of varimax rotation is described by Harman [27] and is outlined below.

In varimax rotation method the final factor loadings are determined so that the function

$$V = n \sum_{j=1}^m \sum_{i=1}^n (a_{ij}/h_i)^4 - \sum_{j=1}^m \left(\sum_{i=1}^n a_{ij}^2/h_i^2 \right)^2 \quad (5.8)$$

is maximized. In eq. (5.8) h_i is the squareroot of communality for the variable i .

The computing procedure for a varimax solution consists of rotating the factors, two at a time, according to the scheme

$$B = A T_{12} T_{15} \dots T_{pq} \dots T_{(m-1)m} \quad (5.9)$$

where, T is the transformation matrix and A and B are the matrix of factor loadings before and after rotation. The complete cycle of $m(m-1)$ pairings is repeated until the value of V calculated to the specified number of decimal places does not increase any more.

The transformation matrix T is determined by calculating the angle of rotation for a particular pair of factors p and q

$$\tan 4 \phi = \frac{D - 2AB/n}{C - (A^2 - B^2)/n} \quad (5.10)$$

where,

$$A = \sum_{i=1}^n u_i$$

$$B = \sum_{i=1}^n v_i$$

$$C = \sum_{i=1}^n (u_i^2 - v_i^2)$$

$$D = 2 \sum_{i=1}^n (u_i v_i)$$

$$\text{and } u_i = (a_{ip}^2 - a_{iq}^2)/h_i^2$$

$$v_i = 2(a_{ip} \cdot a_{iq})/h_i^2$$

The solution (5.10) which makes V in eq. (5.9) maximum yields a value of ϕ between -45° to 45° . Once the angle ϕ is obtained, the transformation matrix T is calculated as

$$T = \begin{pmatrix} \cos \phi & -\sin \phi \\ \sin \phi & \cos \phi \end{pmatrix} \quad (5.11)$$

Next, the normalized rotated vectors are computed according to the following equation

$$(A_{ip} \quad A_{iq}) = (a_{ip}/h_i \quad a_{iq}/h_i) \begin{pmatrix} \cos \phi & -\sin \phi \\ \sin \phi & \cos \phi \end{pmatrix} \quad (5.12)$$

Finally, the normalization is removed by multiplying each value by the appropriate h_i for the row. Thus, a matrix of rotated factor loadings is obtained.

A measure of the adequacy of the factor analysis solution is whether the factors can reproduce the observed correlation matrix. The relevant comparison is between each observed correlation C_{ij} and the quantity

$$s = \sum_{m=1}^M a_{im} a_{jm} \quad (5.13)$$

From the rotated factor matrix the communality for each variable can be calculated using eq. (5.6). Very small value of communality indicates a unique source for the variable. The fraction of total variance accounted by each factor is calculated as

$$f_j = \sum_{i=1}^n a_{ij}^2 / n \quad (5.14)$$

where n is the total number of variables.

Following the above method of factor analysis a computer program to obtain rotated factor matrix was developed and was applied to the air quality data.

5.1.7 Factor analysis of elemental data in zones A, B and C of Kanpur city

Starting with the correlation coefficient matrix we performed the factor analysis of the data. First six vectors corresponding to the six largest eigenvalues were chosen as the factor axes. These factor axes were rotated using the varimax rotation method. In Table 5.10(a), 5.10(b) and 5.10(c) we have shown the rotated factor pattern for zones A, B and C respectively. Columns are the loadings corresponding to each factor, rows are the various elements. The communality values indicate the total variance of the variable accounted by the six factors. The fraction of total variance accounted by each factor is also shown in the last row. Communality of a variable tells us about how much variation in the observed variable can be accounted for by

Table 5.10(a)

Factor Analysis Loadings (Rotated Six-Factor Solution for Zone A)

Element	Factor Number and Factor Loadings						Communality
	1	2	3	4	5	6	
TSP	-0.952	0.218	0.131	0.055	0.032	0.110	0.98
K	-0.950	0.173	-0.011	0.083	0.137	-0.001	0.91
Ca	-0.925	0.146	0.301	-0.052	0.027	-0.055	0.97
Ti	-0.944	0.015	-0.241	0.159	-0.046	-0.107	0.98
V	-0.781	0.006	-0.074	-0.023	-0.041	-0.546	0.91
Cr	-0.158	0.944	0.076	0.111	-0.024	0.039	0.91
Mn	-0.767	0.122	-0.196	0.172	-0.369	0.079	0.82
Fe	-0.971	0.129	0.067	-0.009	0.086	-0.146	0.99
Ni	-0.119	-0.025	0.847	0.076	-0.015	0.012	0.71
Cu	0.144	-0.015	-0.073	-0.910	-0.029	-0.001	0.81
Zn	-0.336	0.696	-0.407	-0.389	0.095	-0.125	0.91
Pb	-0.425	0.077	-0.209	0.237	0.486	0.076	0.51
Fraction of total variance	0.504	0.126	0.096	0.093	0.035	0.031	

Table 5.10(b)

Factor Analysis Loadings (Rotated Six-Factor Solution for Zone B).

Element	Factor Number and Factor Loadings						6 Communalit
	1	2	3	4	5	6	
TSP	-0.920	0.343	0.094	-0.051	-0.046	-0.039	0.979
K	-0.723	0.137	0.016	0.063	0.495	-0.032	0.792
Ca	-0.430	0.113	-0.019	0.059	0.786	-0.047	0.823
Ti	-0.483	0.762	0.362	-0.199	-0.003	-0.072	0.990
V	-0.102	0.918	-0.147	0.265	0.052	-0.056	0.951
Cr	-0.127	0.080	0.847	-0.032	-0.223	0.051	0.793
Mn	-0.044	0.136	-0.156	-0.163	-0.017	-0.630	0.468
Fe	-0.887	0.031	0.036	0.235	0.236	-0.076	0.906
Ni	-0.002	-0.062	0.812	-0.175	0.223	0.050	0.746
Cu	-0.072	0.165	-0.137	0.916	0.005	0.043	0.892
Zn	-0.528	0.359	-0.012	0.199	0.101	-0.514	0.721
Pb	-0.524	-0.064	-0.114	0.525	0.301	-0.383	0.805
Fraction of total variance	0.263	0.147	0.133	0.116	0.086	0.069	

Table 5.10(c)

Factor Analysis Loadings (Rotated Six-Factor Solution for Zone C)

Element	Factor Number and Factor Loadings						Communality
	1	2	3	4	5	6	
TSP	0.918	0.318	-0.107	0.165	-0.043	0.108	0.996
K	0.708	0.602	-0.098	-0.022	0.231	0.026	0.928
Ca	0.843	0.463	-0.077	-0.143	0.125	0.117	0.981
Ti	0.635	0.755	-0.067	-0.102	-0.035	0.083	0.996
V	0.118	-0.029	0.452	0.233	0.725	0.035	0.800
Cr	-0.018	-0.053	0.101	0.837	0.114	0.033	0.728
Mn	0.763	0.202	0.032	0.165	0.075	0.556	0.966
Fe	0.864	0.435	-0.135	-0.083	-0.005	0.190	0.997
Ni	-0.032	-0.081	0.952	0.055	0.109	-0.003	0.930
Cu	0.887	0.188	0.231	0.099	0.236	-0.123	0.956
Zn	0.821	0.354	0.096	-0.260	-0.168	-0.012	0.905
Rb	0.491	0.842	-0.065	0.014	-0.048	0.013	0.957
Fraction of total variance	0.459	0.196	0.103	0.077	0.060	0.033	

the six factors. The fraction of total variance indicates the capacity of each factor to account for the variation in the total system variance (in this case 12).

To check the adequacy of the analysis the correlation matrix obtained from the observed data was compared with the values obtained using eq. (5.13) and Tables 5.10(a), 5.10(b) and 5.10(c). The agreement is generally very good and sometimes within 5 %. If the factor loading for a variable is 0.5 or greater the variable is generally considered to be a member of the factor. Factor loadings of 0.5 and 0.87 explain 25 and 75 % of a variable's variance respectively. A total of 82 to 90 % variance could be accounted for by the six factor solution. Some of the major loadings shown in Tables 5.10(a) and (b) happen to be negative, but this has no physical significance. The factor could be redefined with an opposite sign. Similar negative loading was also observed in some cases by Gaarenstroom et al. [26] for the data collected at South Arizona, U.S.A.

In Table 5.11 we have given the zone-wise distribution of elements with large factor loadings (>0.5) on various factors. The first factor in all the three zones seems to be heavily loaded with soil-borne elements.

In zone A, independent sources for Ni, Cu and V exist and may be due to the industrial activity (7 to 16 in Fig. 4.1). Low value of communality for Pb indicates an unique source and it may be due to the emissions from the

Table 5.11

Elemental Groups with Large Factor Loadings on Various Factors in Different Zones.

Zone	Factor Number					
		1	2	3	4	5
A (Thickly populated)	TSP, K, Ca, Ti, V, Mn, and Fe	Cr and Zn	Ni	Cu	Mn and Pb	V
B (Thinly Populated)	TSP, K, Fe, Zn and Pb	Ti and V	Cr and Ni	Cu and Pb	K and Ca	Mn and Zn
C (Industrial)	TSP, K, Ca, Ti, Mn, Fe, Cu, Zn and Pb	K and Ga, Pb	Ti and V and Ni	Cr	V	Mn

Railway Station and other automobile exhausts. Factors 2 and 5 indicate some transport mechanism because Cr and Mn have independent sources in zone C.

In zone B, Mn has low communality and indicates an unique source which may be municipal incinerator fly ash. Factors 2, 3, 4 and 6 indicate transport mechanism or common sources. Since zone B has no industries it is more likely that these factors indicate some transport mechanisms of the air particulate matter. Separate factor for K and Ca indicates construction activity. In zone B, Pb is loaded on first and fourth factor. Loading on fourth factor may be due to the transport of Pb and Cu (fine particle) from zone A which has sources of these two elements. But the first factor loading may be due to the fact that on dusty roads a large volume of dust gets raised into the atmosphere along with the auto-exhaust.

In zone C, first factor has heavy loadings for soil-borne elements, Pb as well as Cu and Zn. Factor 2 also has loading on elements (K, Ca and Ti) originating from the soil and Pb. Factor 2 can be attributed to auto-exhaust. High loading for Cu and Zn on factor 1 may be due to the main coal combustion sources (two thermal power plants). Gladney [29] has shown that the element ratios in fly ash are similar to those in earth crust. Fly ash has higher content of Pb and Zn than crustal dust [Table 1.4]. So the first factor can be attributed to the combined effect of soil and coal combustion. Effect of coal combustion can also be seen to some extent on the first factor of zone B. Cr, V and Mn seem to have independent

sources in zone C. The source of Cr may be the large number of tanneries [24 to 29, Fig. 4.1] in Jajmau and I.E.L. [2, Fig. 4.1]. Factor 3 may be representing the transport of V and Ni from zone A. Otherwise it is difficult to understand factor 3. The element Zn seems to arise mainly from the thermal power plants. Zn is loaded in zone A with Cr and with Mn and soil elements in zone B. It is to be noted that Cr, Mn and fly ash appear to have independent sources in zone C.

Thus, the factor analysis has helped us in identifying possible sources of pollution and distribution of the pollutants in various zones.

5.2 Analysis of Air Particulate Matter Collected at the Breathing Level at Some Busy Traffic Crossings in Kanpur City

In the previous section an analysis of the air quality of Kanpur city is given and it has helped us in understanding the general level of pollution. To investigate the chemical composition of air particulate matter, that affects the daily commuters on the road, we collected air particulate samples at some busy traffic crossings at a height of about 1.5 mtrs. The sampling locations are shown in Fig. 4.3. We have also taken some samples by collecting particles from the exhaust of a well-maintained motor-cycle and a car under controlled conditions. The conditions in which the samples were collected are described in Table 5.12 along with the details about other samples. The XRF analysis of these samples was carried out by using the procedure described earlier. Of the eight sites

Information about Air Particulate Samples Collected at Breathing Level at Few Busy Crossings in Nanpur City.

Location no. in Fig. 4.3	Place	Date	Deposition Wind $\mu\text{g}/\text{m}^3$	Wind Direction	Temperature $^{\circ}\text{C}$
I	Vijay Nagar Crossing	15.6.79	673	SE \rightarrow NW	41.5
II	LIC (Phool Bagh)*	20.6.79	359	E \rightarrow W	39.8
III	GEC (Bada Chowrah)	21.6.79	1136	E \rightarrow W	40.0
IV	Moolganj Crossing	5.7.79	747	Still	37.6
V	Jareeb Chowky*	12.7.79	558	Still	32.5
VI	GhantaGhar*	14.7.79	1622	Still	30.4
VII	Transport Nagar*	29.8.79	614	W \rightarrow E	38.6
VIII	Kalyanpur	5.9.79	897	W \rightarrow E	35.5
	Motor-Cycle Exhaust	17.12.79	17154	10' above ground and 2' away from the exhaust pipe. The motor-cycle was run 6 kms. at the speed 60-70 km/hr and sample was then collected at a stationary position unaccelerated.	
	Car Exhaust	19.12.79	3230	Very near exhaust.	

*Indicates places where sampling is carried out at breathing level and also at a nearby location at a higher height for air quality measurement.

studied, maximum TSP concentration was obtained at Bada Chowrah (III, Fig. 4.3) and Ghantaghar (VI, Fig. 4.3). Bada Chowrah has a very high traffic density of tempo-taxis and it is also a crossing of five busy roads. The frequency of cycle rickshaws, buses and trucks is very high near Ghantaghar which is near the railway station and the bus terminus.

The results of the XRF analysis of these samples are presented in Table 5.13. Although the TSP concentration was very high in the motor cycle exhaust, Pb concentration was found to be $77.818 \mu\text{g}/\text{m}^3$. On the other hand it was $11154.35 \mu\text{g}/\text{m}^3$ in the car exhaust. An interesting feature of the data is the detection of Ba at many places. In the air quality data Ba was above detection limit at only two locations. The results obtained at locations II, V, VI and VII were compared with the air quality data obtained at nearby locations (9, 12, 5 and 23 in Fig. 5.1) and discussed in Section 5.1. We found that the TSP and elemental concentrations were generally higher in breathing level samples than in those collected at a greater height ($\sim 5-15$ mtrs.) in air quality data. For Pb, we were expecting a much higher concentration in breathing level samples than in air quality data due to the effect of the auto-exhaust. But we did not observe this and a possible reason could be that due to the enrichment of Pb in the atmosphere over the years its concentration at high levels accumulates more small size concentration (which also has higher residence time).

Table 5.13

Concentration of TSP and Various Elements ($\mu\text{g}/\text{m}^3$) in Air
 Particulate Samples at Some Busy Crossings in Kanpur City.

Location	Site No. in Fig. 4.3	TSP	K	Ca	Ti	V	Cr
Vijay Nagar Crossing	I	710	28.976 (9.8)	32.708 (2.2)	4.674 (7.0)	-	1.350 (15.2)
Phool Bagh	II	355	10.360 (13.1)	9.537 (5.6)	0.750 (18.9)	-	-
Bada Chowrah	III	1196	27.483 (9.7)	33.485 (2.2)	4.305 (6.8)	1.086 (11.5)	-
Moolganj Crossing	IV	779	25.874 (1.6)	28.932 (3.3)	0.457 (42.0)	-	-
Jareeb Chowky	V	572	62.751 (4.5)	48.294 (1.9)	1.361 (20.0)	-	-
Ghantaghar	VI	1651	49.975 (13.6)	59.144 (0.2)	13.045 (5.8)	-	2.478 (18.8)
Transport Nagar	VII	642	25.941 (8.9)	39.129 (0.3)	2.867 (8.3)	0.395 (25.0)	1.455 (11.6)
Kalyanpur	VIII	929	44.513 (8.8)	43.778 (3.5)	10.410 (4.5)	-	1.307 (22.0)

Continued

Table 5.13

Concentration of TSP and Various Elements ($\mu\text{g}/\text{m}^3$) in Air
Particulate Samples at Some Busy Crossings in Kanpur City.

Location	Site No. in Fig. 4.3	Mn	Fe	Ni	Cu	Zn	Ba	Pb
Vijay Nagar Crossing	I	1.043 (14.5)	32.533 (0.6)	-	-	0.652	1.331	0.357
Phool Bagh	II	-	7.340 (1.2)	-	0.026 (11.9)	0.220 (8.1)	-	0.205 (5.4)
Bada Chowrah	III	0.783 (15.5)	17.371 (2.1)	-	0.034 (7.3)	0.389 (6.2)	1.042 (7.2)	0.408 (5.4)
Moolganj Crossing	IV	0.601 (20.8)	19.020 (0.7)	-	-	0.434 (5.8)	0.372 (14.6)	0.407 (5.8)
Jareeb Chowky	V	0.903 (14.4)	3.814 (2.6)	0.676 (6.6)	0.214 (9.5)	0.617 (4.5)	-	0.716 (3.9)
Ghantagharp	VI	1.964 (16.7)	38.802 (1.1)	1.937 (7.0)	1.201 (7.9)	1.182 (6.6)	-	0.564 (11.9)
Transport Nagar	VII	0.998 (12.3)	28.202 (0.6)	0.386 (12.8)	0.213 (10.0)	0.297 (10.7)	1.468 (4.8)	0.668 (4.3)
Kalyanpur	VIII	1.284 (17.1)	41.036 (0.7)	-	0.375 (10.6)	0.671 (7.7)	0.886 (11.2)	0.508 (7.9)

Calculation of enrichment factors and statistical analysis of the data is done following the method explained in Section 5.1. An interesting feature of enrichment analysis is the high enrichment of all elements except Ti at Jareeb Chowky. EF for lead is highest (EF = 626). Jareeb Chowky is surrounded by a large number of factories in an area of high population density and is marked by heavy traffic density of trucks. The linear correlation coefficients for all elemental pairs and the factor analysis solution are presented in Tables 5.14 and 5.15 respectively. Except for Ba and V all other elements and the TSP seem to be correlated with each other to various degrees. A four-factor solution accounts for 90 % of the total variance in the system. Ba and V are loaded on two separate factors indicating two independent sources of pollution. The second factor indicates the source to be auto-exhaust and the first factor seems to be due to the dispersion of soil.

This investigation indicates the levels of various elements in the air at breathing level at some of the very busy areas. It shows the quality of air being inhaled by the moving population at these centres.

5.3 Analysis of Air Particulate Samples Collected Inside Some Factories

To study the effect of air pollution on human health it is essential that other parameters affecting the human health should be controlled. This is hardly possible in a general population group having diffused traffic pattern and

Table 5.14

Linear Correlation Coefficients for Samples Collected at Breathing Level.

	TSP	K	Ca	Ti	V	Cr	Mn	Fe	Ni	Cu	Zn	Ba	Pb
TSP	1.000												
K	a	1.000											
Ca	0.674	0.868	1.000										
Ti	0.801	a	0.682	1.000									
V	a	a	a	a	1.000								
Cr	0.578	a	0.629	0.815	a	1.000							
Mn	0.792	0.670	0.922	0.863	a	0.845	1.000						
Fe	0.583	a	a	0.820	a	0.860	0.757	1.000					
Ni	0.657	0.577	0.738	0.593	a	0.637	0.734	a	1.000				
Cu	0.763	0.545	0.754	0.829	a	0.770	0.830	0.536	0.925	1.000			
Zn	0.756	0.696	0.807	0.821	a	0.715	0.888	0.579	0.798	0.856	1.000		
Ba	-0.629	a	a	a	a	a	a	a	a	a	a	1.000	
Pb	a	0.764	0.805	a	a	0.571	a	a	a	a	a	a	1.000

a - Not significant at 5 % level.

Table 5.15

Factor Analysis Loadings (Rotated Four-Factor Solution for Samples at Breathing Level).

Element	Factor Number and Factor Loadings				4 Communality
	1	2	3	4	
TSP	-0.786	0.174	-0.216	-0.428	0.878
K	-0.250	0.883	-0.275	0.131	0.935
Ca	-0.554	0.802	-0.066	-0.032	0.956
Ti	-0.970	0.186	-0.099	-0.016	0.986
V	0.092	-0.038	0.024	-0.961	0.993
Cr	-0.843	0.178	0.203	0.219	0.826
Mn	-0.805	0.530	0.039	0.009	0.931
Fe	-0.896	0.031	0.401	0.137	0.983
Ni	-0.509	0.420	-0.482	0.025	0.668
Cu	-0.768	0.328	-0.421	0.043	0.876
Zn	-0.747	0.382	-0.301	0.192	0.831
Ba	-0.096	-0.037	0.964	0.233	0.994
Pb	-0.064	-0.955	0.086	-0.027	0.924
Fraction of total variance	0.42	0.18	0.14	0.10	

undergoing diverse living conditions. It is a formidable task to correlate the health of a population to the general air quality. But such a possibility exists in factories where a large number of workers are exposed regularly to a fairly higher level of elemental pollution. The values given in Table 1.8 are in fact threshold limit values for such work-room atmosphere where workers stay for about eight hours a day. Realising the medical significance of such studies, we decided to investigate the elemental levels inside a few factories, so that we could obtain some idea about the quality of air inhaled by the workers.

A few air particulate samples were collected at breathing level (~ 1.5 mtrs.) inside a few factories following the method described in Chapter 4. The samples were collected inside a paints factory, a leather processing factory and an iron and steel factory. The work-room conditions in which the samples were collected are described in Table 5.16. The XRF analysis of these samples was carried out by the method explained in Chapter 3. The results are presented in Table 5.17. In Table 5.18 we have given the maximum concentrations for work-room (labelled as class A) atmosphere in a factory and for a commercial zone (labelled as class B) as recommended by the World Health Organization [29]. The exposure levels indicated in class A are intended to represent the air breathed by the worker. It is assumed that any individual exposed to class A atmosphere is healthy and that the

Table 5.16

Information about Air Particulate Samples Collected Inside Some Factories in Kanpur

City.

S.No.	Place	Deposition $\mu\text{g}/\text{m}^3$	Comments
1.	Nagarath Paints	6044	Dry grinding section with 4 grinders. One was operating during the sampling period.
2.	Nagarath Paints	809	Varnishing kitchen. (3 furnace capsules)
3.	TAFCO Leather Processing Unit	389	Sampling is done in spray section. Distance from automatic spray - 3.5mtr. Distance from manual spray - 7.5 mtrs.
4.	J.K. Iron and Steel	3560	Foundry Section. Two mouldings were covered. <ol style="list-style-type: none"> 1) distance from mould to sampler was 4 mtrs. Wind direction was unfavourable. 2) distance from mould to sampler was 9.5 mtrs. 3) in furnace section.
5.	J.K. Iron and Steel	506	The sample was collected at night when no molten iron was poured.

Table 5.17

Elemental Concentration ($\mu\text{g}/\text{m}^3$) at Various Places Inside Some Factories in Kanpur City.

Location	Element				
	K	Ca	Ti	Cr	Mn
Nagarath Paints (Grinding Section)	44.640 (6.2)	283.947 (0.2)	13.887 (1.6)	-	2.671 (6.8)
Nagarath Paints (Varnishing Kitchen)	28.434 (11.3)	23.776 (5.7)	36.154 (1.0)	1.705 (14.6)	0.898 (19.3)
TAFCO (Spray Section)	-	6.939 (11.1)	19.645 (3.8)	1.980 (7.5)	-
J.K. Iron and Steel (During Moulding)	277.115 (2.6)	-	11.286 (6.6)	5.088 (10.1)	37.813 (1.5)
J.K. Iron and Steel (After Moulding in Furnace Section)	13.096 (16.9)	22.451 (4.6)	4.536 (5.6)	1.307 (13.6)	3.813 (4.0)

Continued

Table 5.17

Elemental Concentration ($\mu\text{g}/\text{m}^3$) at Various Places Inside Some Factories in Kanpur City.

Location	Fe	Ni	Element		Zn	Ba	Pb
			Cu				
Nagarath Paints (Grinding Section)	83.511 (0.3)	0.244 (24.7)	0.266 (12.0)	2.098 (1.8)	54.147 (0.3)	2.635 (1.6)	
Nagarath Paints (Varnishing Kitchen)	27.179 (0.8)	-	0.172 (12.2)	0.550 (5.9)	-	0.504 (7.5)	
TAFCO (Spray Section)	5.854 (1.6)	-	0.079 (9.7)	0.897 (3.2)	-	4.017 (1.1)	
J.K. Iron and Steel (During Moulding)	661.077 (0.3)	0.385 (24.7)	2.518 (5.1)	345.057 (0.1)	2.358 (8.7)	35.822 (0.5)	
J.K. Iron and Steel (After Moulding in Furnace Section)	45.509 (0.4)	-	0.336 (9.1)	20.385 (0.3)	-	2.110 (1.6)	

Table 5.18

Maximum Concentration in $\mu\text{g}/\text{m}^3$ Recommended by the W.H.O.
[29].

Substance	Class A	Class B
Ba	100	10
Calcium arsenate	1000	10
Calcium oxide	100	5
Chromates	100	1
Chromic acid	100	1
Chromium	50	0.5
Copper dust and mist	1000	100
Copper fumes	100	10
Iron oxide fume	10000	50
Lead (AsPb)	100	1
Manganese oxide	10000	500
Manganese oxide fume	15000	700
Manganese	2000	2
Nickel	200	2
Titanium	10000	100
Titanium dioxide	15000	150
Vanadium dust	500	5
Vanadium fume	100	1
Zinc	10000	100
Zinc oxide fume	5000	50

exposure is limited to not more than 8 hrs. a day and five days a week. Class B concentration limits are ideal maximum values which are decided arbitrarily and are recommended for the commercial zone of a city where the occupants normally work 8 hrs. per day and 5 days per week, plus one hour commuting time entering and leaving the area. Comparison of elemental levels in Table 5.17 and class A of Table 5.18 indicates that the elemental levels in work-room atmosphere are not higher than the maximum recommended value. But it is also true that the preconditions mentioned for class A values are not fulfilled in most of the factories in Kanpur. In fact, incidence of tuberculosis among the workers in Kanpur city is one of the highest.

The present investigation provides some data which can be useful for further medical studies of the workers in these factories. Before fixing regulatory standards for any work-room atmosphere it is essential that an extensive study regarding the correlation of health to the level of pollution in the work-room atmosphere be undertaken. For a working population with a low level of physical fitness, it is expected that the regulatory standards will have much lower values than given in class A (Table 5.18). Hence, it is suggested that a systematic medical survey of workers in various factories in Kanpur be undertaken immediately from an environmental point of view.

(Fig. 5.1) is the most polluted area in Kanpur city. iii) The concentration of the soil-borne elements is higher in Kanpur than in other cities and the concentrations of elements like Zn, Cu and Pb are comparable. iv) Calculation of enrichment factor shows that the elements Zn and Pb are less enriched than in other cities and their enrichment due to man-made sources is comparable with their enrichment in natural aerosols at remote areas in western countries and also over the Arabian Sea. We have also been able to point out a few locations where enrichment of some elements due to anthropogenic sources is quite high. v) Zone-wise statistical analysis of the data has helped us in understanding the behaviour of various elements and also in identifying some sources of pollution in each zone. We could identify a soil source in each zone, sources of pollution for Ni, Cu, V and Pb in zone A and for Cr, Mn, V and Pb in zone C and for Mn in zone B. vi) The analysis of the air particulate data collected at breathing level indicates fairly uniform increase in the TSP and elemental concentrations than those in the air quality data at nearby locations. The expected high value of Pb was not observed and this may be due to the possibility that the aerosol at greater height is enriched over the years by small size Pb particles whereas at breathing level Pb may be present mainly in large particle size. In this context, a particle-size study of composition of aerosol at various heights may provide valuable information. We were also able

to point out a location (Jareeb Chowky) with very high level of pollution due to nearby anthropogenic sources. vii) The concentrations of elements observed inside various factories was found to be less than the prescribed concentrations, but it should also be noted that the prescribed control condition are generally not satisfied in the factories under study.

In view of the above findings further investigations could help in understanding the nature of pollution due to air particulate matter in our country. A study of background level of the TSP is necessary to decide the national air quality criteria for the TSP. An investigation of composition of natural aerosols at remote parts in the country will also help in understanding the relative importance of long range transport of pollutants and natural processes in enriching the elements Zn and Pb. On the local level it is hoped that the present data provide some basis for the urban planners and local authorities to take appropriate measures to prevent pollution hazards in the area.

The present study was undertaken on an experimental level to standardize and develop various techniques and methods of analysis necessary to study chemical composition of air particulate matter. For further nation-wide study of the similar pollution problems it is necessary to establish XRF analysis laboratories where the technique could be standardized and kept ready for routine analysis. It is also necessary to select different cities in various parts of the country to study the nature of industrial pollution.

A need for a systematic plan to investigate the background aerosol at remote areas exists. The study should cover different seasons in the year. Various methods of sample collection should be developed and standardized to perform particle size analysis of elemental composition of air particulate matter. The statistical methods used to analyze the data in the present work can also be extended to similar studies made elsewhere in India.

It is hoped that the present research project has provided an application of nuclear detection techniques for studying a problem of sociological and national relevance. The present study will remain incomplete unless it is followed up by some executive measures by those who are in charge of the municipal supervision and urban planning of our cities.

REFERENCES

1. H.A. Trindade, W.C. Pfeiffer, H. Londers, and C.L. Costa-Ribeiro, *Environ. Sci. Technol.*, 15, 84 (1981).
2. R.C. Ragaini, H.R. Ralston and N. Roberts, *Environ. Sci. Technol.*, 11, 773 (1977).
3. J.L. Moyers, L.E. Ranweiler, S.B. Hopf and N.E. Korte, *Environ. Sci. Technol.*, 11, 789 (1977).
4. P.K. Hopke, E.S. Gladney, G.E. Gordon, W.H. Zoller and A.G. Jones, *Atmos. Environ.*, 10, 1015 (1976).
5. R.N. Khandekar, D.N. Kelkar and K.G. Vohra, *Atmos. Environ.*, 14, 457 (1980).
6. M.T. Kleinman, Ph.D. Dissertation, New York University, (1977).
7. A. Donagi, E. Ganor, A. Shenhav and H. Cember, *J. Air Pollut. Control Assoc.*, 29, 53 (1979).
8. R.E. Lee, Jr. and S. Goranson, *Environ. Sci. Technol.*, 10, 1022 (1977).
9. P.K. Yennawar, S.N. Dixit, V.L. Pampattiwar, J.M. Dave and S.J. Arceivala, *Environ. Health*, 12, 355 (1970).
10. V.P. Sharma, H.C. Arora, S.N. Chattopadhyay and T. Routh, *Indian J. Environ. Health*, 15, 132 (1973).
11. C. McDonald and H.J. Duncan, *Atmos. Environ.*, 13, 413 (1979).
12. V.V. Egorov, T.N. Zhigalovskaya and S.G. Malakhov, *J. Geophys. Res.*, 75, 3650 (1970).
13. J.A. Cooper, Review of Workshop on X-Ray Fluorescence Analysis of Aerosols, Battelle Pacific Northwest Laboratory Report BNWL-SA-4690, June 1, 1973.
14. G.E. Gordon, W.H. Zoller and E.S. Gladney, in Trace Substances in Environmental Health-VII, ed. D.D. Hemphill, University of Missouri, Columbia (1973), p. 167.
15. W. John, R. Kaifer, K. Rahn, and J.J. Wesolowski, *Atmos. Environ.*, 7, 107 (1973).

16. W.J. Pattenden, presented at the 41st Ann. Conf. of the National Society for Clean Air, 14-13 Oct., Cardiff, U.K. (1974).
17. J. Bogen, *Atmos. Environ.*, 7, 1117 (1973).
18. I.J.M. Bowen, Trace Elements in Chemistry, Academic Press Inc., London Ltd. (1966), p. 39.
19. J.W. Winchester, *Nucl. Instrum. Methods*, 142, 85 (1977).
20. K.A. Rahn, Ph.D. Thesis, University of Michigan, Ann Arbor, (1971).
21. W.L. Zoller, E.S. Gladney and R.A. Duce, *Science*, 183, 198 (1974).
22. R.E. Jervis, J.J. Paciga, A. Chattopadhyay, *Proc. Int. Symp.*, STI/PUB/432, (1976).
23. S. Sadasivan, *Atmos. Environ.*, 12, 1677 (1978).
24. R.A. Fisher, Statistical Methods for Research Workers, Hafner, New York, (1958), p. 356.
25. C.W. Lewis and E.S. Macias, *Atmos. Environ.*, 14, 185 (1980).
26. F.D. Gaarenstroom, S.P. Perone and J.L. Moyers, *Environ. Sci. Technol.*, 11, 795 (1977).
27. H.H. Harman, Modern Factor Analysis, The University of Chicago Press, (1960).
28. E.S. Gladney, Ph.D. Thesis, University of Maryland, (1974).
29. M.J. Suess and S.R. Craxford, eds. Manual on Urban Air Quality Management, WHO Regional Publications, European Series No. 1 (1976).

VITAE

Veena Ramrao Joshi was born in Ichalkarnji, in Kolhapur District, Maharashtra, India on 7th July 1954. She obtained her B.Sc. degree in Physics from Karnataka College, Dharwar, Karnataka, and the M.Sc. degree in Physics from Indian Institute of Technology, Bombay, Maharashtra. She joined the Ph.D. program in Physics at the Indian Institute of Technology, Kanpur in July 1974. She was a recipient of National Merit Scholarship from the Government of India from 1968 to 1974. At present she is a Research Scholar at I.I.T. Kanpur

Publications:

- 1) Electron Hopping in $\text{Eu}_{1-x}\text{Sr}_x\text{FeO}_3$ and $\text{Nd}_{1-x}\text{Sr}_x\text{CoO}_3$, Veena Joshi, Om Prakash, G.N. Rao and C.N.R. Rao, J. Chem. Soc., Faraday Trans. II, 75, 1199 (1979).
- 2) Trace Element Analysis using Energy Dispersive X-Ray Fluorescence Technique, Veena Joshi, K.K. Dwivedi, Prem Sagar, R.M. Singru and G.N. Rao, to be published in Transactions of Indian Institute of Metals.
- 3) Energy Dispersive X-Ray Fluorescence Technique and its Applications to Trace Element Analysis of Environmental Samples, Veena Joshi, K.K. Dwivedi, Prem Sagar, R.M. Singru and G.N. Rao, presented at International Symposium on Trace Analysis and Technological Development held at Bombay, Feb. 16-19, 1981.